

SUMMARY REPORT FOR A

TITAN MT SURVEY

OVER

KOPER LAKE PROJECT

(NORTHERN ONTARIO)

ON BEHALF OF

KWG RESOURCES INC.



March 8, 2023
CA01329T

Quantec Geoscience Ltd.
146 Sparks Ave., Toronto, ON, M2H 2S4, Canada
+1-416-306-1941



QUANTEC
Geoscience

Report Disclaimer:

Quantec Geoscience Limited holds a Certificate of Authorization from the Association of Professional Geoscientists of Ontario (PGO) to perform the work presented in this report. Quantec employed qualified professionals to carry out the work presented in this geophysical report.

Statements made in this report represent opinions that consider information available at the time of writing. Although every effort has been made to ensure the accuracy of the material contained in this report, complete certainty cannot be guaranteed due to the interpretive nature of the work which may include mathematically derived solutions that are inherently non-unique. Therefore, the estimated physical parameters of the subsurface may have no direct relation to the real geology and possible economic value of any mineralization.

There is no guarantee or representation to the user as to the level of accuracy, currency, suitability, completeness, usefulness, or reliability of this information for any purpose. Therefore, decisions made based on this work are solely the responsibility of the end user. It is incumbent upon the end user to examine the data and results delivered and make Quantec aware of any perceived deficiencies.

EXECUTIVE SUMMARY

This report presents the data analysis, inversion results and the interpretation of the Titan MT Survey, carried out from 19/01/2023 to 11/02/2023, over the Koper Lake Project by Quantec Geoscience Ltd. on behalf of KWG Resources Inc.

In this project, a total of 13 MT lines were acquired over the Koper Lake Project. Eight lines were located over a detailed grid (Grid-1), oriented at 317° true north and spaced at 100 m to 150 m. All lines on Grid- 1 used an array of 100 m inline dipoles and crossline dipoles of same size at every 200 m. Other five lines were located over a regional grid (Grid-2), where four lines were oriented at 315° and one line at 0° true north. Each line on Grid-2 was deployed with an array of 100 m and 200 m inline dipole combinations and crossline dipoles of 100 m at every other inline dipole. Titan MT sites along all lines were acquired and processed at the respective line azimuth, within a nominal frequency range from 10 kHz to 0.01 Hz.

2D inversions were completed for the acquired Titan MT data. The inversion results are presented as MT resistivity sections, plans and 3D-view maps in this report. The maps presented in this report use a consistent colour range of 500-20,000 Ω -m to accommodate the wide range of sub-surface resistivities observed over the Koper Lake Project.

MT inversions resolved a low resistivity surficial layer, which represents the Quaternary deposits that extends to an approximate depth of 50 m throughout the project area. Besides this top layer, inversion results show the underlying bedrocks with high resistivity. These underlying rocks are resolved with multiple zones of low resistivity responses, including sub-vertical structures possibly indicating the shear/fault zones or lithological contacts.

The main sub-vertical low resistivity zones resolved in the 2D resistivity models show some correlation to the known shear zones in the region. The available drill data shows chromite mineralization within these shear zones and within the underlying medium resistivity zones. The main anomalies resolved are briefly discussed in this report using the resistivity section and plan maps and an overview of the results are presented in 3D views.

The results and any interpretation presented in this report are purely based on the inversions completed using available MT data. It is recommended to integrate these results with other geological and geophysical data to help with any follow up exploration efforts.

TABLE OF CONTENTS

List of Figures and Tables.....	7
1. Introduction	11
1.1. Client Information.....	11
1.2. General Project Information	11
1.3. Survey Logistics	11
1.4. Deliverables	15
1.5. Digital Archive Attached to the Report.....	15
2. Previous Work and Geology.....	17
3. Inversion Procedures	19
3.1. Magnetotelluric Inversions	19
3.1.1. 2D inversion parameters	19
4. Inversion Results and Interpretation	21
4.1. Koper Lake MT 2D Results	22
4.1.1. L4700E.....	23
4.1.2. L4800E.....	24
4.1.3. L4900E.....	25
4.1.4. L5000E.....	26
4.1.5. L5100E.....	27
4.1.6. L5250E.....	28
4.1.7. L5350E.....	29
4.1.8. L5450E.....	30
4.1.9. L1E.....	31
4.1.10. L1aE.....	31
4.1.11. L2E.....	31
4.1.12. L3E.....	31
4.1.13. L4E.....	36
4.1.14. Resistivity Plan Maps (Depth levels)	38
4.1.15. 3D view of the MT Resistivity Sections	57
5. Conclusions and Recommendations.....	64
APPENDIX A. References	65

APPENDIX B. Resistivity Section Maps 67
APPENDIX C. Resistivity Plan Maps (Depth Levels) 81
APPENDIX D. Geotools 2D (CGG) Inversion Code..... 133

LIST OF FIGURES AND TABLES

Figure 1-1: General location map.	12
Figure 1-2: Titan MT coverage over Koper Lake Grid-1.	13
Figure 1-3: Titan MT coverage over Koper Lake Grid-2.	14
Figure 2-1: Simplified geology of Ontario (by Ontario Geological Survey, copied from KWG website).	17
Figure 2-2: Magnetic map of the McFaulds Lake, highlighting the Ring of Fire (copied from KWG website).	18
Figure 4-1: MT resistivity colour range used for the Koper Lake Project.	21
Figure 4-2: 2D MT resistivity section along L4700E.	23
Figure 4-3: 2D MT resistivity section along L4800E.	24
Figure 4-4: 2D MT resistivity section along L4900E.	25
Figure 4-5: 2D MT resistivity section along L5000E.	26
Figure 4-6: 2D MT resistivity section along L5100E.	27
Figure 4-7: 2D MT resistivity section along L5250E.	28
Figure 4-8: 2D MT resistivity section along L5350E.	29
Figure 4-9: 2D MT resistivity section along L5450E.	30
Figure 4-10: 2D MT resistivity section along L1E.	32
Figure 4-11: 2D MT resistivity section along L1aE.	33
Figure 4-12: 2D MT resistivity section along L2E.	34
Figure 4-13: 2D MT resistivity section along L3E.	35
Figure 4-14: 2D MT resistivity section along L4E.	37
Figure 4-15: MT resistivity plan map over Koper Lake Grid-1 at the surface; the resistivity is well below 500 Ω -m over the entire survey area.	38
Figure 4-16: MT resistivity plan map over Koper Lake Grid-1 at the surface; shown using 10-500 Ω -m colour range.	39
Figure 4-17: MT resistivity plan map over Koper Lake Grid-1 at 50 m depth.	40
Figure 4-18: MT resistivity plan map over Koper Lake Grid-1 at 100 m depth.	41
Figure 4-19: MT resistivity plan map over Koper Lake Grid-1 at 300 m depth.	42
Figure 4-20: MT resistivity plan map over Koper Lake Grid-1 at 500 m depth.	43
Figure 4-21: MT resistivity plan map over Koper Lake Grid-1 at 800 m depth.	44

Figure 4-22: MT resistivity plan map over Koper Lake Grid-2 at the surface; the resistivity is well below 500 Ω -m over the entire survey area.....	45
Figure 4-23: MT resistivity plan map over Koper Lake Grid-2 at the surface; shown using 10-500 Ω -m colour range.	46
Figure 4-24: MT resistivity plan map over Koper Lake Grid-2 at 50 m depth.....	47
Figure 4-25: MT resistivity plan map over Koper Lake Grid-2 at 100 m depth.....	48
Figure 4-26: MT resistivity plan map over Koper Lake Grid-2 at 200 m depth.....	49
Figure 4-27: MT resistivity plan map over Koper Lake Grid-2 at 300 m depth.....	50
Figure 4-28: MT resistivity plan map over Koper Lake Grid-2 at 500 m depth.....	51
Figure 4-29: MT resistivity plan map over Koper Lake Grid-2 at 800 m depth.....	52
Figure 4-30: MT resistivity plan map over Koper Lake Grid-2 at 1000 m depth.....	53
Figure 4-31: MT resistivity plan map over Koper Lake Grid-2 at 1200 m depth.....	54
Figure 4-32: MT resistivity plan map over Koper Lake Grid-2 at 1400 m depth.....	55
Figure 4-33: MT resistivity plan map over Koper Lake Grid-2 at 1600 m depth.....	56
Figure 4-34: 2D MT resistivity sections over Koper Lake Grid-1; all lines shown together in the 3D view.	57
Figure 4-35: 2D MT resistivity sections over Koper Lake Grid-2; all lines shown together in the 3D view.	58
Figure 4-36: 3D view of the Grid-1 (top) and Grid-2 (bottom) MT2D sections plotted with the drill data showing chromite mineralization (in blue).....	59
Figure 4-37: Line L2E plotted with a drill hole showing minor chromite mineralization, coincident with the low resistivity shear zone.....	60
Figure 4-38: Line L3E plotted with a drill hole showing chromite mineralization.	61
Figure 4-39: Line L4700E resistivity section and drill data showing chromite mineralization.....	62
Figure 4-40: Lines L4800E (left) and L4900E (right) resistivity sections and drill data showing chromite mineralization.	63
Figure 4-41: Lines L5000E (left) and L5100E (right) resistivity sections and drill data showing chromite mineralization.	63

Table 1-1: Contents of the digital archive included with this report.....	16
Table 3-1: 2D inversion details of the Titan MT data over the Koper Lake Project.....	20
Table 4-1: Resistivity anomaly classification for the Koper Lake Project.....	21

1. INTRODUCTION

This report presents the data analysis, inversion results and the interpretation of the Titan MT Survey, carried out from 19/01/2023 to 11/02/2023, over the Koper Lake Project by Quantec Geoscience Ltd. on behalf of KWG Resources Inc.

Details of the data acquisition are provided in a separate Logistics Report completed for the project.

1.1. CLIENT INFORMATION

Name: KWG Resources Inc.

Address: 141 Adelaide Street West, Suite 240
Toronto, ON, M5H 3L5, Canada

Representative: Maurice Lavigne
Phone: +1-807-627-0132
Email: toolbuck@gmail.com

1.2. GENERAL PROJECT INFORMATION

Quantec Project Manager: Mark Morrison

Quantec Project Number: CA01329T

Report prepared by: Jimmy Stephen, PhD, PGeo

Project Name: Koper Lake Project

Survey Type: Titan MT

General Location: Approximately 170 km NE of Fort Hope (Figure 1-1).
Lat /Long: 52°44'38.4"N, 086°15'41.6"W
UTM: 549850m E, 5844050m N
Datum: WGS84, UTM Zone 16N

Survey Period: From 19/01/2023 to 11/02/2023

1.3. SURVEY LOGISTICS

Logistic report: Logistic Report for a Titan MT survey over Koper Lake Project (Northern Ontario) by Quantec Geoscience Ltd. on behalf of KWG Resources Inc.

PDF File: CA01329T_KWG_KoperLake_Logistics_Report.pdf



Figure 1-1: General location map.

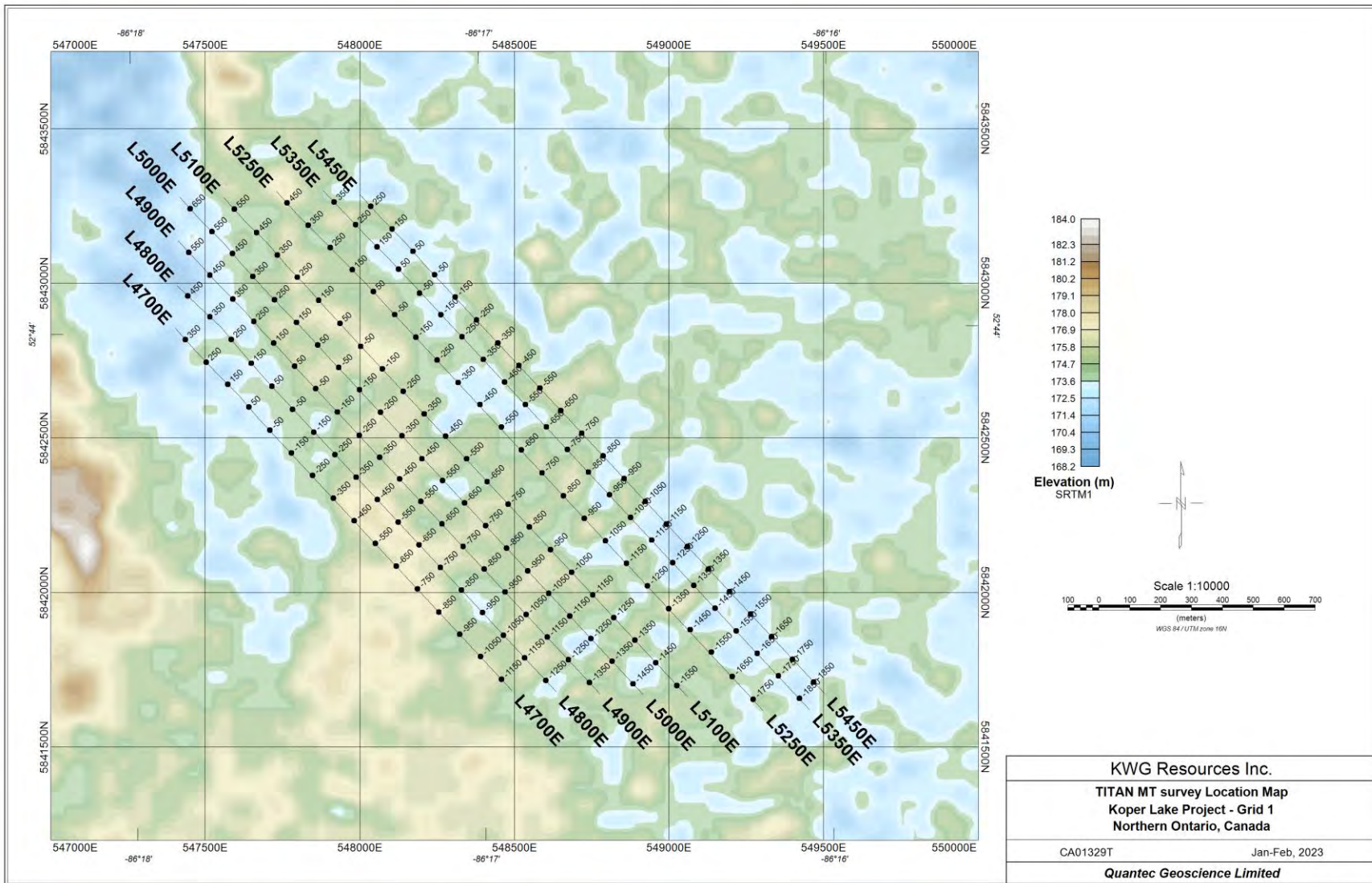


Figure 1-2: Titan MT coverage over Koper Lake Grid-1.

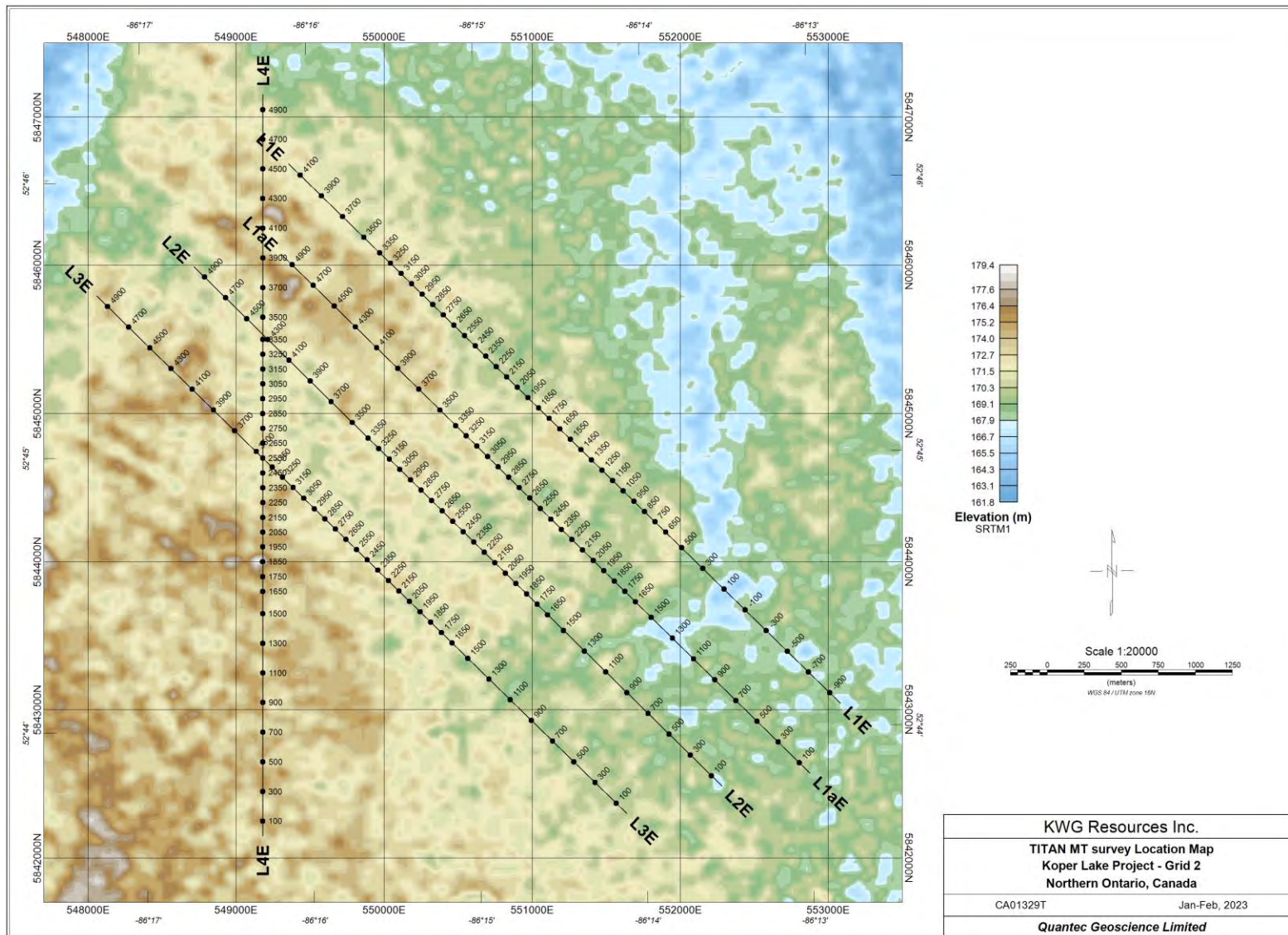


Figure 1-3: Titan MT coverage over Koper Lake Grid-2.

1.4. DELIVERABLES

The final survey results delivered with this report are:

- 2D inversion products
 - 2D models for each line, provided as Geosoft maps (.MAP), images (.PNG) and ASCII (.XYZ) files.
 - One MT resistivity model
 - Plan maps at selected depth levels (gridded from 2D models).
 - Each level as Geosoft map (.MAP) and image (.PNG) files
 - Geosoft format 3D section views prepared from 2D models.

1.5. DIGITAL ARCHIVE ATTACHED TO THE REPORT

The digital archive accompanying this report contains a copy of the results, including model files and map products. Copy of the logistics report and the final processed data are also included.

Table 1-1: Contents of the digital archive included with this report.

Folder	Sub-folder	Contents
\Report		Geophysical report (.PDF) Logistics report (.PDF)
\Data	\Line#\EDI	Final processed MT data (.EDI) Raw spectra EDI files for each site. Sub-folders with images of sounding plots (.PNG) and daily remote EDI files (referenced and unreferenced).
	\Line#\GPS	Survey location data for each line (.TXT)
	\Line#\Documents	Compilation of Various field documents including operator and processing notes.
\Geosoft	\Basemap	Survey location map and database
	\MT2D	Geosoft documents related to the 2D inversions including model databases, section / plan maps and corresponding PNG files. (This folder also comprises additional TM only inversion models in a sub-folder)
\Miscellaneous		Extra documents (final survey .KML, etc.).

2. PREVIOUS WORK AND GEOLOGY

The Koper Lake Project is located within the Ring of Fire, a mineral rich area of the James Bay Lowlands of the Northern Ontario. The mineral exploration efforts are generally hampered in the region due to the thick cover of Quaternary deposits. Geophysical methods play a vital role here to map beneath this overburden.

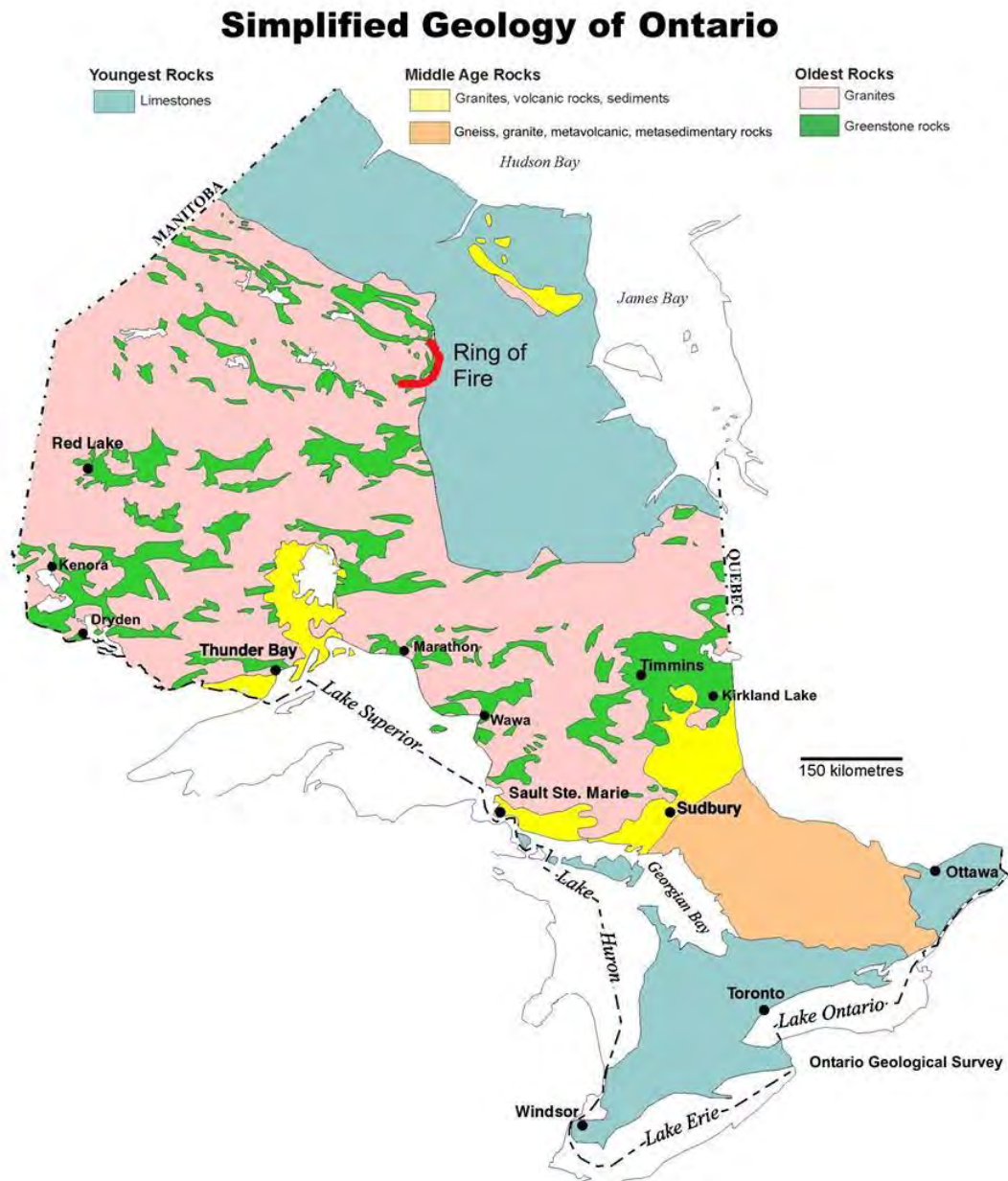


Figure 2-1: Simplified geology of Ontario (by Ontario Geological Survey, copied from KWG website).

Some of the previous geophysical work include airborne and ground surveys, including gravity and magnetic. Current Titan MT survey is to map beneath the surficial low resistivity layer and delineate the underlying resistivity structures possibly helping with the ongoing exploration efforts to identify chromite targets.

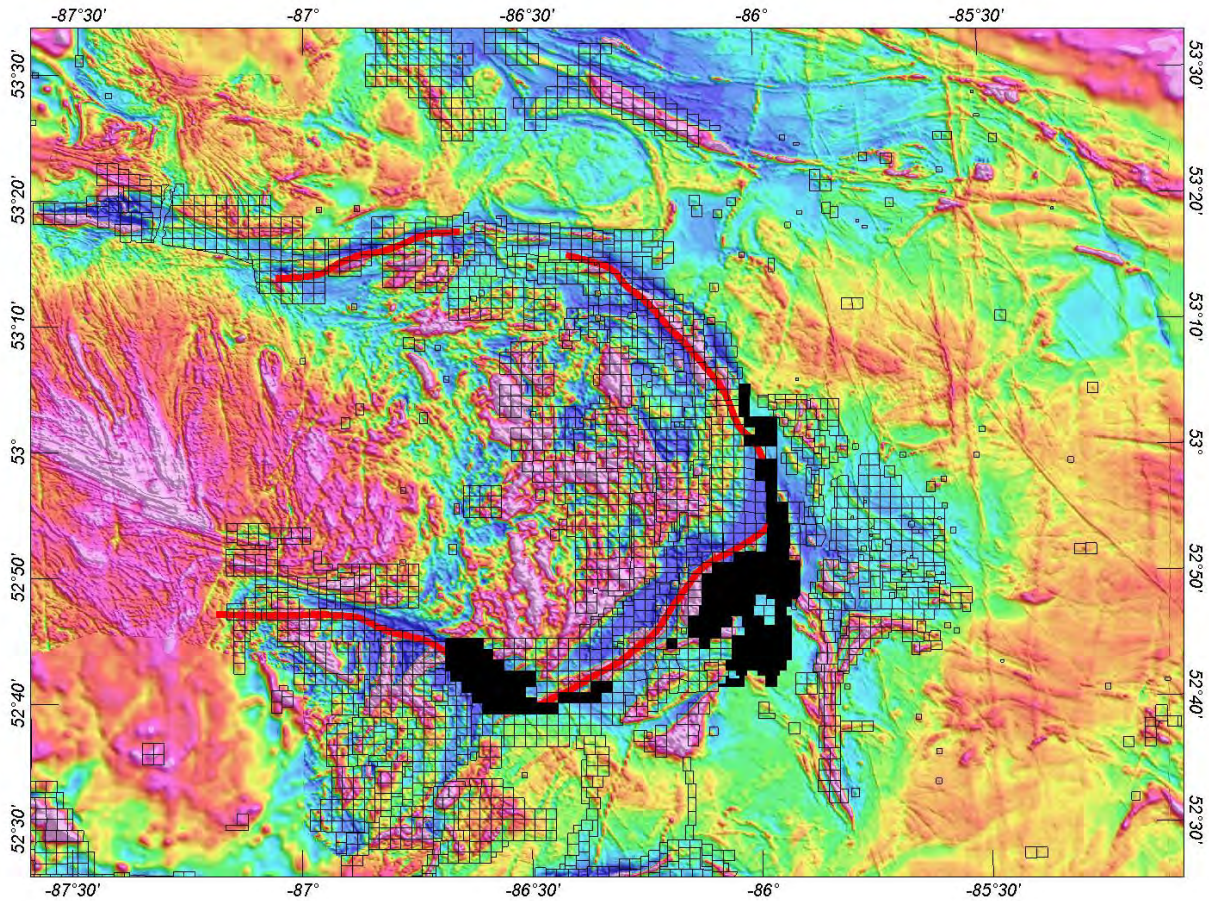


Figure 2-2: Magnetic map of the McFaulds Lake, highlighting the Ring of Fire (copied from KWG website).

3. INVERSION PROCEDURES

3.1. MAGNETOTELLURIC INVERSIONS

The Magnetotelluric (MT) method is a natural source EM method that measures the variation of both the electric (E) and magnetic (H) field on the surface of the earth to determine the distribution at depth of the resistivity of the underlying rocks. A complete review of the method is presented in Vozoff (1972) and Orange (1989).

The measured MT impedance Z , defined by the ratio between the E and H fields, is a tensor of complex numbers. This tensor is generally represented by an apparent resistivity (a parameter proportional to the modulus of Z) and a phase (argument of Z). The variation of those parameters with frequency relates the variations of the resistivity with depth, the high frequencies sampling the sub-surface and the low frequencies the deeper part of the earth. However, the apparent resistivity and the phase have an opposite behaviour. An increase of the phase indicates a more conductive zone than the host rocks and is associated with a decrease in apparent resistivity. The objective of the inversion of MT data is to compute a distribution of the resistivity of the surface that explains the variations of the MT parameters, i.e. the response of the model that fits the observed data. The solution however is not unique and different inversions must be performed (different programs, different conditions) to test and compare solutions for artefacts versus a target anomaly.

The depth of investigation is determined primarily by the frequency content of the measurement. Depth estimates from any individual sounding may easily exceed 20 km. However, the data can only be confidently interpreted when the aperture of the array is comparable to the depth of investigation.

The inversion model is dependent on the data, but also on the associated data errors and the model norm. The inversion models are not unique, may contain artefacts of the inversion process and may not therefore accurately reflect all the information apparent in the actual data. Inversion models need to be reviewed in context with the observed data, model fit. The user must have an understanding of the model norm used and evaluate whether the model is geologically plausible.

3.1.1.2D inversion parameters

For this project, 2D inversions were performed on all surveyed Titan MT lines.

The 2D inversions presented in this report were carried out using the CGG Geotools MT-2D inversion algorithm (Rodi and Mackie, 2001; Geotools, 2012); more details provided in APPENDIX D.

For each profile, we assume the strike direction is perpendicular to the profile for all sites: the TM mode is then defined by the inline E-field (and cross line H-field), and the TE mode is defined by the crossline E-field (and inline H-field) data.

The 2D inversions were performed using resistivity and phase data interpolated at 6 frequencies per decade, assuming 10% and 5% error for the resistivity and phase respectively, which is equivalent to 5% error on the impedance component Z . Since the Titan MT deployment uses a shared crossline dipole for two inline dipoles, a minimum of 7.5% error is assigned on the TE mode impedance data for meaningful TETM inversion.

The topography was included in the inversions of each profile. The topography along the line is accommodated with 10 m thick vertical mesh cells. Then the thickness of cells increased by a factor of 1.03 with depth, from 10 m up to 100 m size to cover the depth of interest. The horizontal mesh was defined with 25 m wide cells to have a minimum of 4 cells between MT sites.

Each 2D inversion started from a half space model of 2000 Ω -m.

A summary of the inverted MT lines over the Koper Lake Project showing the number of inverted sites, line extents and the achieved data misfit is provided in Table 3-1.

Table 3-1: 2D inversion details of the Titan MT data over the Koper Lake Project.

Line	# Sites	Line Start	Line End	Final_RMS
Koper Lake Grid-1				
L4700E	16	-1150	350	2.0
L4800E	18	-1250	450	2.6
L4900E	20	-1350	550	2.5
L5000E	22	-1450	650	2.6
L5100E	22	-1550	550	3.0
L5250E	23	-1750	450	2.4
L5350E	23	-1850	350	2.5
L5450E	22	-1850	250	2.0
Koper Lake Grid-2				
L1E	40	-900	4100	3.4
L1aE	34	100	4900	2.4
L2E	34	100	4900	2.8
L3E	34	100	4900	2.6
L4E	34	100	4900	2.2

4. INVERSION RESULTS AND INTERPRETATION

This section presents the 2D inversion results of the Titan MT data acquired over the Koper Lake Project. Figure 1-2 and Figure 1-3 show the data coverage. 2D MT inversions were primarily carried out using the TETM mode data and used for the discussions in this report. The inversion models are presented as MT resistivity sections, plans at depth levels and 3D views, as appropriate from the 2D inversion models, along with an interpretation overlay. The accompanying digital archive comprises additional inversions completed exclusively using the TM mode MT data, which may be useful for any follow up references. However, this is to be noted that the TETM and TM models could show significant differences between those due to differences in the inverted data.

Over the Koper Lake Project, the sub-surface resistivities vary over several decades (Ω -m). All maps presented in this report use a consistent colour range from 500 Ω -m to 20,000 Ω -m. The observed anomalies are classified into three categories for the purpose of discussions in this report (Table 4-1). Figure 4-1 shows the resistivity colour bars used to present the resistivity maps for both grids.

Table 4-1: Resistivity anomaly classification for the Koper Lake Project.

Description	Resistivity Range
Low resistivity	<1,400 Ω -m
Medium resistivity	1,400 Ω -m – 5,000 Ω -m
High resistivity	>5,000 Ω -m

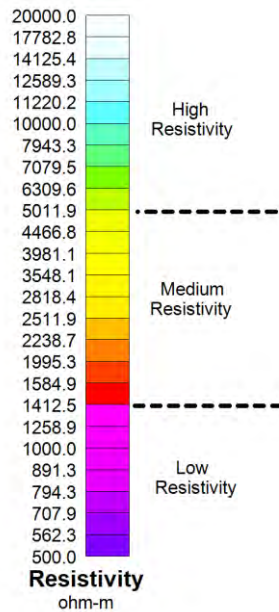


Figure 4-1: MT resistivity colour range used for the Koper Lake Project.

4.1. KOPER LAKE MT 2D RESULTS

Overview of the 2D MT resistivity models show a low resistivity surficial layer covering the entire region, which extends to an approximate depth of 50 m. Based on the available geology, this overburden represents four extensive layers; limestone, glacial till, lake-bottom mud, and muskeg of the James Bay lowlands, which covers the Canadian Shield bed rock. The MT resistivity sections help to identify the structures hidden beneath this top low resistivity layer. The most significant anomaly resolved on all lines is a NW dipping low resistivity feature extending from the near-surface to depth, possibly indicating a major shear zone.

The resistivity section maps along Grid-1 lines L4700E – L5450E and Grid-2 lines L1E – L4E are presented from Figure 4-2 through Figure 4-14. Anomalies of interest are discussed briefly. Any vertical/sub-vertical conductive lineaments / shear zones identified on the resistivity sections are marked with black dashed lines.

4.1.1.L4700E

Figure 4-2 shows the 2D MT resistivity section along the Koper Lake line L4700E. The main anomaly resolved on this line is the sub-vertical low resistivity zone below station 150, which shows a steep NW dip. This zone is possibly representing a shear zone, which dips outwards the NW end of the line at -800 m elevation (i.e., an approximate depth of 950 m below surface).

There is also another sub-vertical medium resistivity feature resolve on line L4700E in the SE. A simplified interpretation overlay is shown on the following section map. Mainly any low resistivity lineaments are highlighted with black dashed lines.

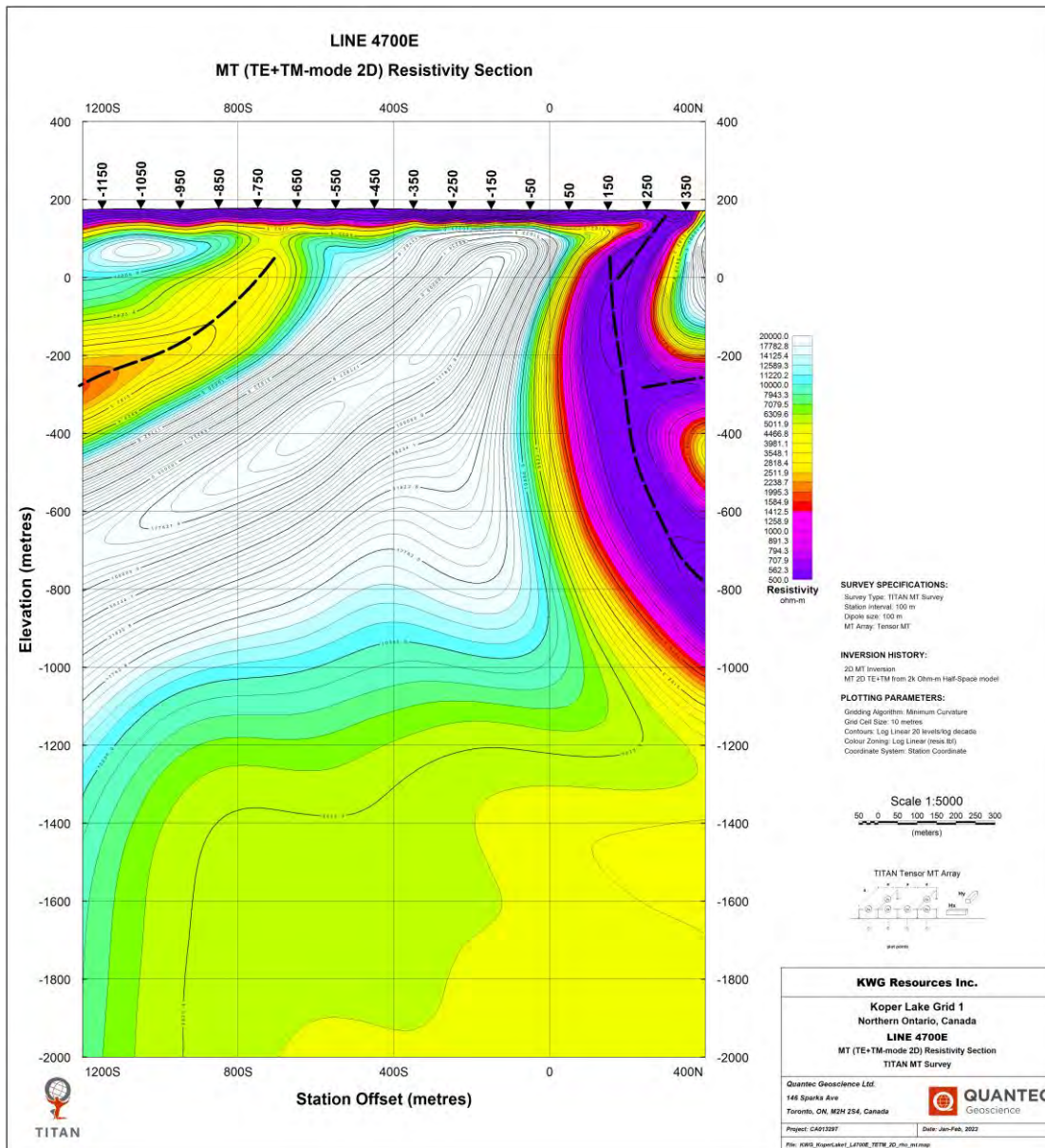


Figure 4-2: 2D MT resistivity section along L4700E.

4.1.2.L4800E

Figure 4-3 shows the 2D MT resistivity section along the Koper Lake line L4800E. On this line, the sub-vertical low resistivity zone is resolved below station 200. It is dipping NW to an approximate depth of 380 m, below which a medium resistivity zone appears to be extending from -200 m elevation down to about -800 m elevation. The entire anomaly zone is then continuing outside the NW end of the line.

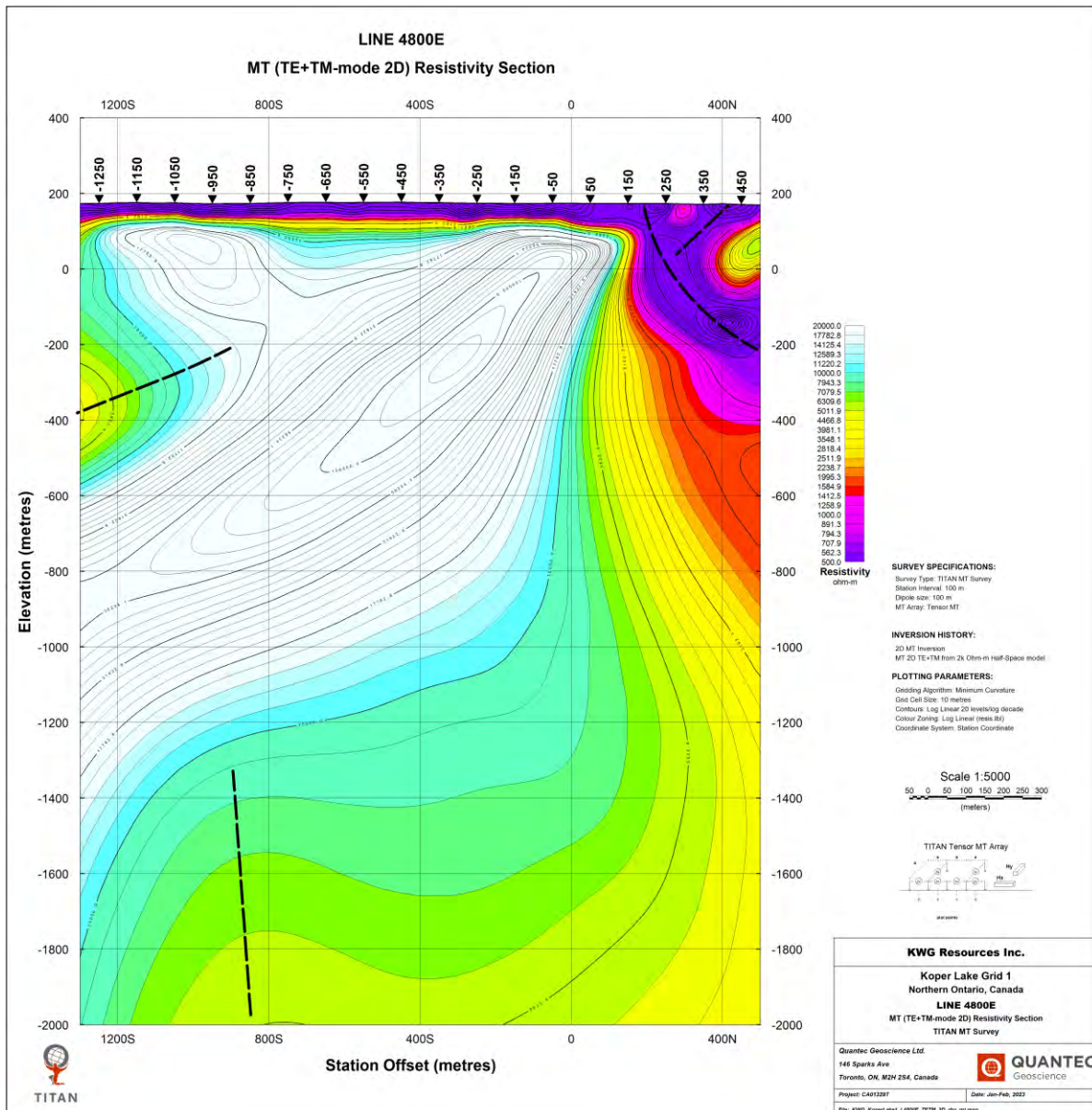


Figure 4-3: 2D MT resistivity section along L4800E.

4.1.3.L4900E

Figure 4-4 shows the 2D MT resistivity section along the Koper Lake line L4900E. Like the previous lines, this line also resolved the NW dipping sub-vertical zone with low resistivity responses, below station 200. The line also resolved another deep-seated medium resistivity zone, centered below station -1000 at -1400 m elevation (~1560 m depth).

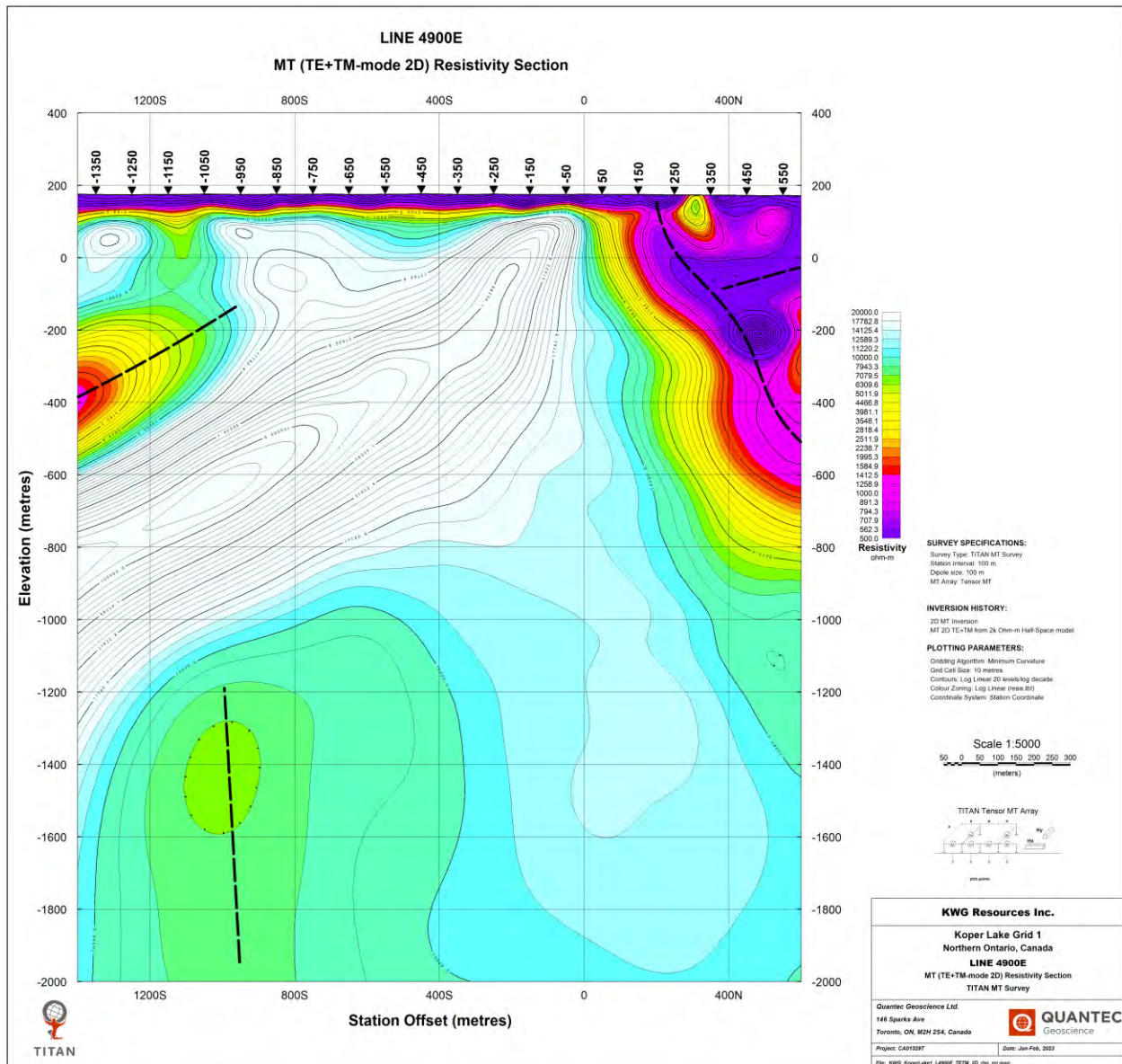


Figure 4-4: 2D MT resistivity section along L4900E.

4.1.4.L5000E

Figure 4-5 shows the 2D MT resistivity section along the Koper Lake line L5000E. The NW dipping low resistivity zone is resolved below station 200. A major discontinuity in the low resistivity structure is observed at about -300 m elevation (~500 m depth). In the southeast, a prominent medium resistivity zone is also resolved on this line, centered below station -800 at -1400 m elevation (~1560 m depth).

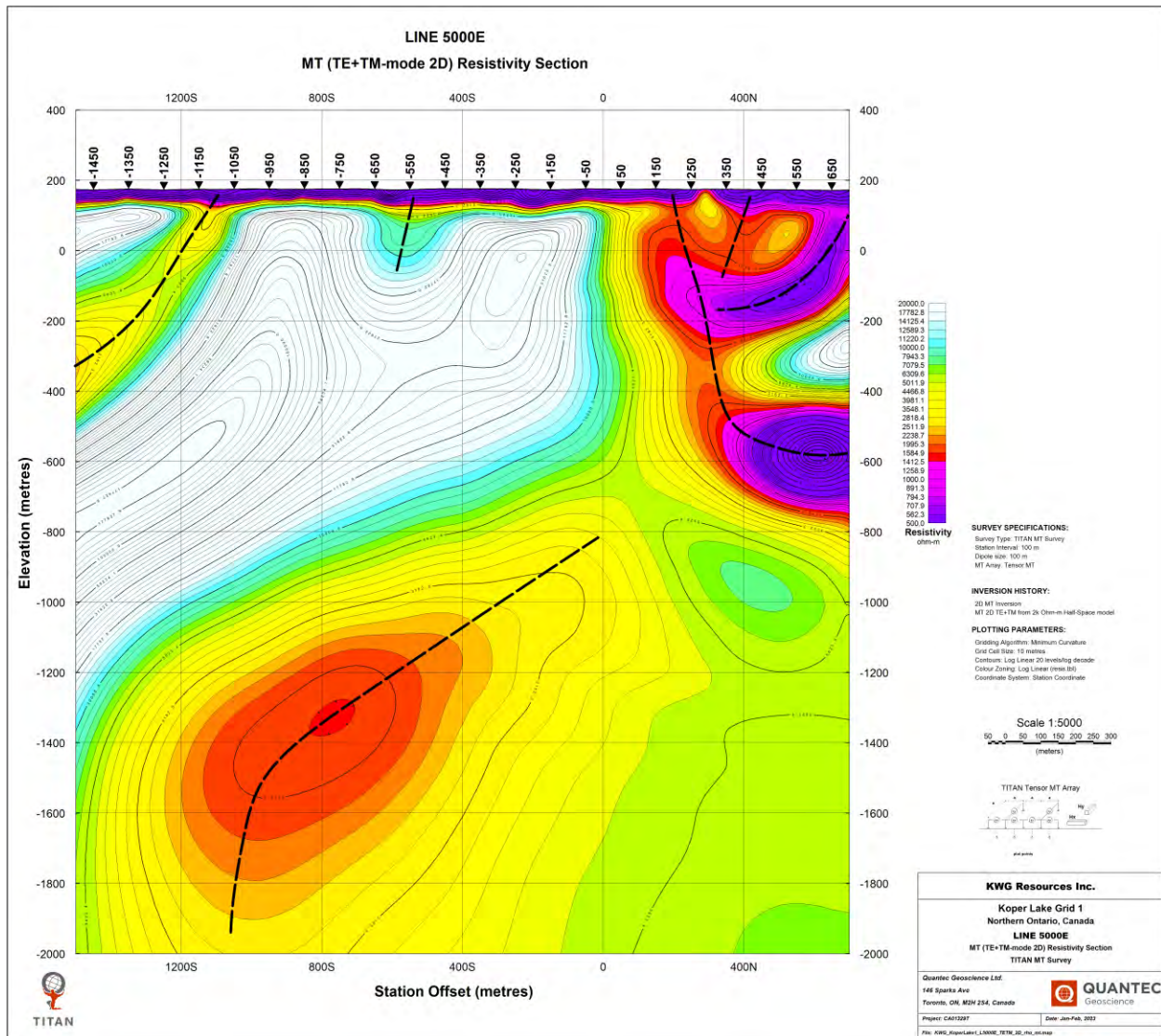


Figure 4-5: 2D MT resistivity section along L5000E.

4.1.5.L5100E

Figure 4-6 shows the 2D MT resistivity section along the Koper Lake line L5100E. The main low resistivity zone resolved on this line shows almost near vertical extension below station 200. At about -600 m elevation this zone dips NW and then runs near horizontal out of this line. At depth, a medium resistivity segment extending southeast from this main low resistivity zone is also observed. This medium resistivity zone extends deeper and is resolved somewhat like that on the previous line L5000E (marked with black dashed line extending to -2000 m elevation).

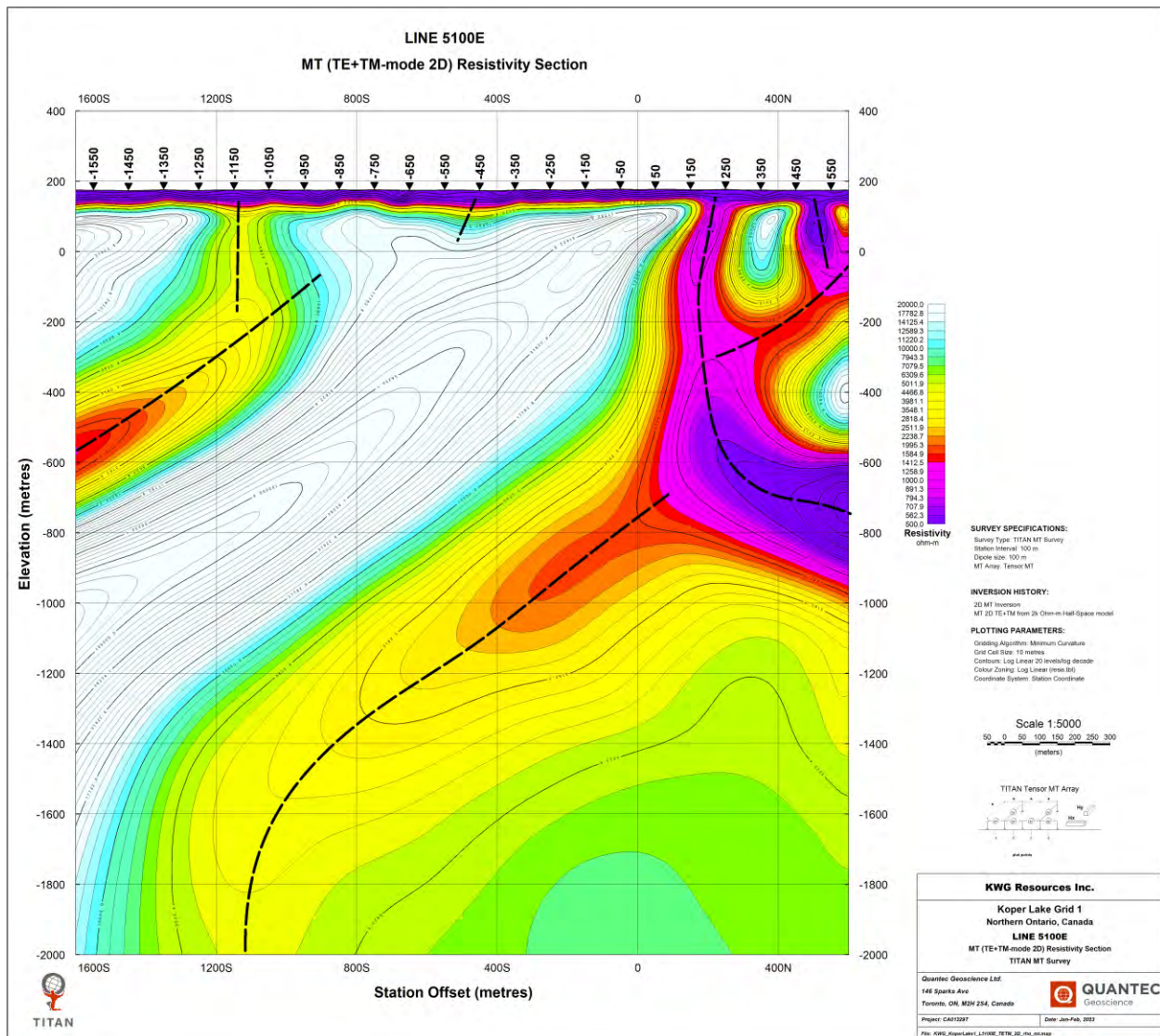


Figure 4-6: 2D MT resistivity section along L5100E.

4.1.6.L5250E

Figure 4-7 shows the 2D MT resistivity section along the Koper Lake line L5250E. Contrary to other lines discussed before, the NW dipping zone is resolved with relatively medium resistivity responses below station 150.

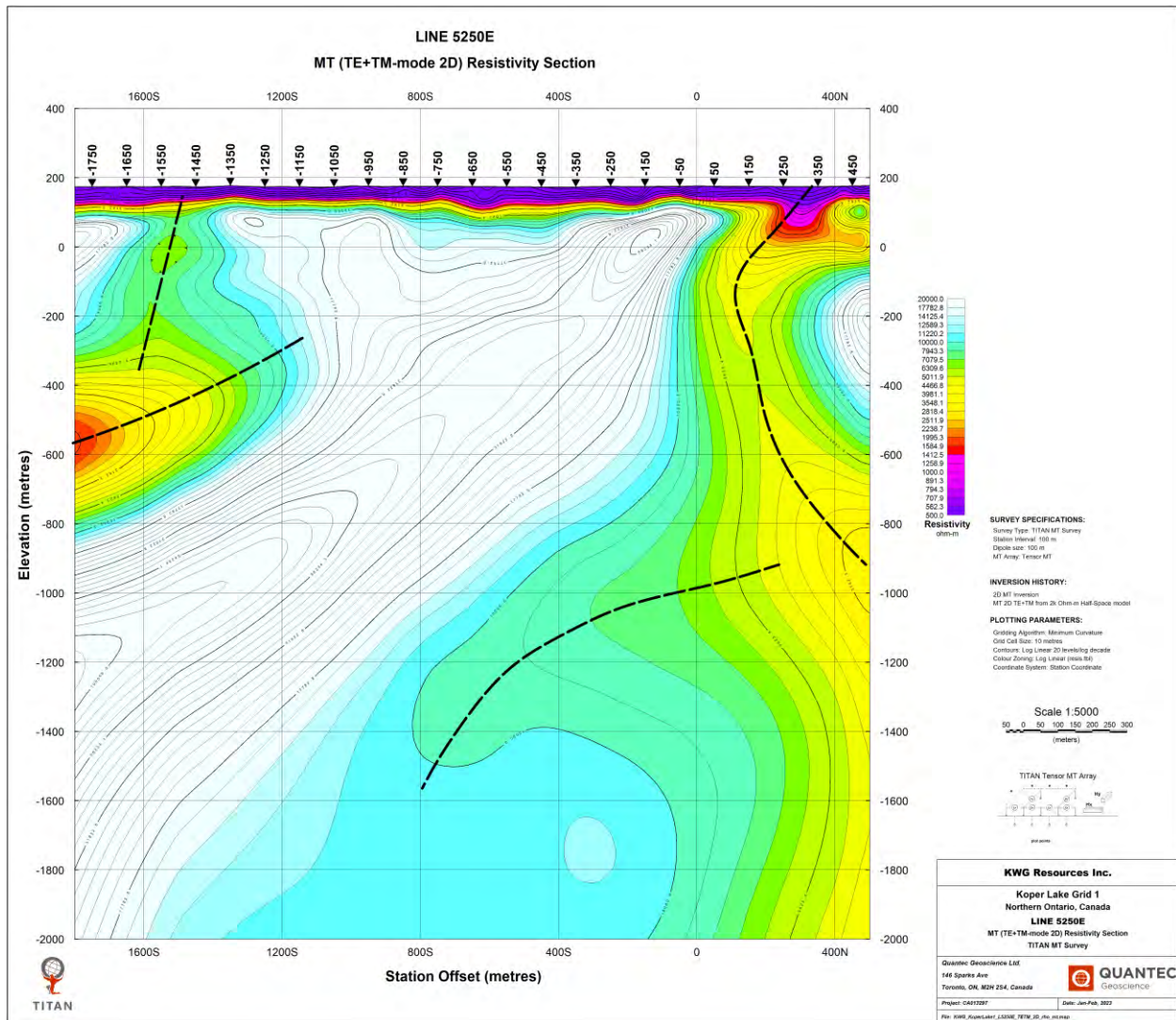


Figure 4-7: 2D MT resistivity section along L5250E.

4.1.7.L5350E

Figure 4-8 shows the 2D MT resistivity section along the Koper Lake line L5350E. The main anomaly resolved on this line is the steep NW dipping low resistivity zone, centered below station 50. This zone extends down to almost -800 m elevation. Other linear medium resistivity features are also resolved on this line as highlighted with dashed lines in the SE and center of the line.

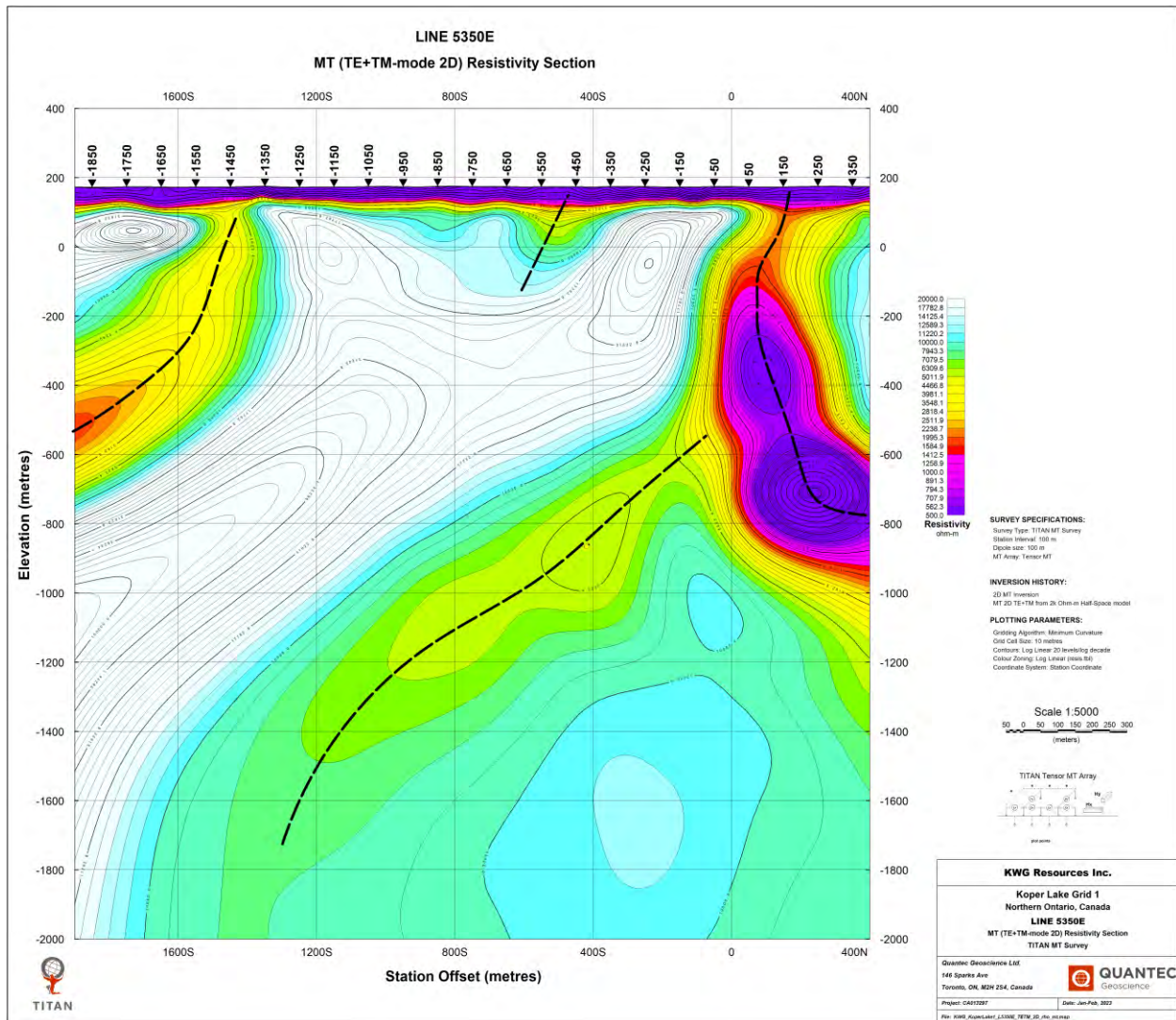


Figure 4-8: 2D MT resistivity section along L5350E.

4.1.8.L5450E

Figure 4-9 shows the 2D MT resistivity section along the Koper Lake line L5450E. The low resistivity sub-vertical anomaly zone is resolved below station 100. This zone extends to -800 m elevation and then shows a wide lateral extension.

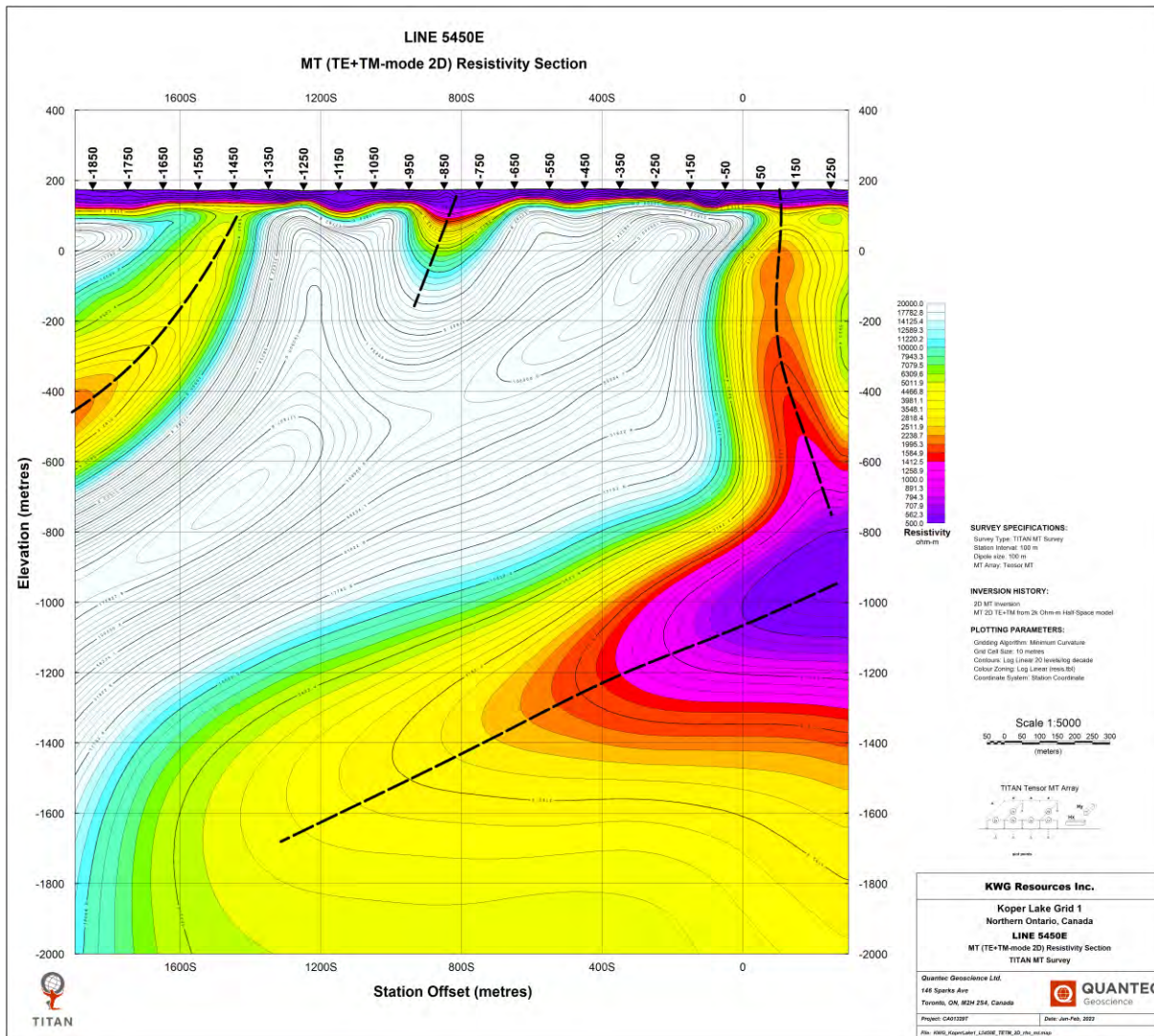


Figure 4-9: 2D MT resistivity section along L5450E.

4.1.9.L1E

Figure 4-10 shows the 2D MT resistivity section along the Koper Lake line L1E. The 2D MT inversion resolved multiple low resistivity sub-vertical structures along this line. The prominent ones are resolved below stations 0, 1550, 1950 and 2900. The one below station 1550 appears to be inline with a known NW dipping shear zone. The main target zone is expected to be underlying this shear zone, possibly showing low to medium resistivity responses.

The low resistivity zone below station 1950 is also significant and it shows some medium resistivity extensions to its NW, right from surface to -200 m elevation (i.e., ~370 m depth below surface), between stations 1950 and 2350.

4.1.10. L1aE

Figure 4-11 shows the 2D MT resistivity section along the Koper Lake line L1aE. This line is located 475 m SW of line L1E. The MT resistivity responses resolved on this line are not as intense as seen on L1E. However, the main sub-vertical anomaly zone is resolved with medium resistivity responses below station 2700, which is inline with the main anomaly zone identified on L1E.

Other sub-vertical zones identified on L1aE are located below stations 1150, 2250, 3500 and 4600. The one extending below station 4600 shows a prominent low resistivity response, centered at -800 m elevation. Other ones below 1200, 2250 and 3500 show relatively medium to high resistivity responses.

4.1.11. L2E

Figure 4-12 shows the 2D MT resistivity section along the Koper Lake line L2E. This line is located 475 m SW of L1aE. The main sub-vertical low resistivity anomaly is resolved below station 2400 on this line. This is inline with the known shear zone in the region. This zone shows a clear NW dip and runs almost horizontal after about 800 m distance (i.e., NW of the station 3200). A broad medium resistivity zone is resolved below this main low resistivity anomaly at an approximate depth of 1380 m, centered below station 3700. This zone is extending to further depth.

4.1.12. L3E

Figure 4-13 shows the 2D MT resistivity section along the Koper Lake line L3E. This line is located approximately 600 m SW of L2E. The NW dipping low resistivity anomaly is resolved below station 2500 and extends deeper than 1200 m. At depth, this anomaly shows a major low resistivity zone, centered below station 4300 at an approximate depth of 1150 m below surface (at -1000 m elevation). This zone shows some vertical medium resistivity extensions to the surface, as observed below stations 4100 and 4700. Another prominent low resistivity sub-vertical feature resolved on this line is below station 2150.

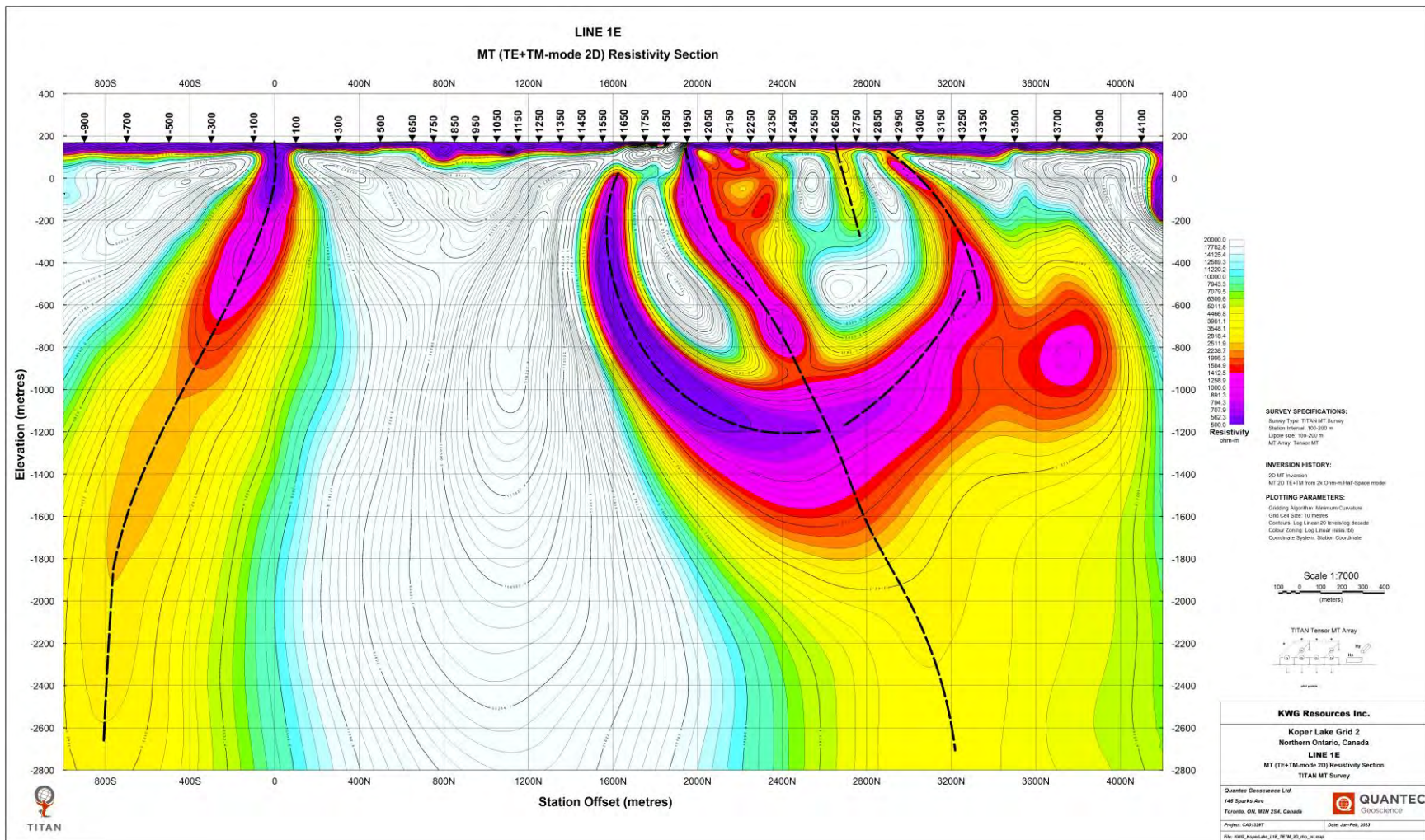


Figure 4-10: 2D MT resistivity section along L1E.

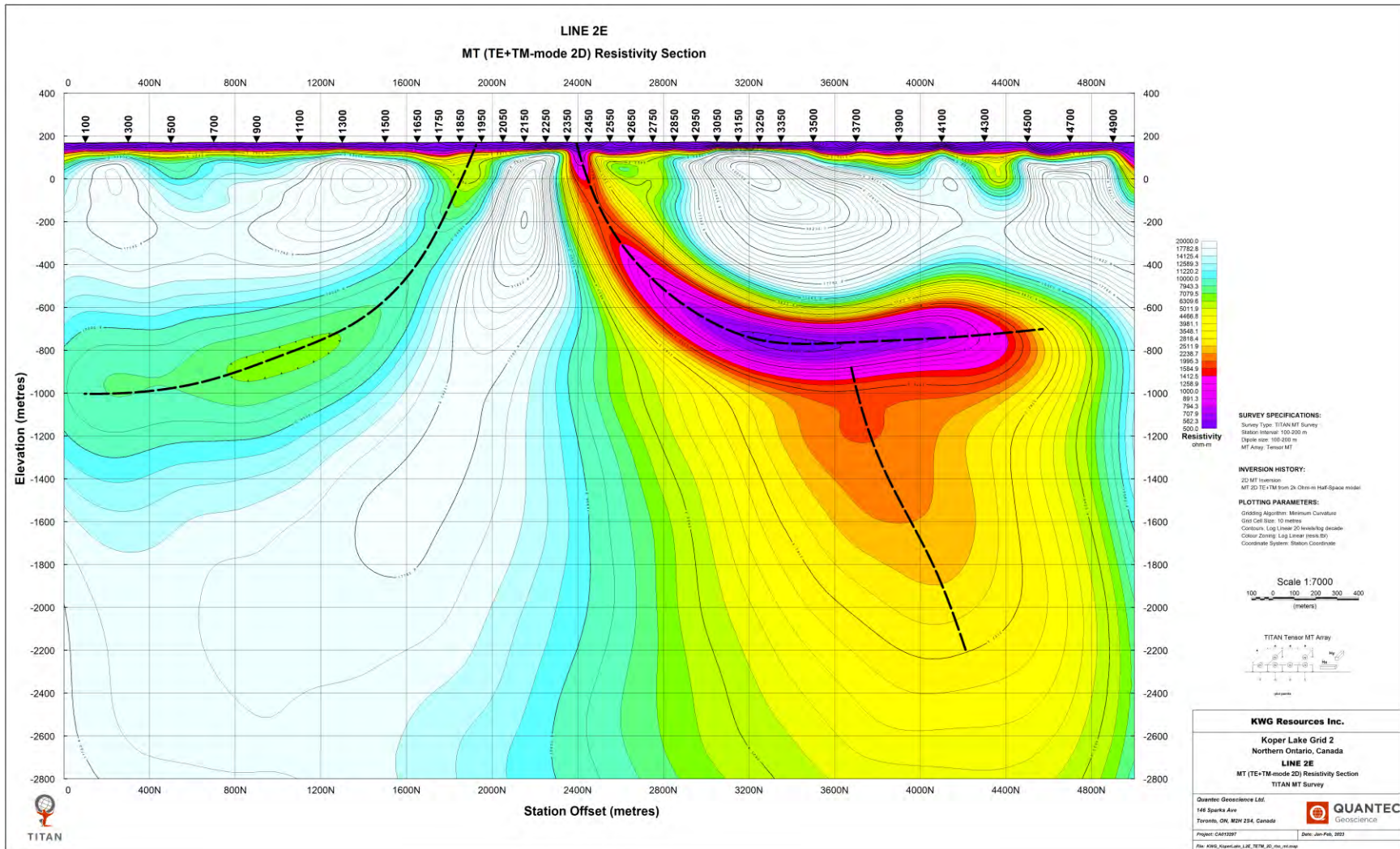


Figure 4-12: 2D MT resistivity section along L2E.

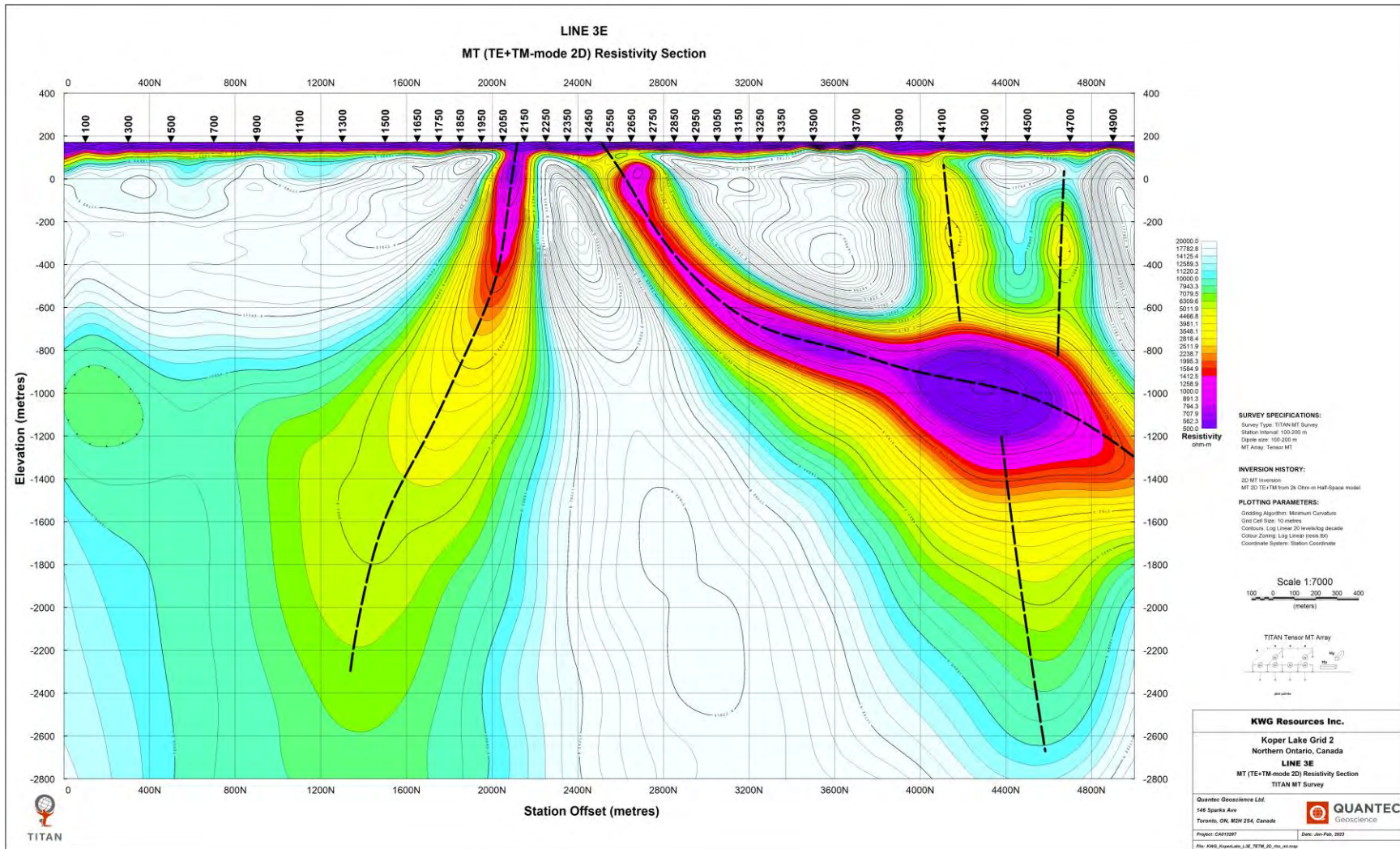


Figure 4-13: 2D MT resistivity section along L3E.

4.1.13. L4E

Figure 4-14 shows the 2D MT resistivity section along the Koper Lake line L4E. This is a NS oriented Titan MT line acquired over the Koper Lake Project. The line mainly resolved a low resistivity anomaly zone, centered below station 2250 at an approximate depth of 675 m (-500 m elevation). This anomaly also shows a medium resistivity sub-vertical extension to the surface (below station 1950).

The main low resistivity zone resolved on L4E coincides with the NW dipping low resistivity zone resolved on line L3E, which is inline with the known shear zone over the grid.

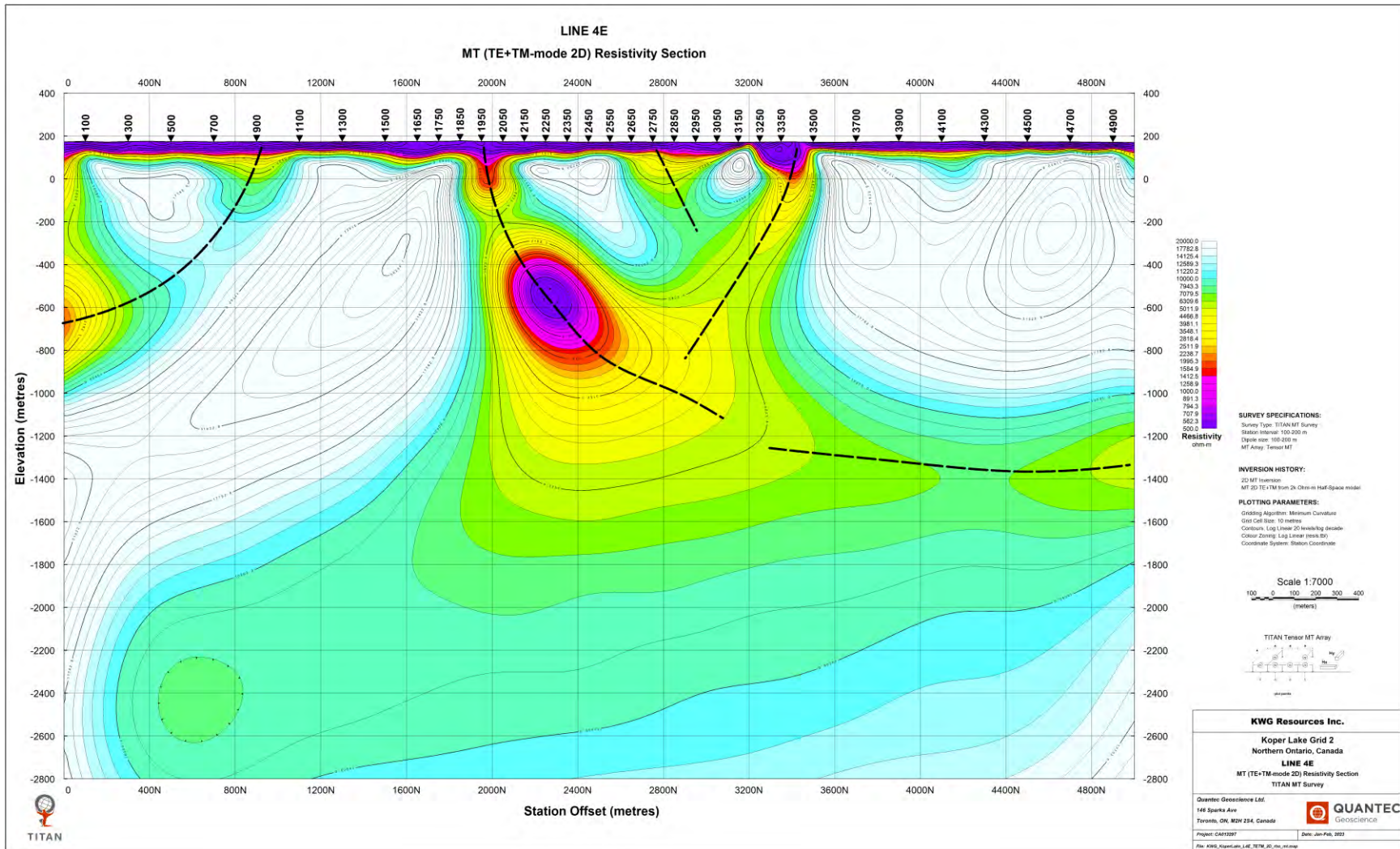


Figure 4-14: 2D MT resistivity section along L4E.

4.1.14. Resistivity Plan Maps (Depth levels)

MT resistivity plan maps for Grid-1 and Grid-2 are presented in the following section. Figure 4-15 shows the resolved resistivity over the Koper Lake Grid-1 at the surface. The overburden masking the bed rock in the region is well resolved with low resistivities below 500 Ω-m. The resistivity colour range (500-20,000 Ω-m) used for all other maps cannot show any variations at surface. Therefore, this plan map is also plotted using a different colour range of 10-500 Ω-m as shown in Figure 4-16. This map clearly shows some of the resistivity variations at the surface. Multiple NE trending low resistivity zones are identified, as highlighted with dashed black lines (Figure 4-16). These low resistivity trends show some correlation to the trends identified in the magnetic data over the region.

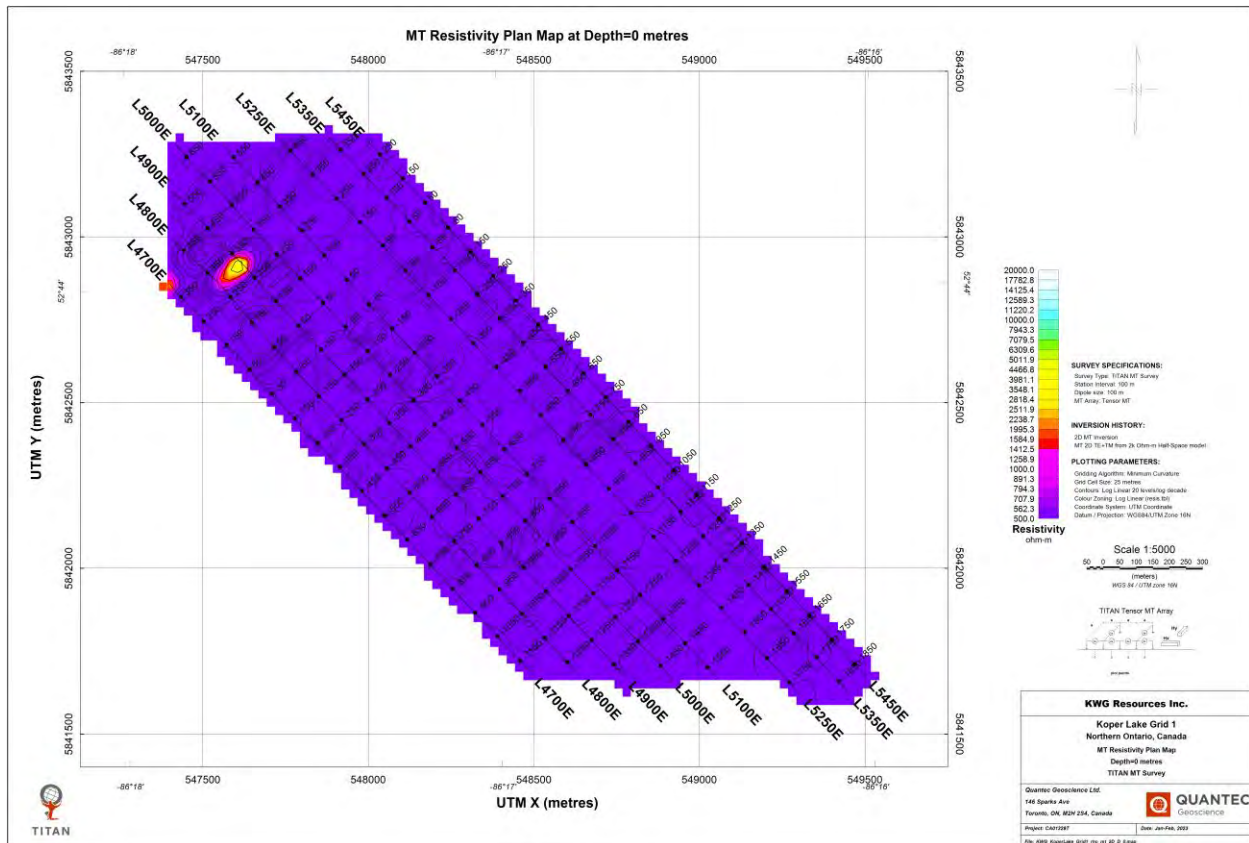


Figure 4-15: MT resistivity plan map over Koper Lake Grid-1 at the surface; the resistivity is well below 500 Ω-m over the entire survey area.

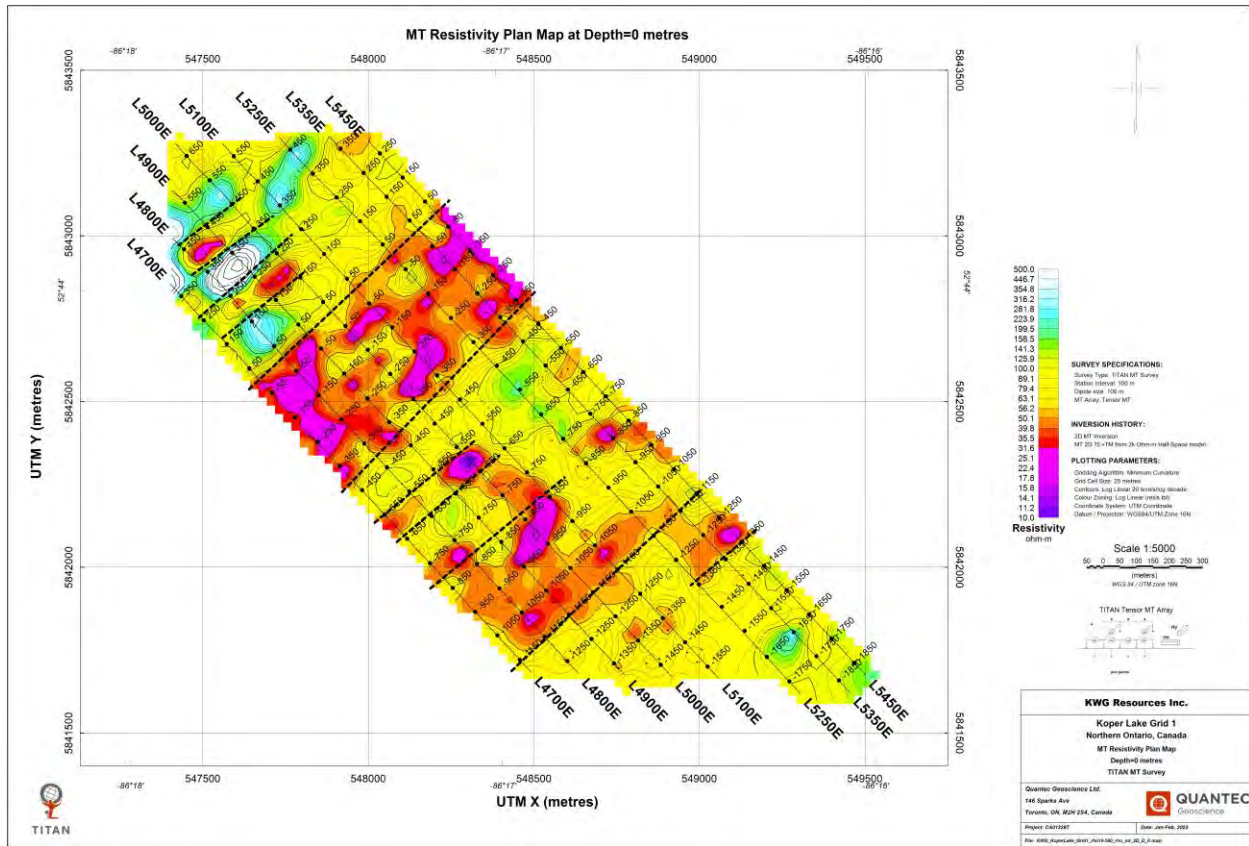


Figure 4-16: MT resistivity plan map over Koper Lake Grid-1 at the surface; shown using 10-500 Ω -m colour range.

The surficial low resistivity layer seems to be showing very low resistivities ($< 100 \Omega$ -m) up to an approximate depth of 25 m and then slightly increases with depth. This overburden layer is nearly 50 m thick and is underlain by high resistivity bedrock.

Figure 4-17 shows the resistivity plan map at 50 m depth. Multiple low resistivity zones are resolved at this depth. The prominent one is in the northwest side of the grid. There are also other low resistivity anomaly zones resolved as highlighted on the plan map. In the northwest, a linear low resistivity trend is marked with black dashed line. This is inline with the sub-vertical anomaly zone identified on the resistivity section maps.

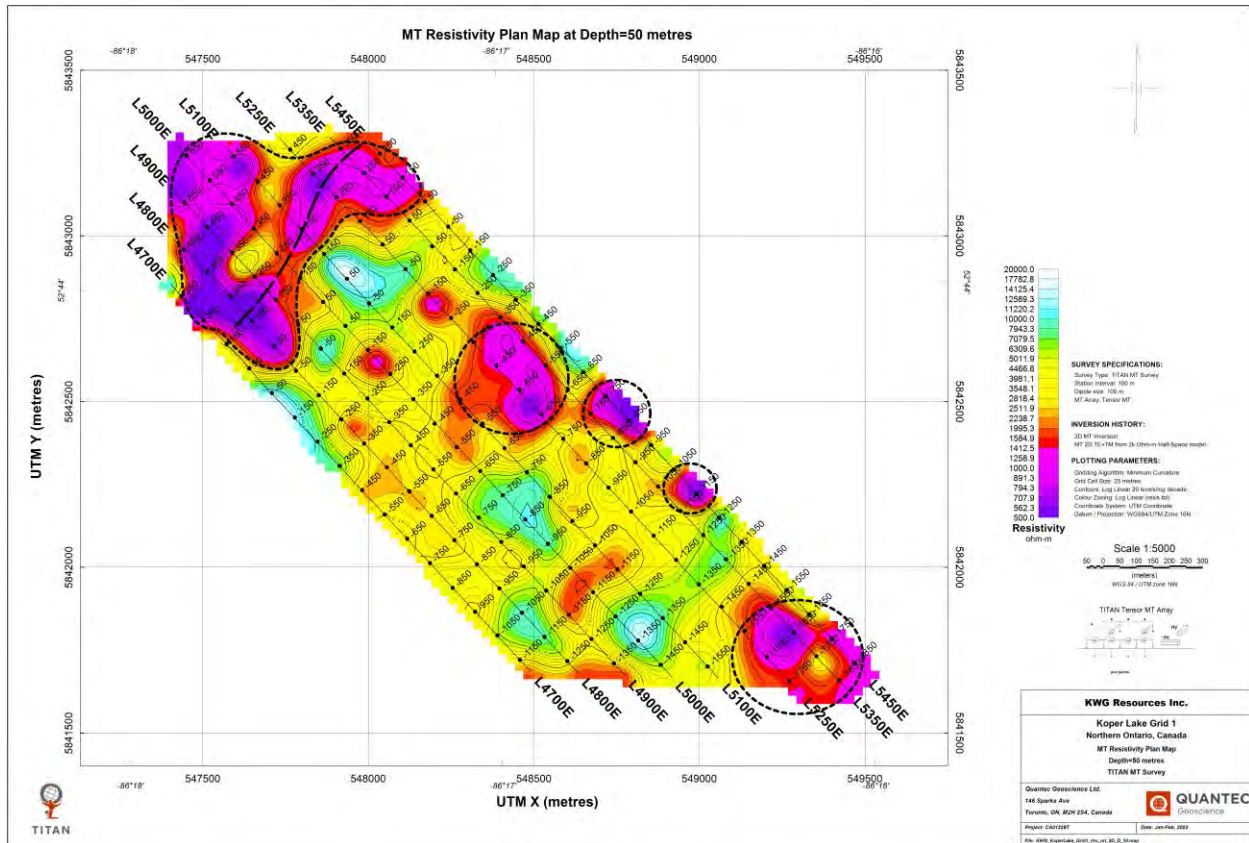


Figure 4-17: MT resistivity plan map over Koper Lake Grid-1 at 50 m depth.

At 100 m depth, all lines over the Grid-1 mainly resolved the low resistivity zone in the northwest (Figure 4-18). The NE trending low resistivity linear feature is well resolved at this depth (black dashed line). This is possibly representing the shear zone in the region, which is dipping NW. At increased depth, this dips outside the current survey limits. Resistivity plan maps at 300 m, 500 m and 800 m depth levels are shown in Figure 4-19, Figure 4-20 and Figure 4-21, respectively.

A complete set of plan maps from surface to 2000 m depth are provided in the APPENDIX C.

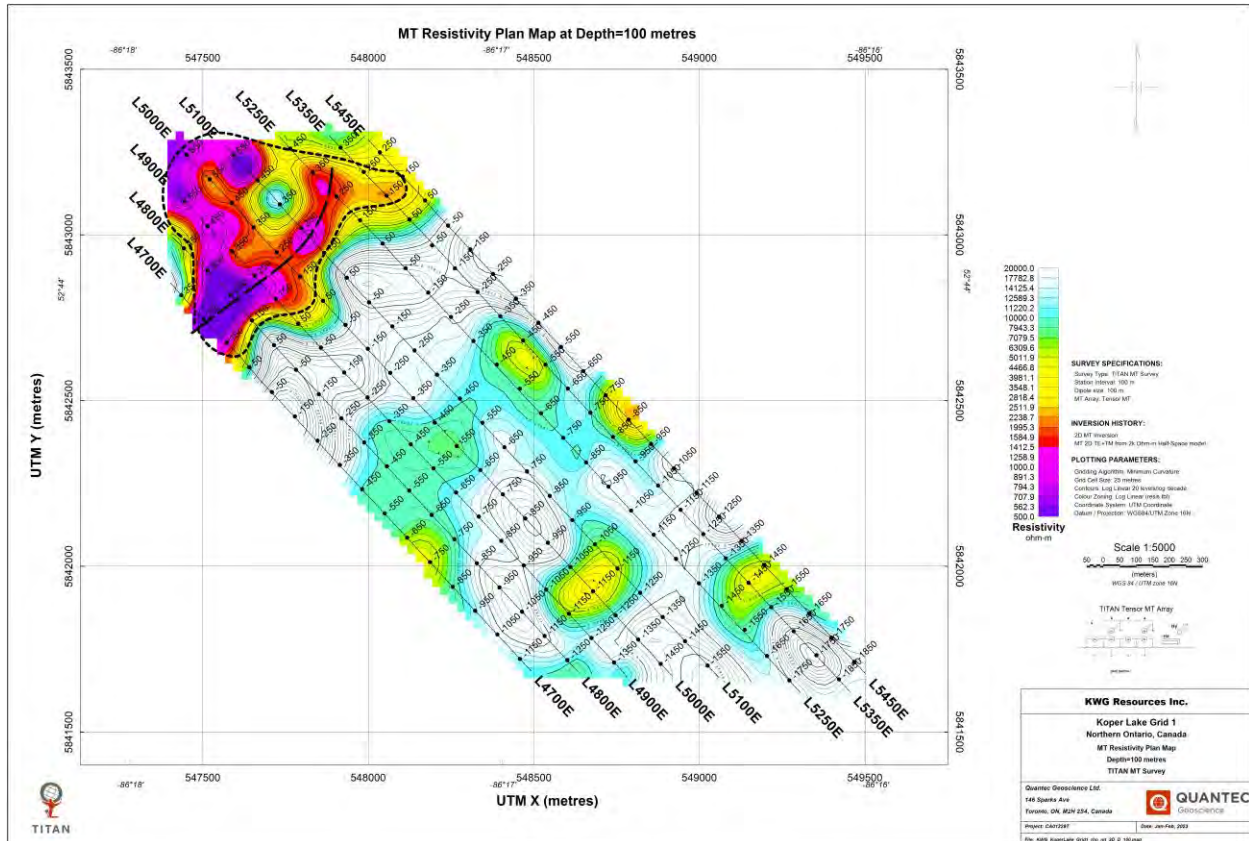


Figure 4-18: MT resistivity plan map over Koper Lake Grid-1 at 100 m depth.

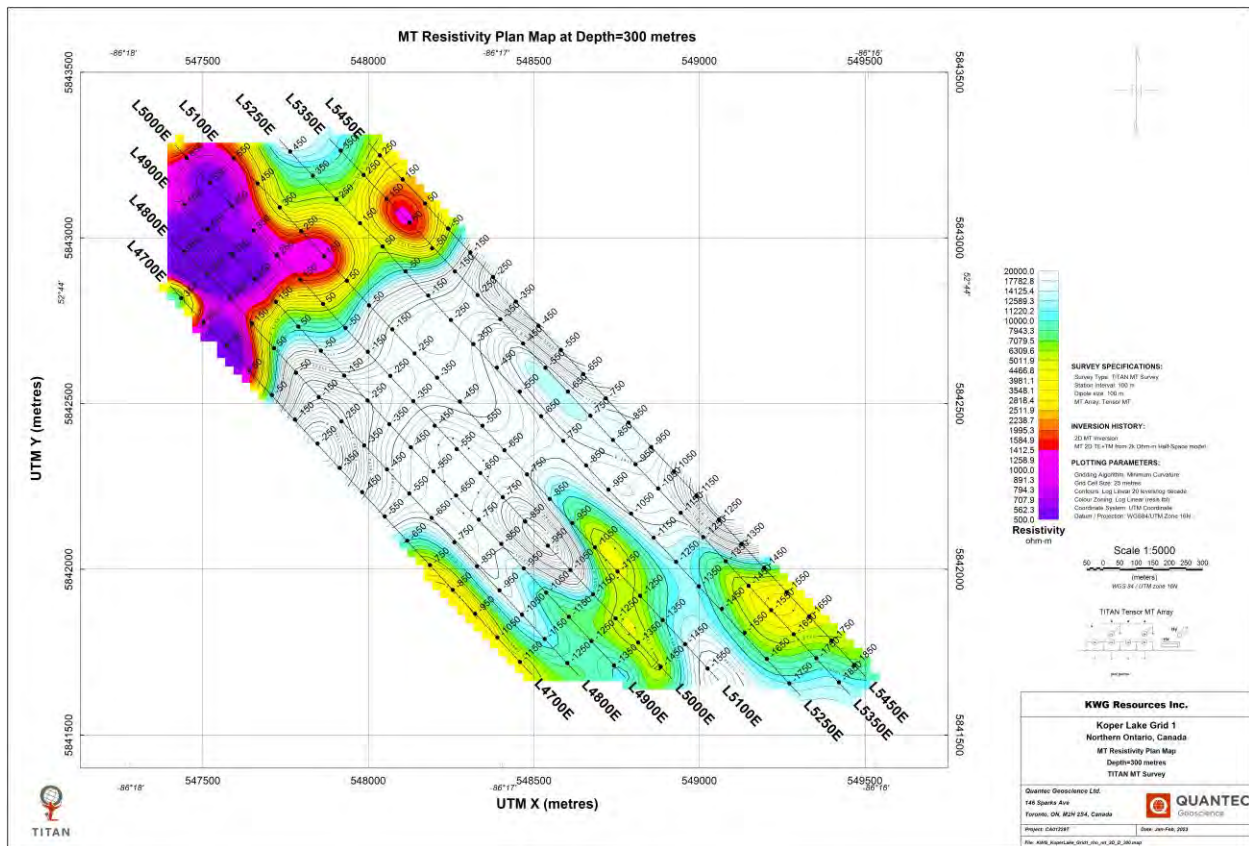


Figure 4-19: MT resistivity plan map over Koper Lake Grid-1 at 300 m depth.

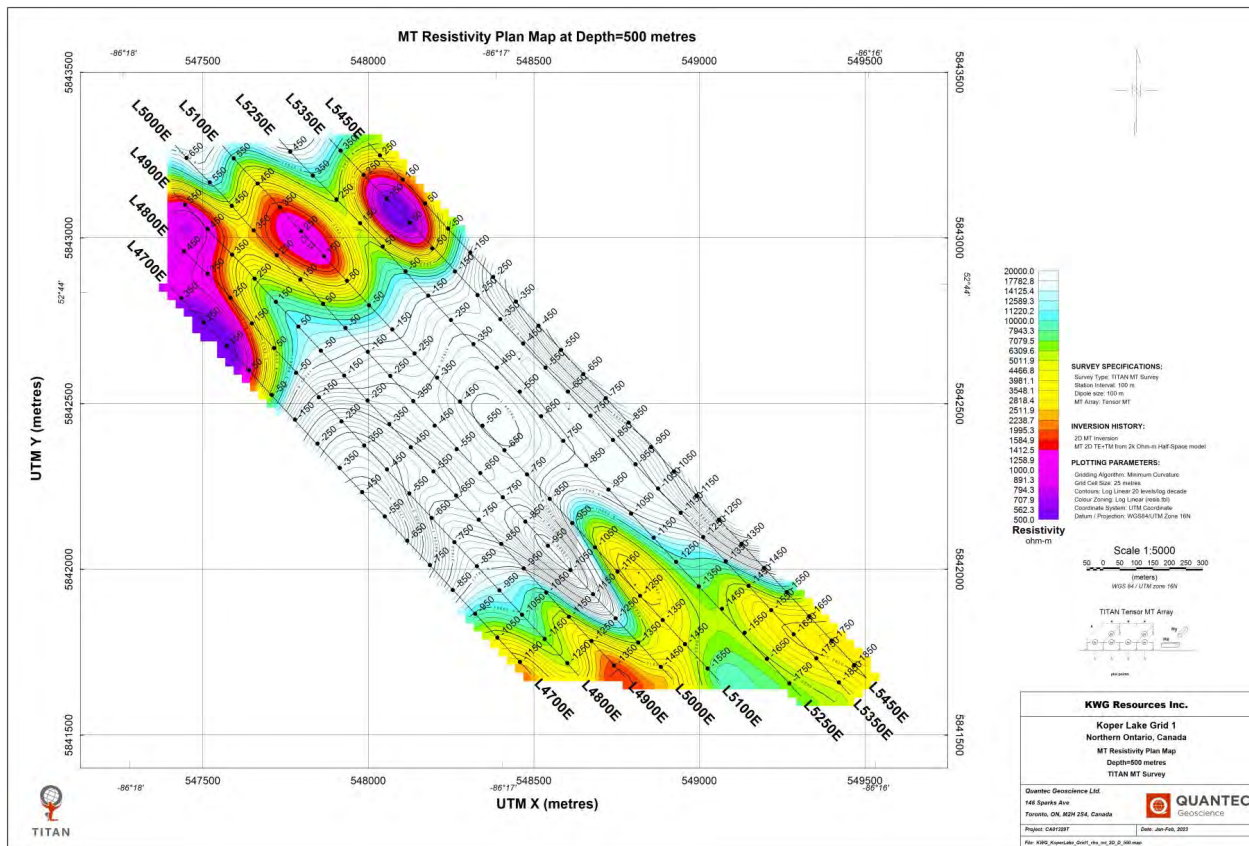


Figure 4-20: MT resistivity plan map over Koper Lake Grid-1 at 500 m depth.

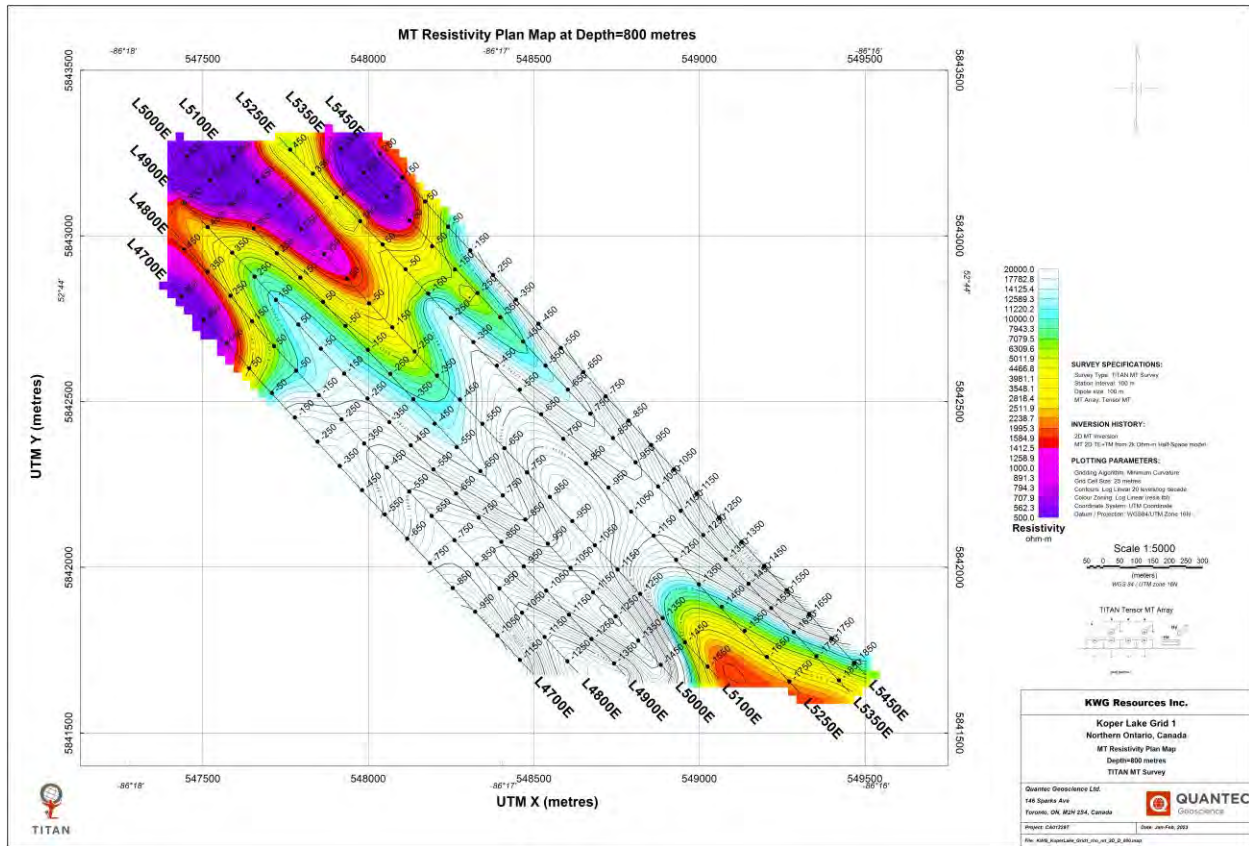


Figure 4-21: MT resistivity plan map over Koper Lake Grid-1 at 800 m depth.

Like the Koper Lake Grid-1, the resistivity plan maps over Grid-2 at different depth levels also show the near-surface low resistivity layer and other sub-vertical features underneath the overburden. Figure 4-22 and Figure 4-23 show the resistivity distribution at the near surface (0 m depth) plotted at two different colour ranges. In general, this surficial layer is resolved with resistivities below 200 Ω -m for the most part.

Note that the data from station 2250 to 3700 from the NS oriented line L4E are not used in the gridding of these plan maps, to avoid discrepancies at the intersection of the NW oriented lines L3E and L2E.

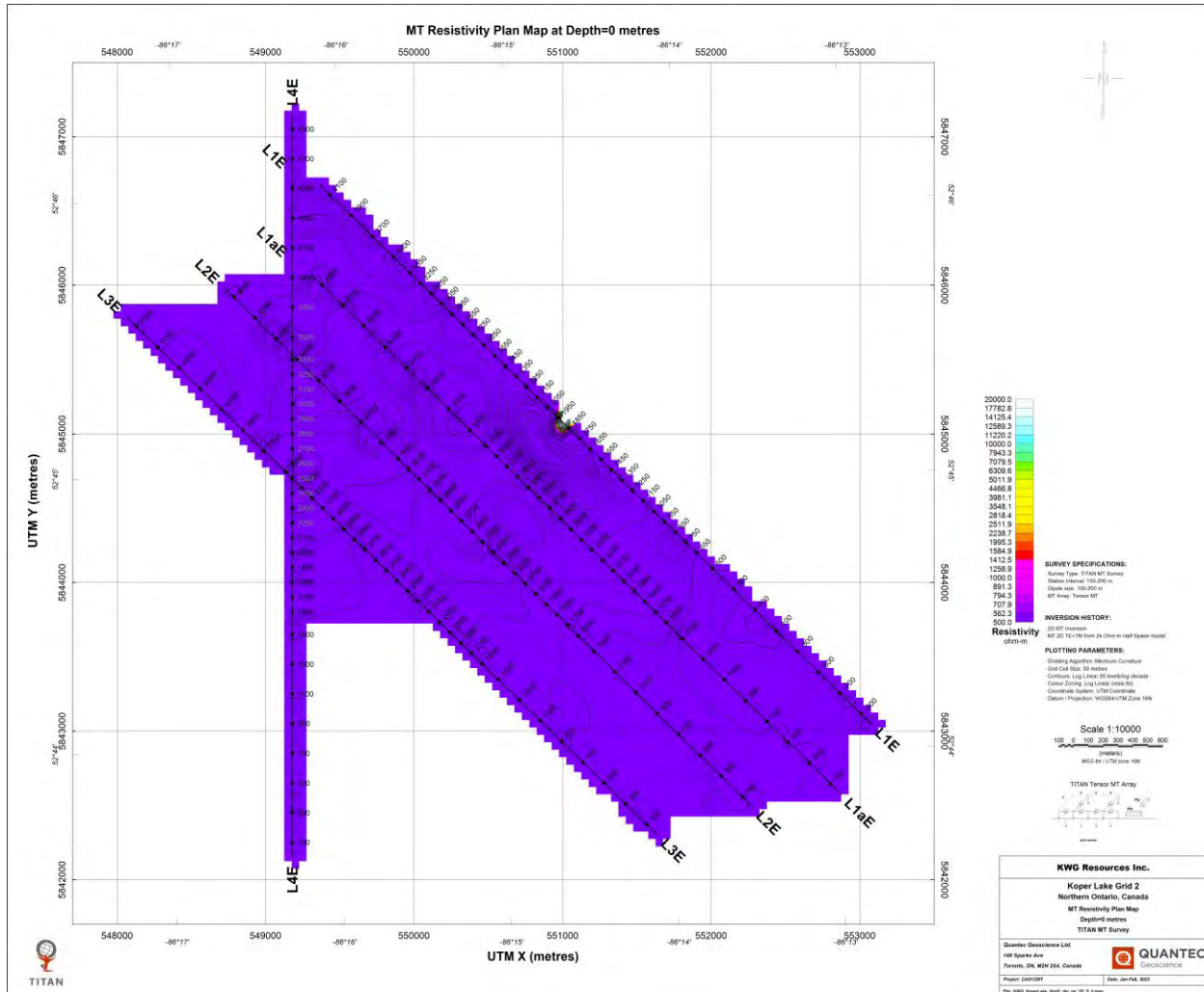


Figure 4-22: MT resistivity plan map over Koper Lake Grid-2 at the surface; the resistivity is well below 500 Ω -m over the entire survey area.

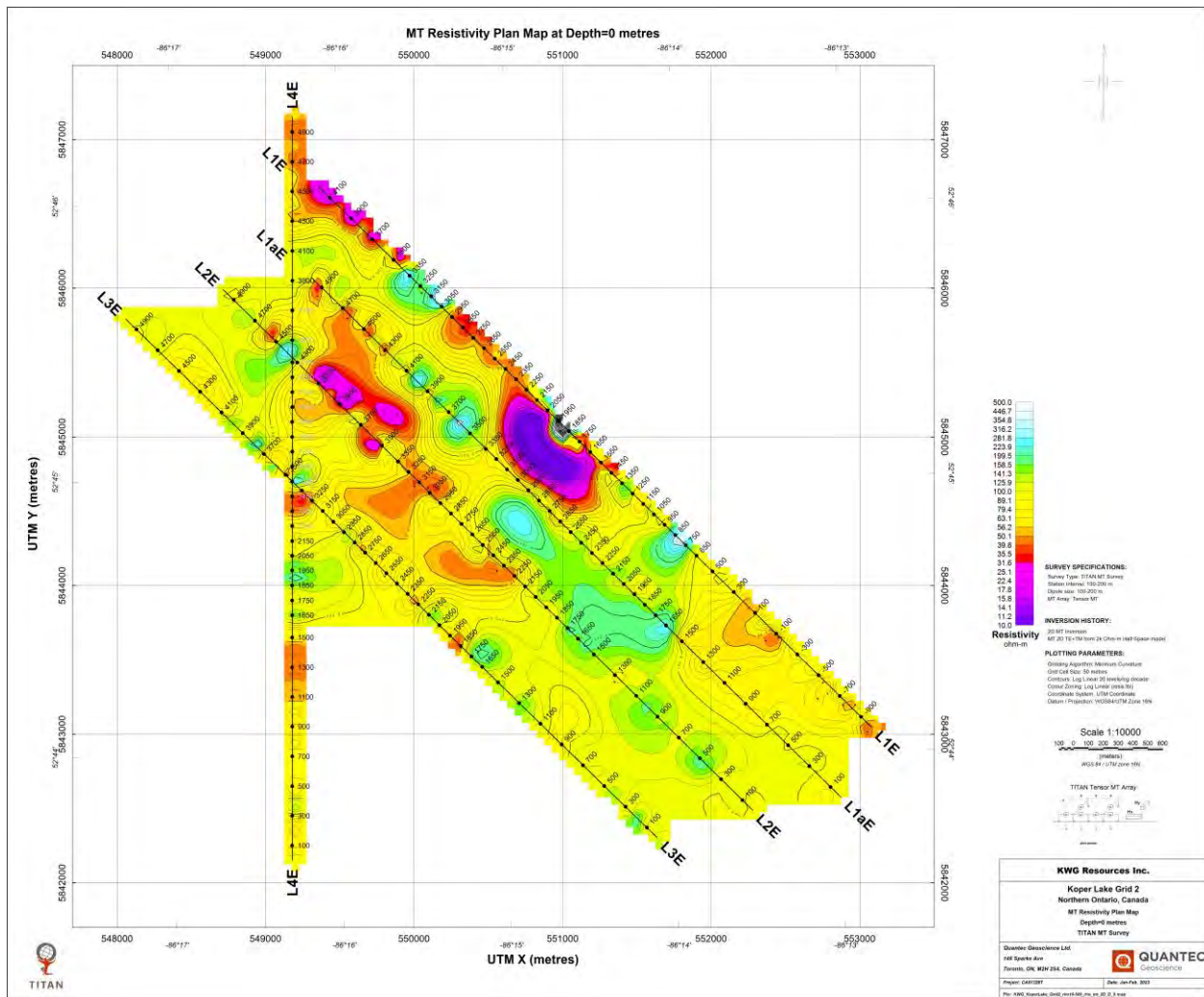


Figure 4-23: MT resistivity plan map over Koper Lake Grid-2 at the surface; shown using 10-500 Ω-m colour range.

Figure 4-24 shows the resistivity plan map at 50 m depth over Grid-2. Multiple low resistivity zones are resolved at this depth, immediately below the overburden layer. Linear northeast trending low resistivity zones are also evident (highlighted with black dashed lines).

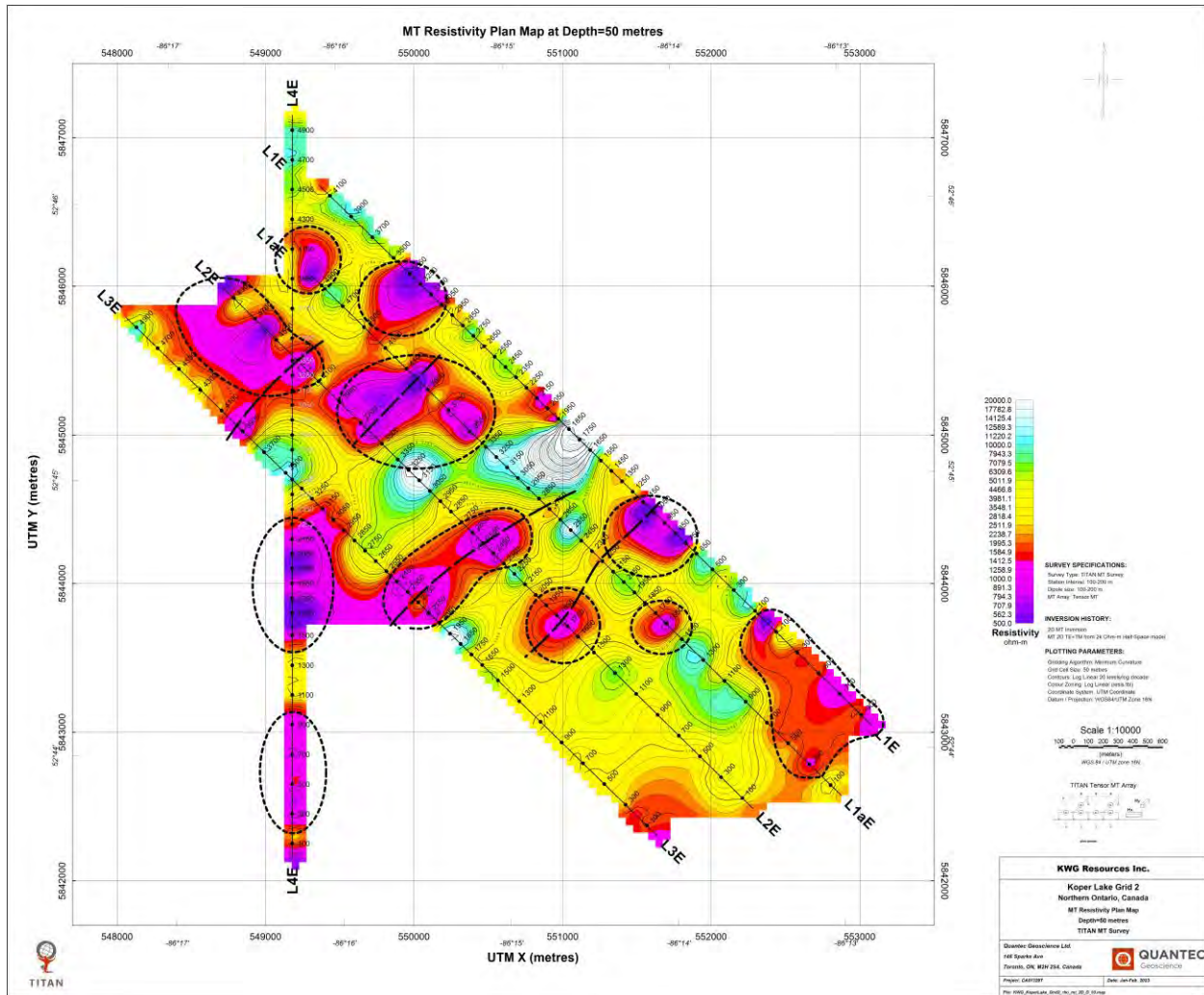


Figure 4-24: MT resistivity plan map over Koper Lake Grid-2 at 50 m depth.

At 100 m depth, the plan map shows mostly high resistivity features with some linear zones of medium to low resistivity responses. One of the main linear features identified at this depth cut across the lines L3E, L2E and L1aE at their center. This is believed to be inline with the known NW dipping shear zone in the region.

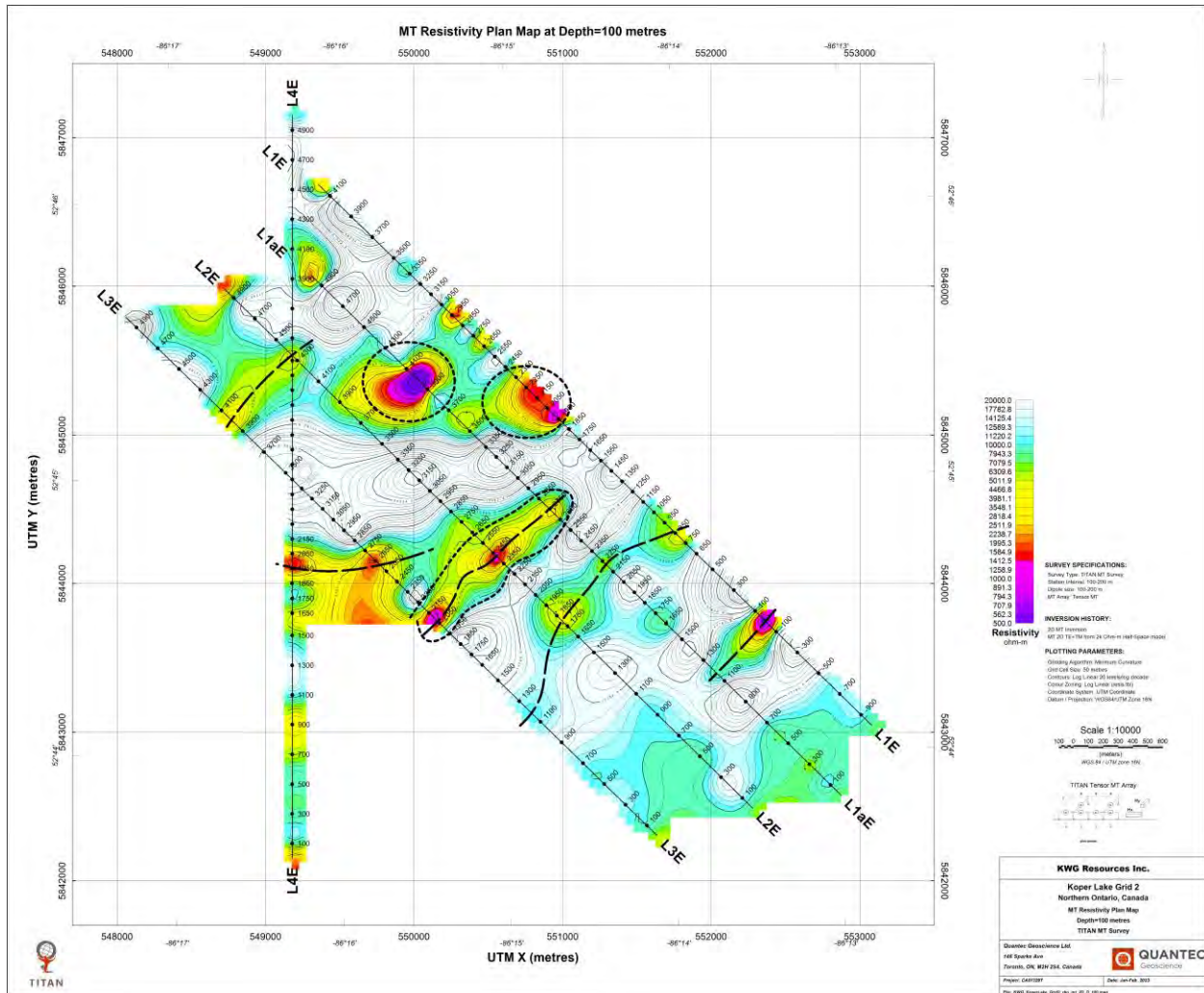


Figure 4-25: MT resistivity plan map over Koper Lake Grid-2 at 100 m depth.

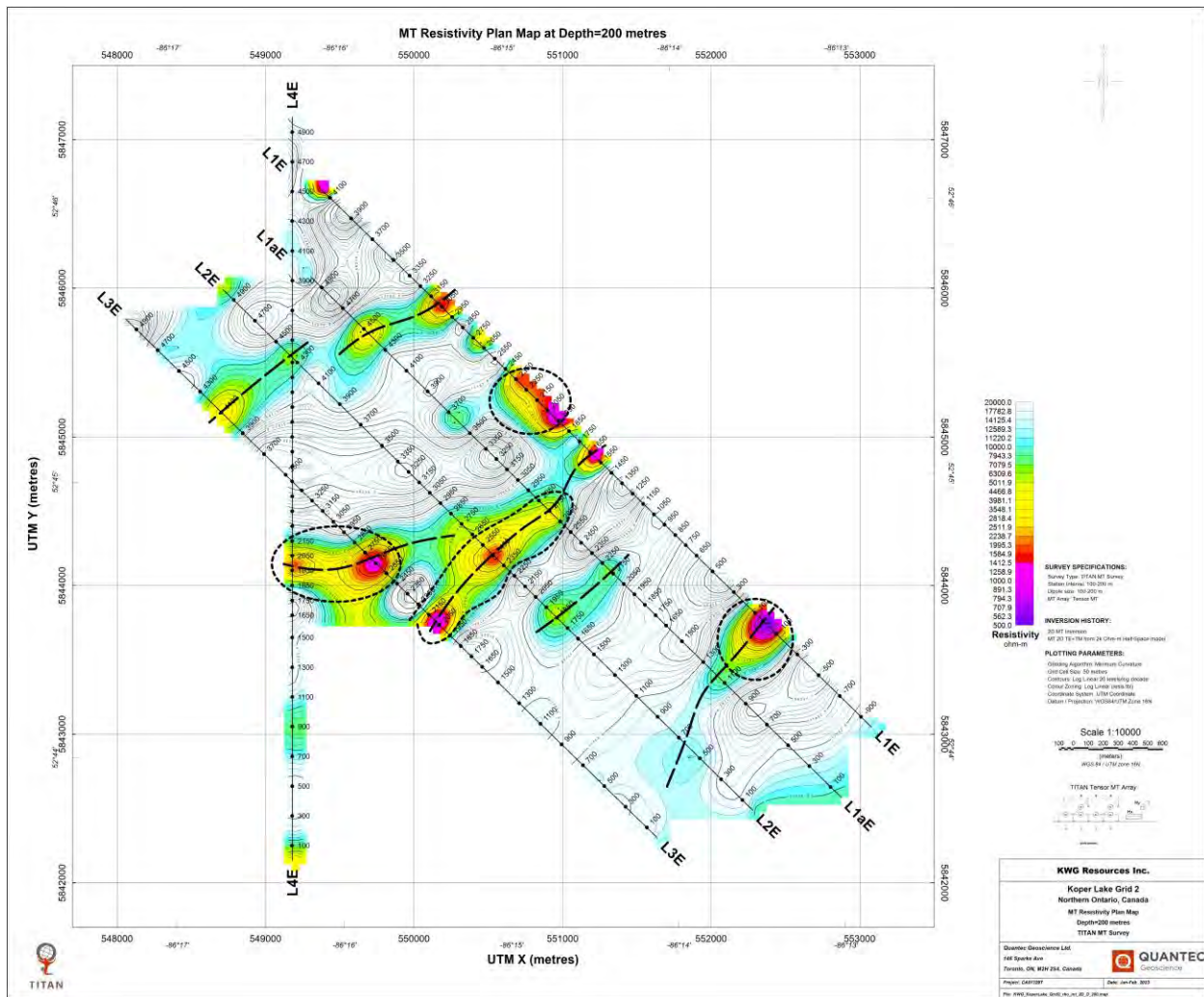


Figure 4-26: MT resistivity plan map over Koper Lake Grid-2 at 200 m depth.

Resistivity plan map at 200 m and 300 m depths are shown in Figure 4-26 and Figure 4-27, respectively. Many NE trending linear resistivity zones are identified at this depth. The resistivities of these zones generally vary from low to medium.

At further depth, these linear zones show more intense low resistivities. Plan maps at 500m and 800 m depths are shown in Figure 4-28 and Figure 4-29, respectively. At 800 m depth, an interesting circular low resistivity zone is resolved in the northeastern half of the grid.

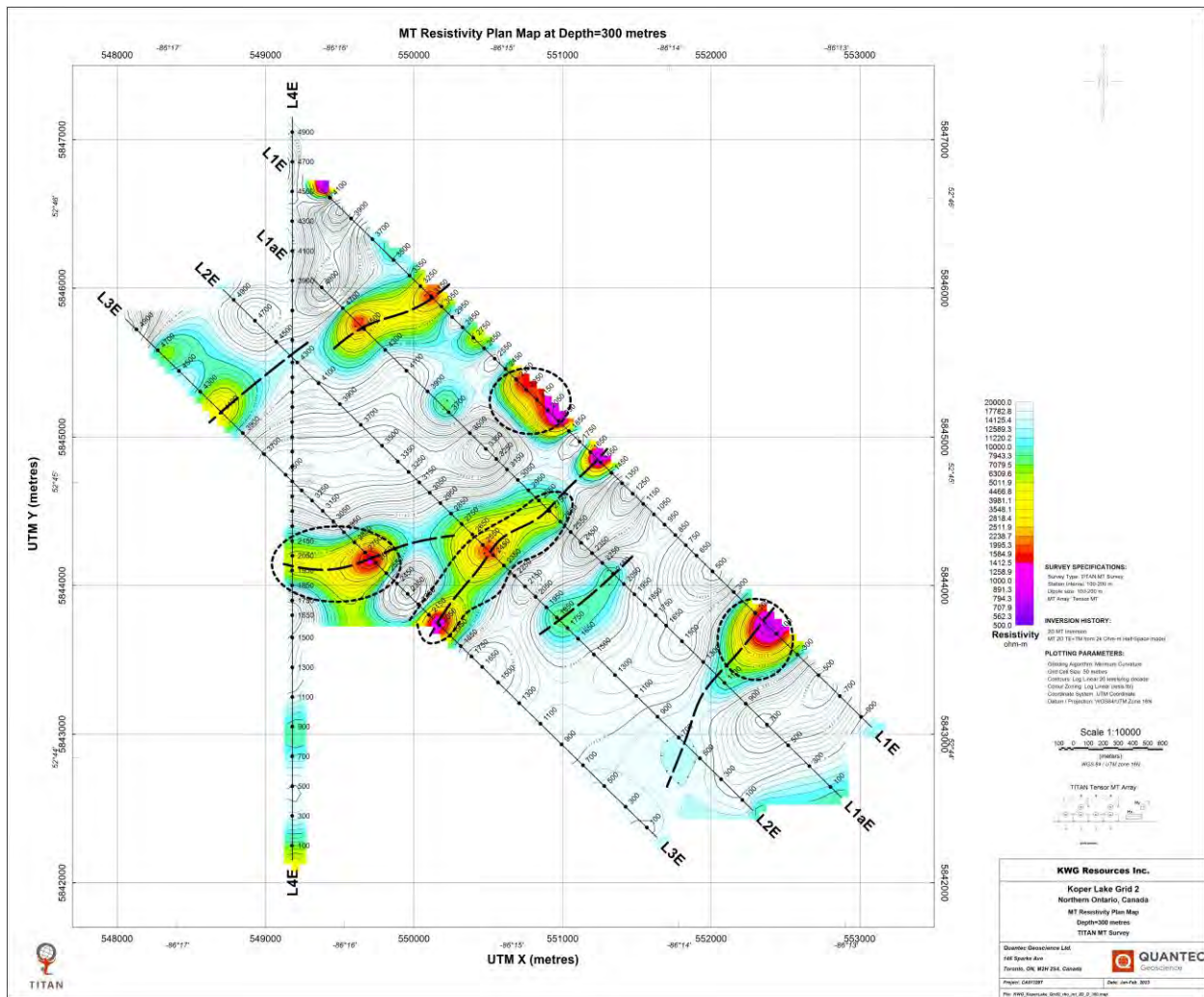


Figure 4-27: MT resistivity plan map over Koper Lake Grid-2 at 300 m depth.

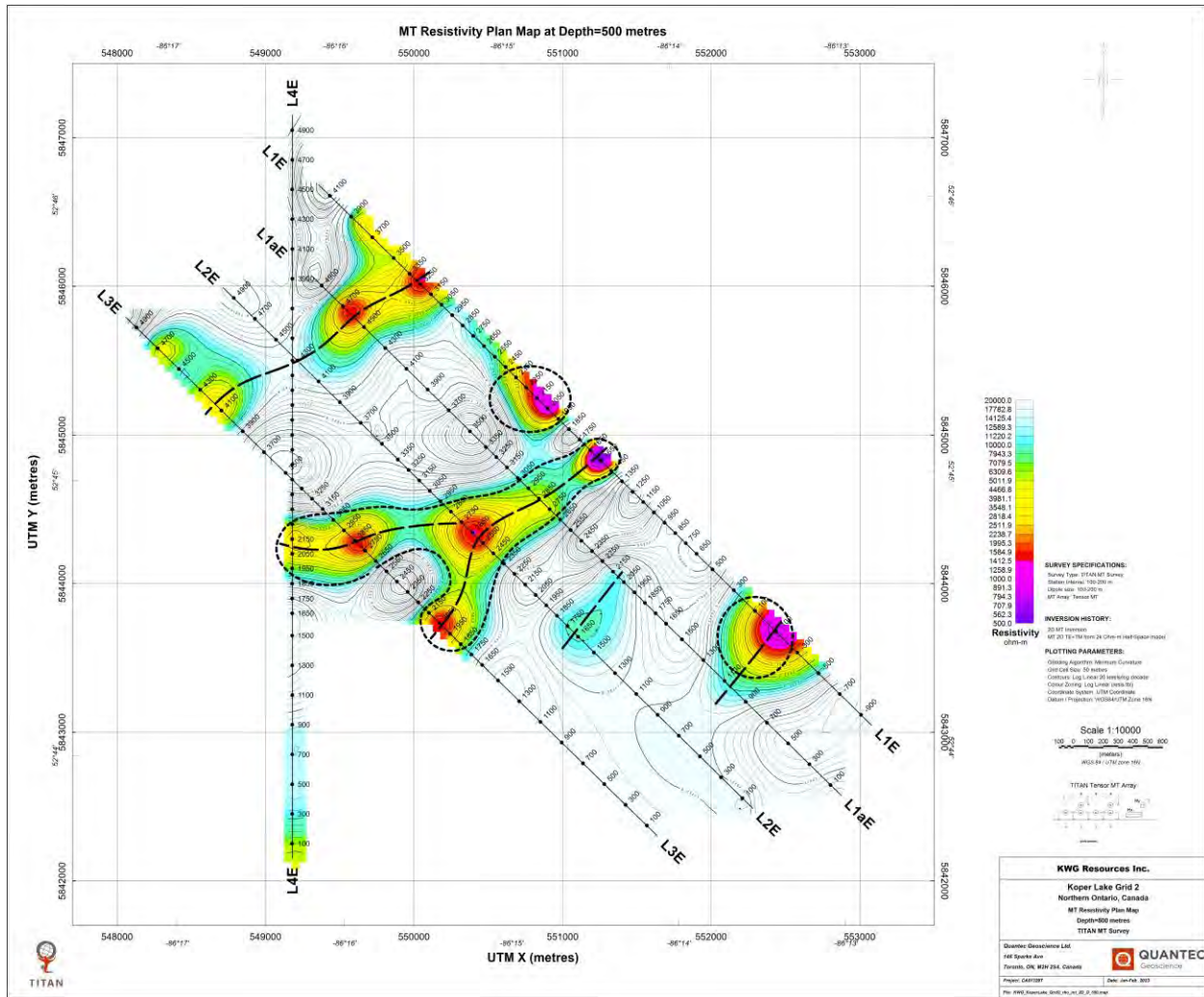


Figure 4-28: MT resistivity plan map over Koper Lake Grid-2 at 500 m depth.

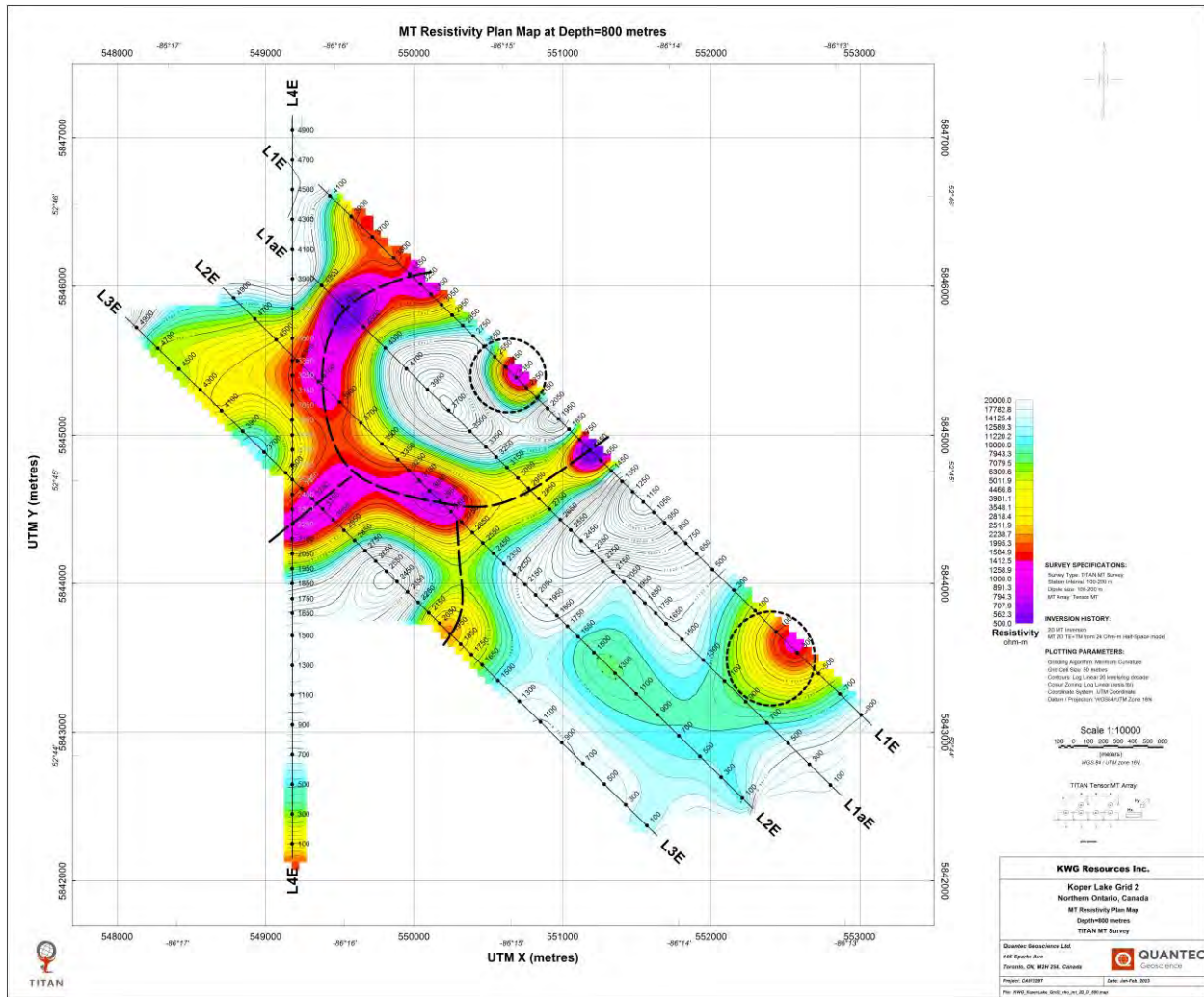


Figure 4-29: MT resistivity plan map over Koper Lake Grid-2 at 800 m depth.

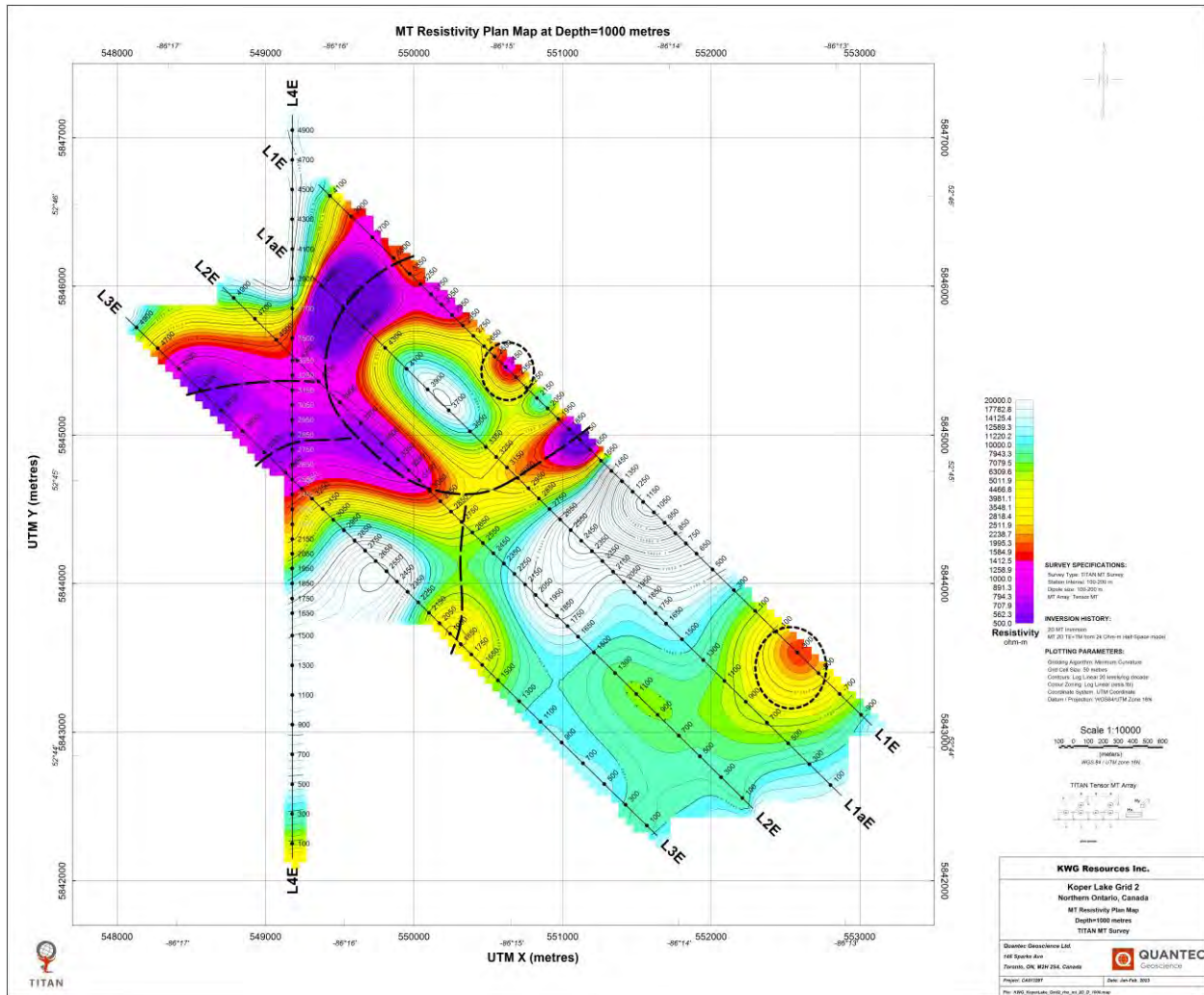


Figure 4-30: MT resistivity plan map over Koper Lake Grid-2 at 1000 m depth.

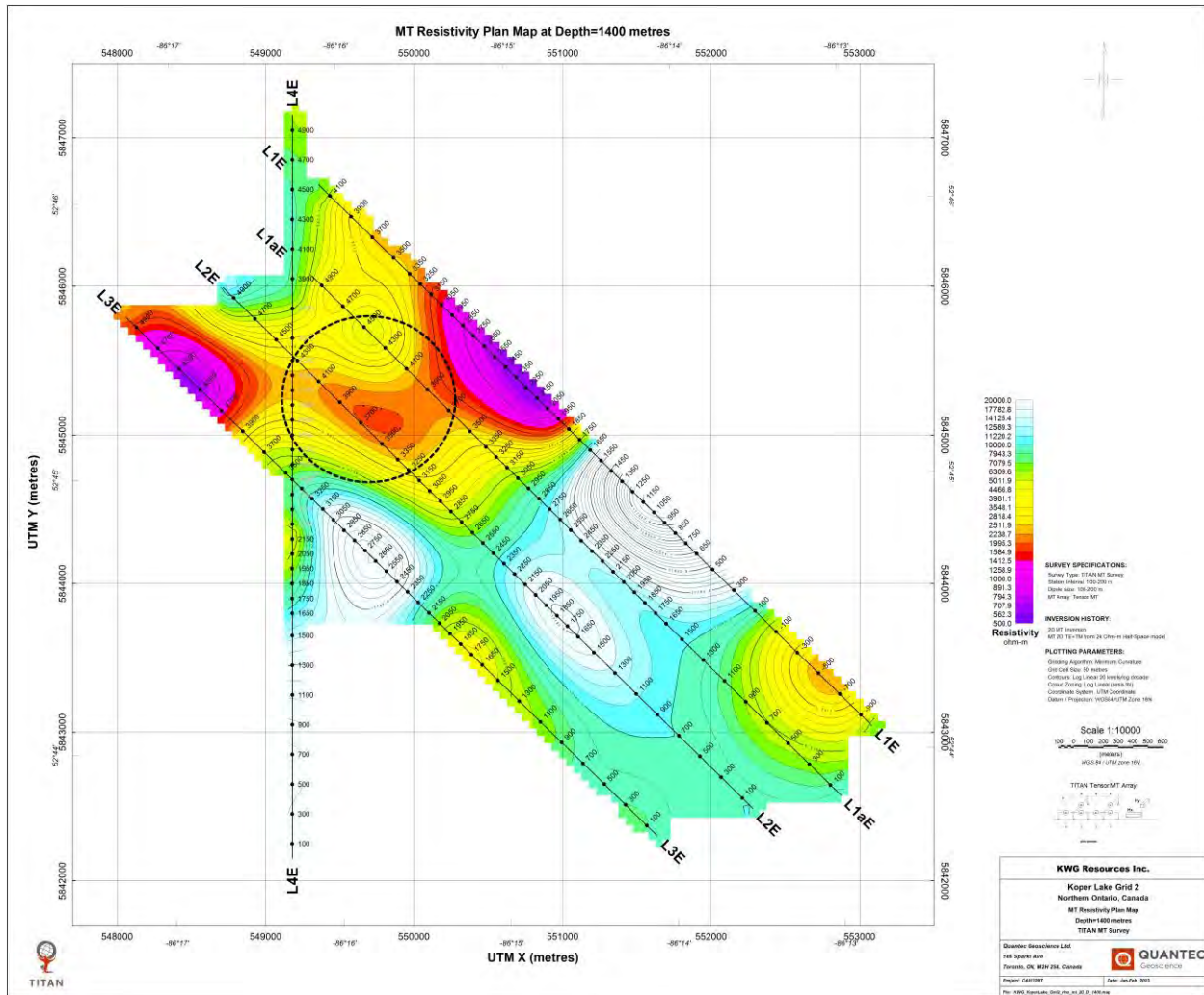


Figure 4-32: MT resistivity plan map over Koper Lake Grid-2 at 1400 m depth.

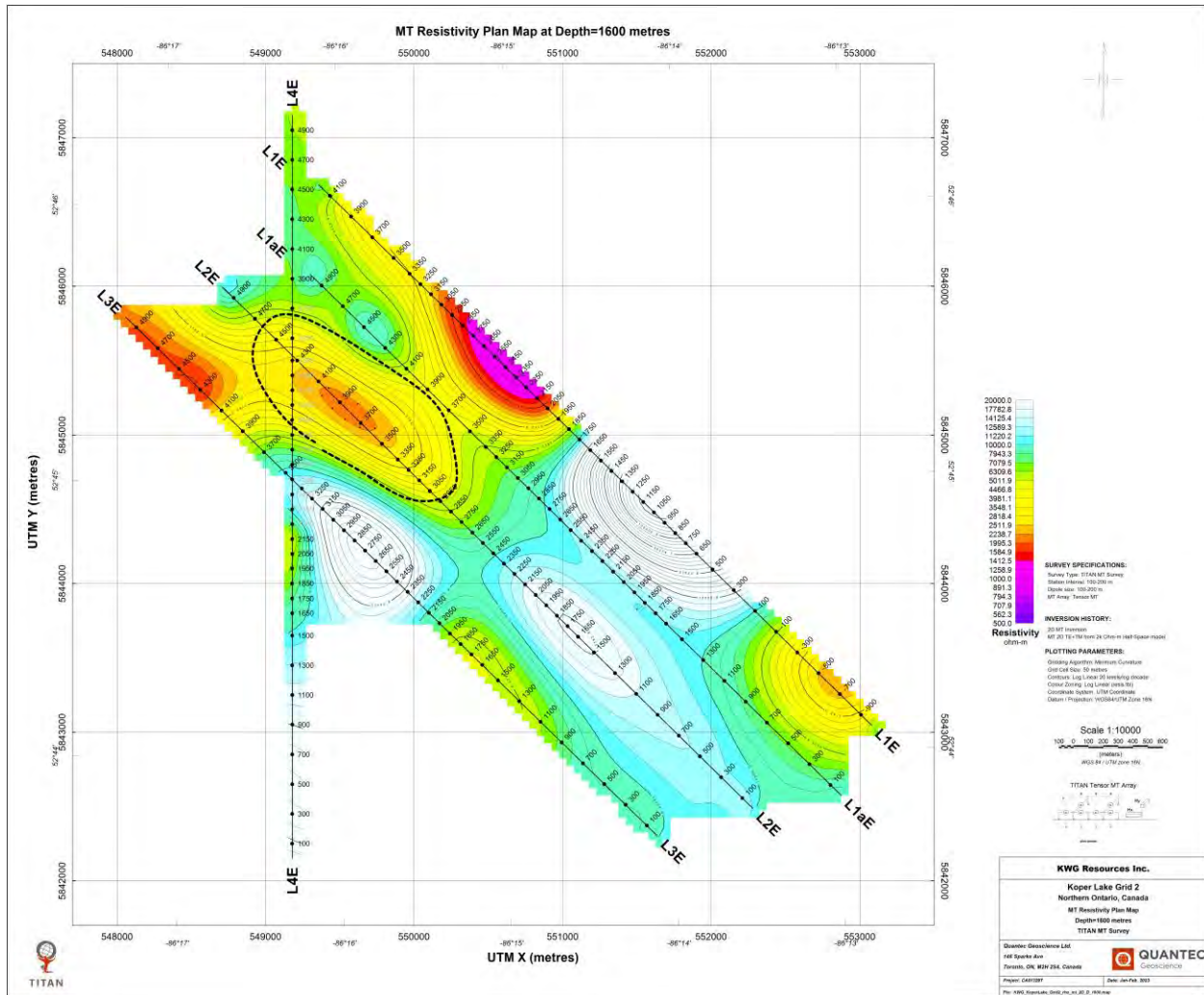


Figure 4-33: MT resistivity plan map over Koper Lake Grid-2 at 1600 m depth.

4.1.15. 3D view of the MT Resistivity Sections

This section presents the 2D MT inversion results as different 3D views. Figure 4-34 and Figure 4-35 show the 2D MT sections of surveyed Titan MT lines shown in 3D view over the Koper Lake Grid-1 and Grid-2, respectively. These 3D views allow a quick comparison of models across multiple lines. On Grid-1, the results show good correlation from line to line. The low resistivity sub-vertical features in the NW are well resolved on all lines.

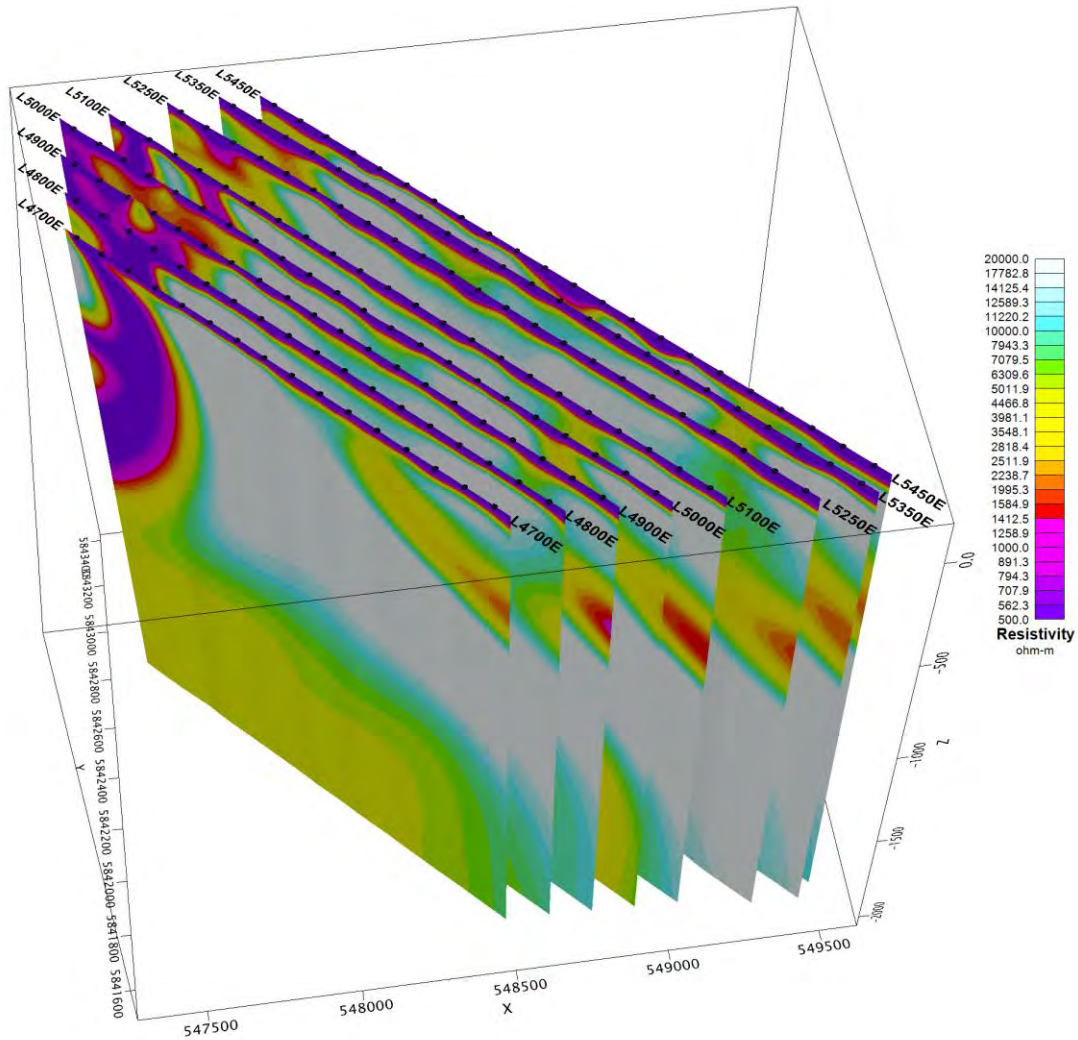


Figure 4-34: 2D MT resistivity sections over Koper Lake Grid-1; all lines shown together in the 3D view.

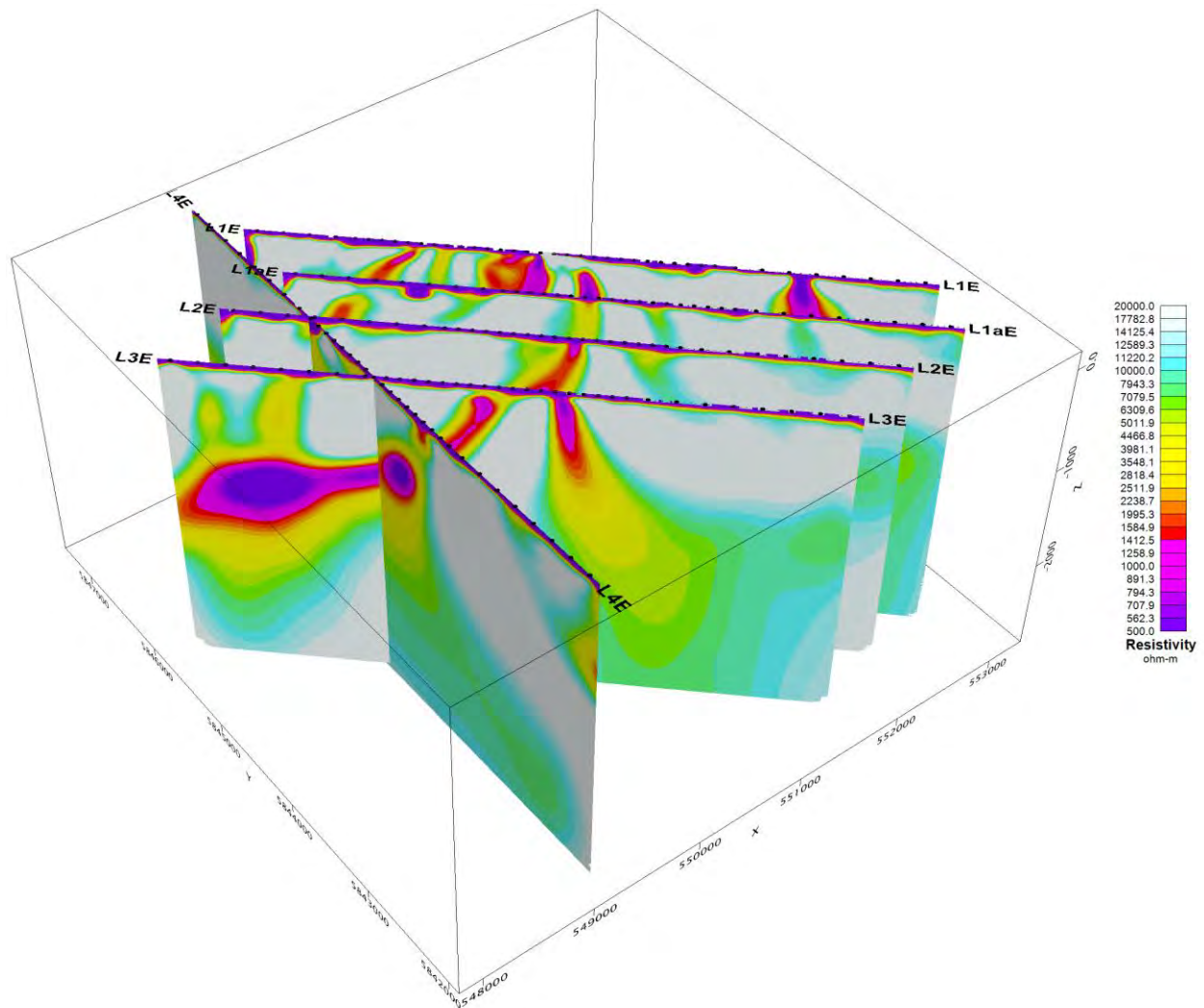


Figure 4-35: 2D MT resistivity sections over Koper Lake Grid-2; all lines shown together in the 3D view.

The low resistivity anomalies resolved on Grid-2 also show distinct sub-vertical structures (Figure 4-35). A good correlation is observed between the resolved resistivity features along the NW oriented lines L1E- L3E and the NS oriented line L4E. This is well reflected between L3E and L4E, where the low resistivity shear zone mapped on line L3E is consistently mapped on the NS line L4E with a coincident low resistivity response (Figure 4-35).

Drill data¹ showing chromite mineralization (light blue bars) are presented for Grid-1 and Grid-2 in Figure 4-36. Over the Grid-1, many occurrences of chromite mineralization were detected at depth. These show some correlation with the major low resistivity anomalies resolved in the 2D MT models. Over Grid-2, most of the drill holes showing chromite appear to be located outside the surveyed Titan MT lines.

¹ Drill data over the project area provided by KWG representative through personal communication.

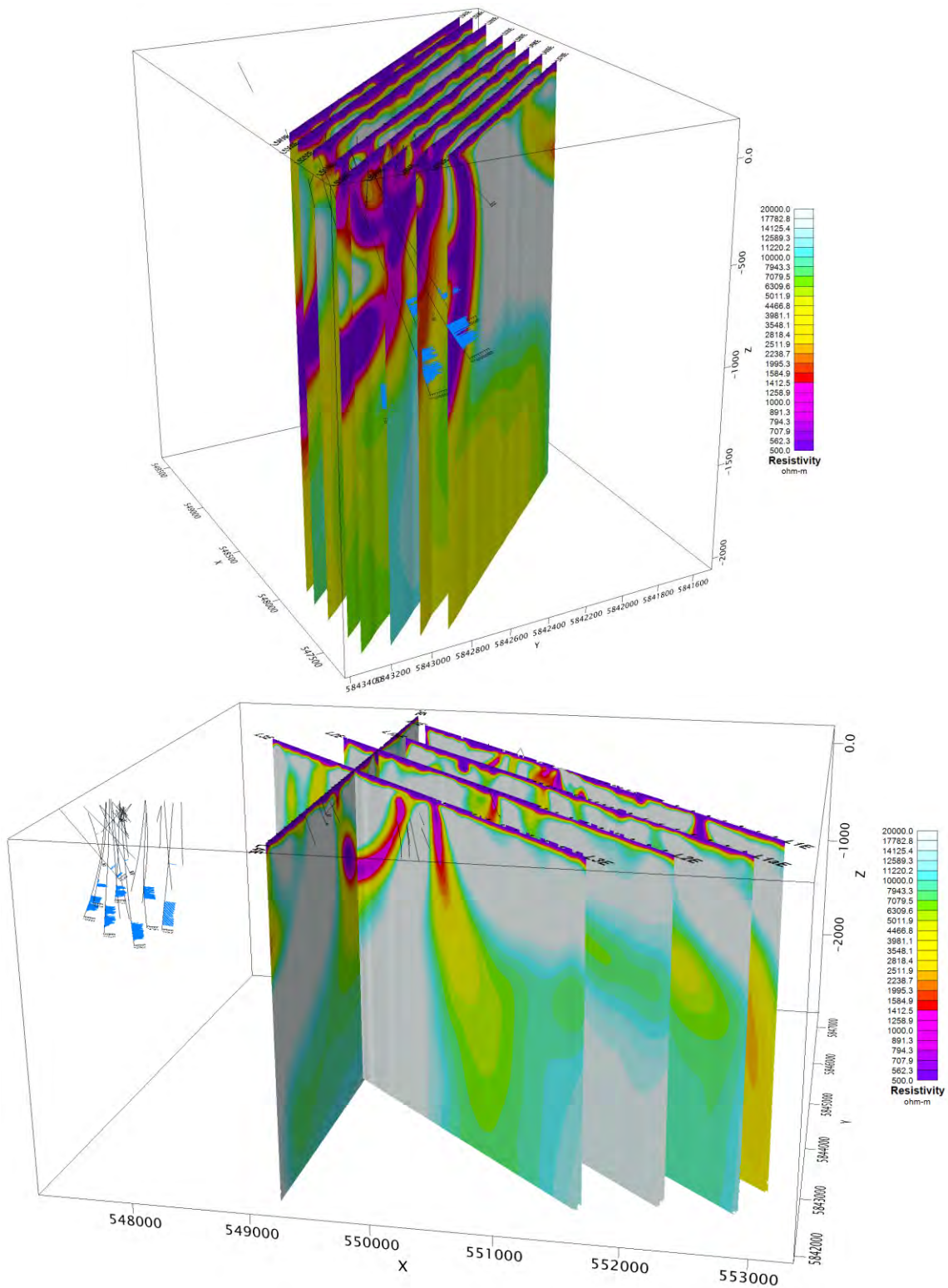


Figure 4-36: 3D view of the Grid-1 (top) and Grid-2 (bottom) MT2D sections plotted with the drill data showing chromite mineralization (in blue).

Some of the selected drill holes in the vicinity of the MT lines are shown here to correlate the resistivity responses to the known chromite mineralization (shown with light blue bars on the drill hole trace). Figure 4-37 shows a drill hole coincident with the line L2E. Minor chromite mineralization is detected inline with the low resistivity shear zone. Another drill hole showing relatively higher percentage of chromite mineralization is shown on line L3E in Figure 4-38. However, this drill hole is not passing through the main low resistivity zone and the chromite mineralization appears to be coincident with high resistivity zones.

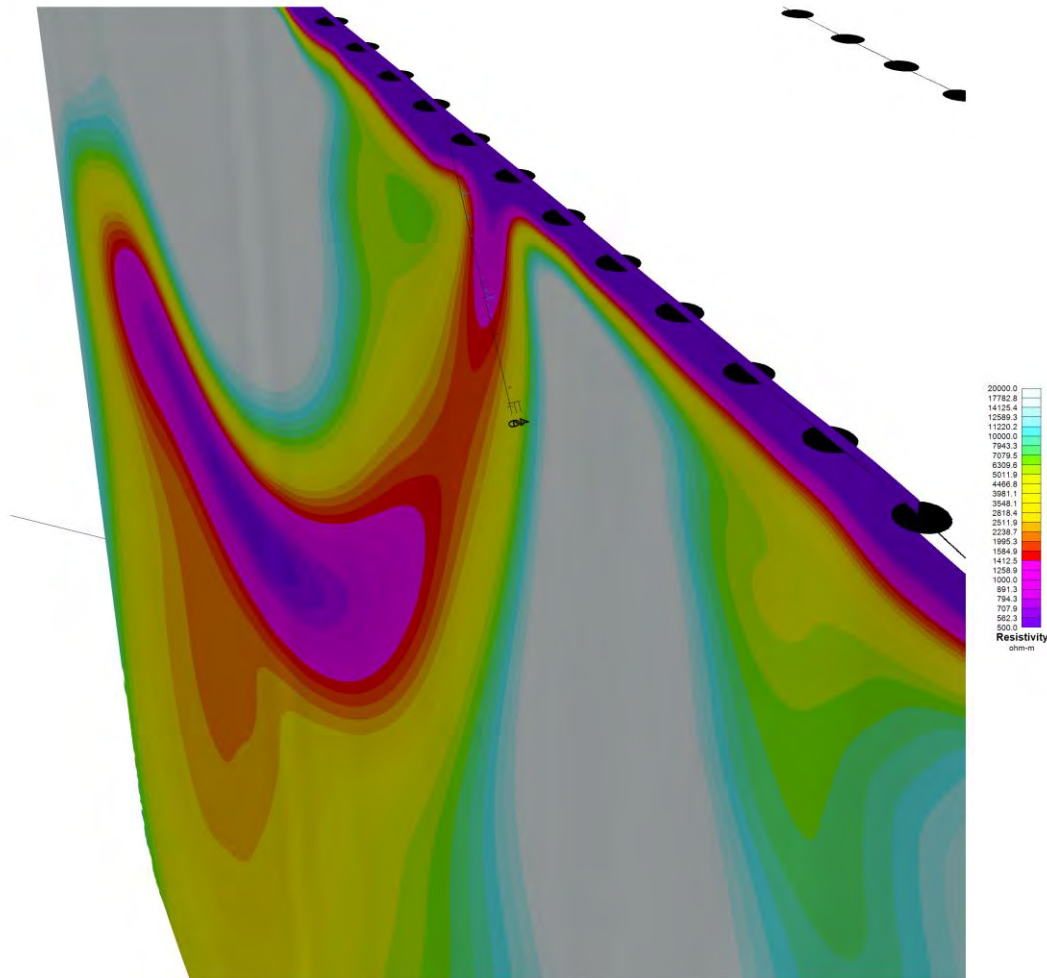


Figure 4-37: Line L2E plotted with a drill hole showing minor chromite mineralization, coincident with the low resistivity shear zone.

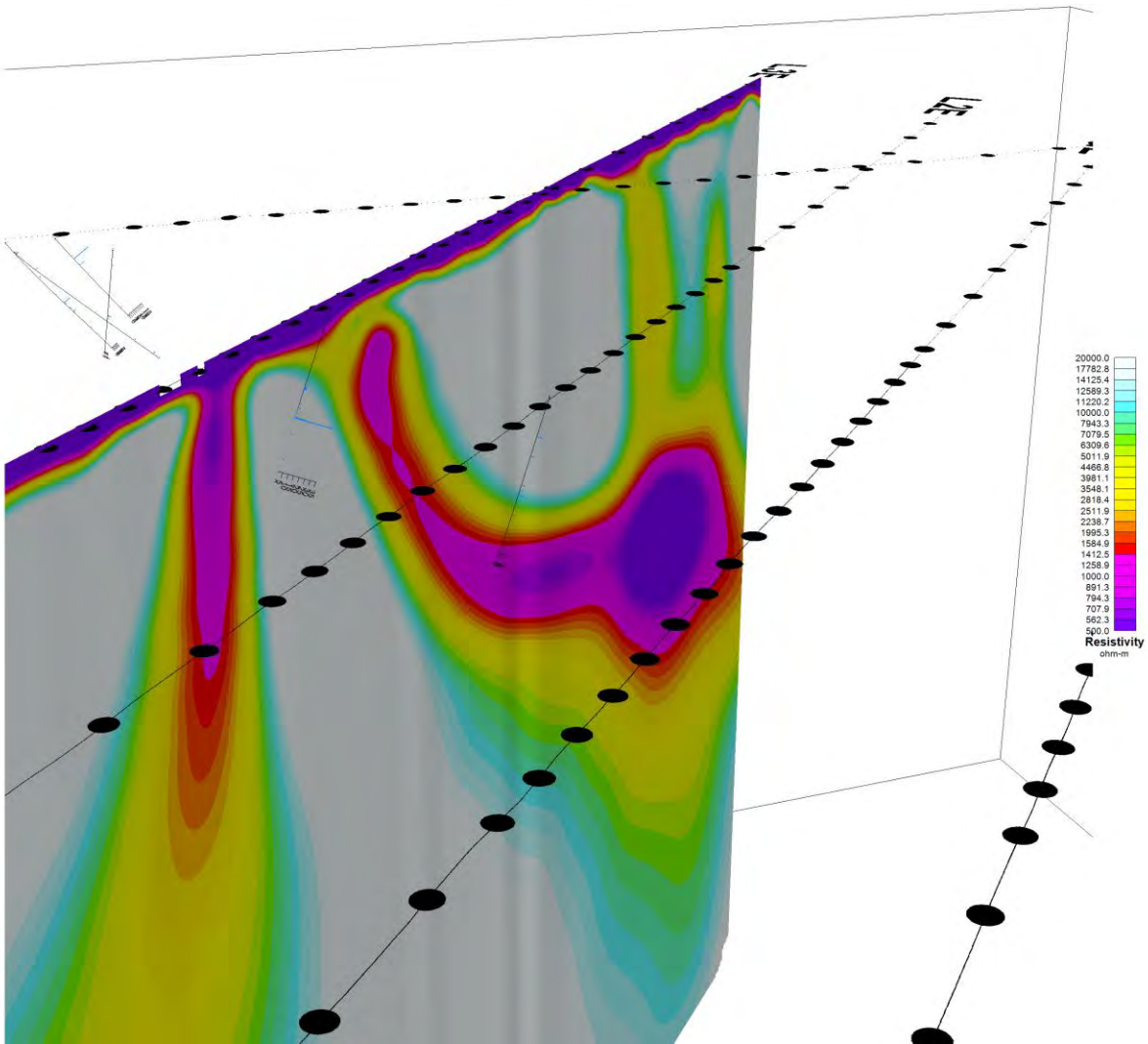


Figure 4-38: Line L3E plotted with a drill hole showing chromite mineralization.

Drill data showing chromite mineralization and 2D MT sections along the Grid-1 lines L4700E, L4800E, L4900E, L5000E and L5100E are shown in Figure 4-39, Figure 4-40 and Figure 4-41. From these drill holes, it is evident that the major chromite mineralization occurs at depth and generally associated with low resistivity zones or with the underlying medium resistivity zones. The medium resistivity association is well evident from the drill holes cutting the resistivity sections of L4800E and L5000E at depth (Figure 4-40 and Figure 4-41).

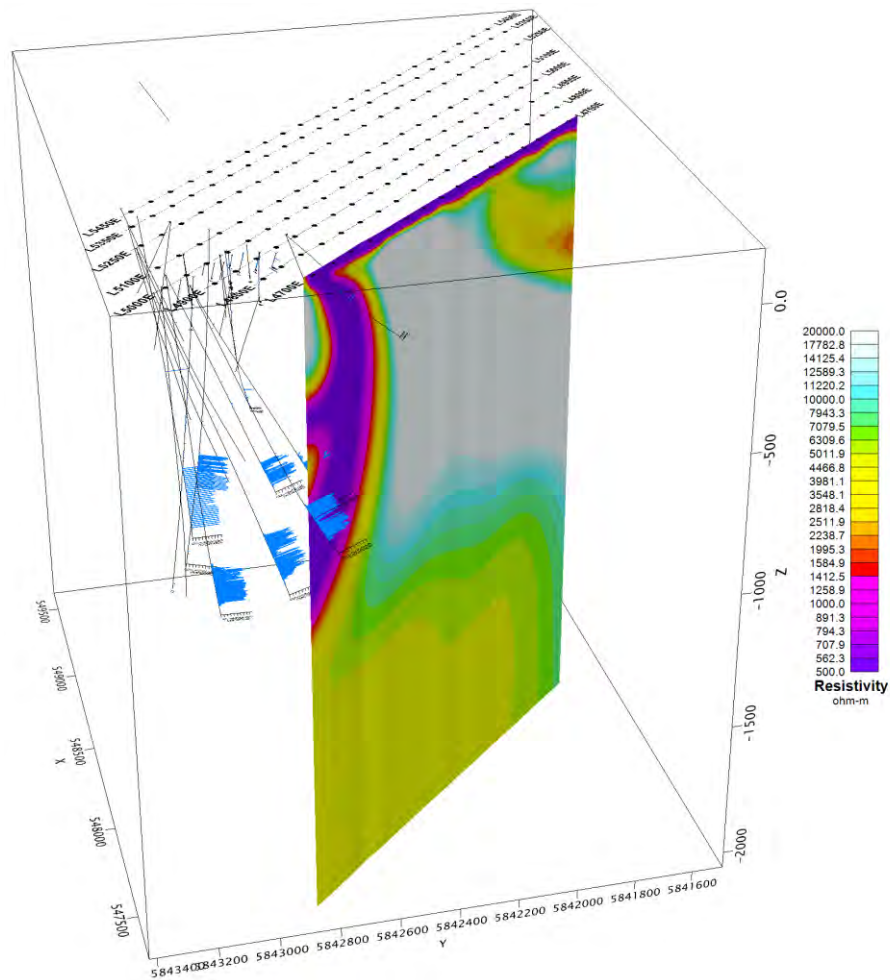


Figure 4-39: Line L4700E resistivity section and drill data showing chromite mineralization.

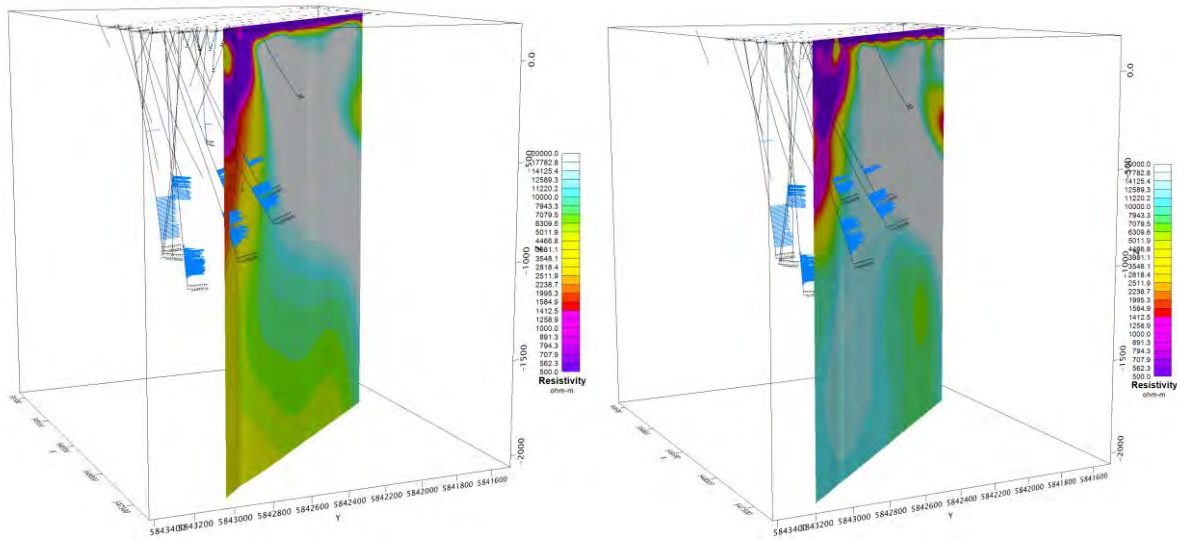


Figure 4-40: Lines L4800E (left) and L4900E (right) resistivity sections and drill data showing chromite mineralization.

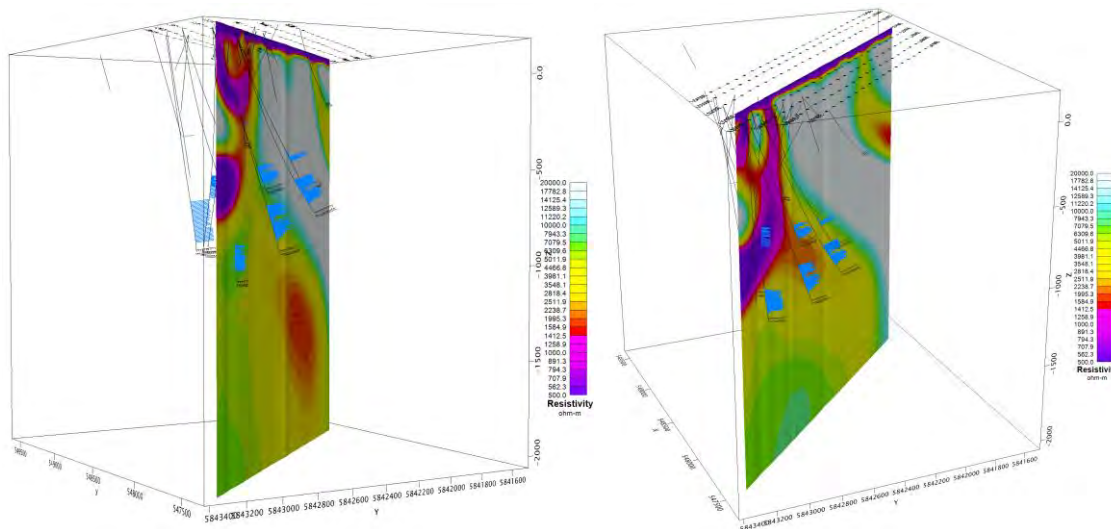


Figure 4-41: Lines L5000E (left) and L5100E (right) resistivity sections and drill data showing chromite mineralization.

5. CONCLUSIONS AND RECOMMENDATIONS

This report presents the data analysis, inversion results and the interpretation of the Titan MT Survey, carried out from 19/01/2023 to 11/02/2023, over the Koper Lake Project by Quantec Geoscience Ltd. on behalf of KWG Resources Inc.

In this project, a total of 13 MT lines were acquired over the Koper Lake Project. Eight lines were located over a detailed grid (Grid-1), oriented at 317° true north and spaced at 100 m to 150 m. All lines on Grid-1 used an array of 100 m inline dipoles and crossline dipoles of same size at every 200 m. Other five lines were located over a regional grid (Grid-2), where four lines were oriented at 315° and one line at 0° true north. Each line on Grid-2 was deployed with an array of 100 m and 200 m inline dipole combinations and crossline dipoles of 100 m at every other inline dipole. Titan MT sites along all lines were acquired and processed at the respective line azimuth, within a nominal frequency range from 10 kHz to 0.01 Hz.

2D inversions were completed for the acquired Titan MT data. The inversion results are presented as MT resistivity sections, plans and 3D-view maps in this report. The maps presented in this report use a consistent colour range of 500-20,000 Ω -m to accommodate the wide range of sub-surface resistivities observed over the Koper Lake Project.

MT inversions resolved a low resistivity surficial layer, which represents the Quaternary deposits that extends to an approximate depth of 50 m throughout the project area. Besides this top layer, inversion results show the underlying bedrocks with high resistivity. These underlying rocks are resolved with multiple zones of low resistivity responses, including sub-vertical structures possibly indicating the shear/fault zones or lithological contacts.

The main sub-vertical low resistivity zones resolved in the 2D resistivity models show some correlation to the known shear zones in the region. The available drill data shows chromite mineralization within these shear zones and within the underlying medium resistivity zones. The main anomalies resolved are briefly discussed in this report using the resistivity section and plan maps and an overview of the results are presented in 3D views.

The results and any interpretation presented in this report are purely based on the inversions completed using available MT data. It is recommended to integrate these results with other geological and geophysical data to help with any follow up exploration efforts.

Report dated March 8, 2023 by Jimmy Stephen, PhD, PGeo

Quantec Geoscience Limited



APPENDIX A. REFERENCES

Mackie, R.L. and Watts, D.M. 2012. Detectability of 3-D sulphide targets with AFMAG. SEG Technical Program Expanded Abstracts 2012: pp. 1-4.

Orange, A.S., 1989. Magnetotelluric exploration for hydrocarbons. Proceedings of the IEEE, 77, 287-317.

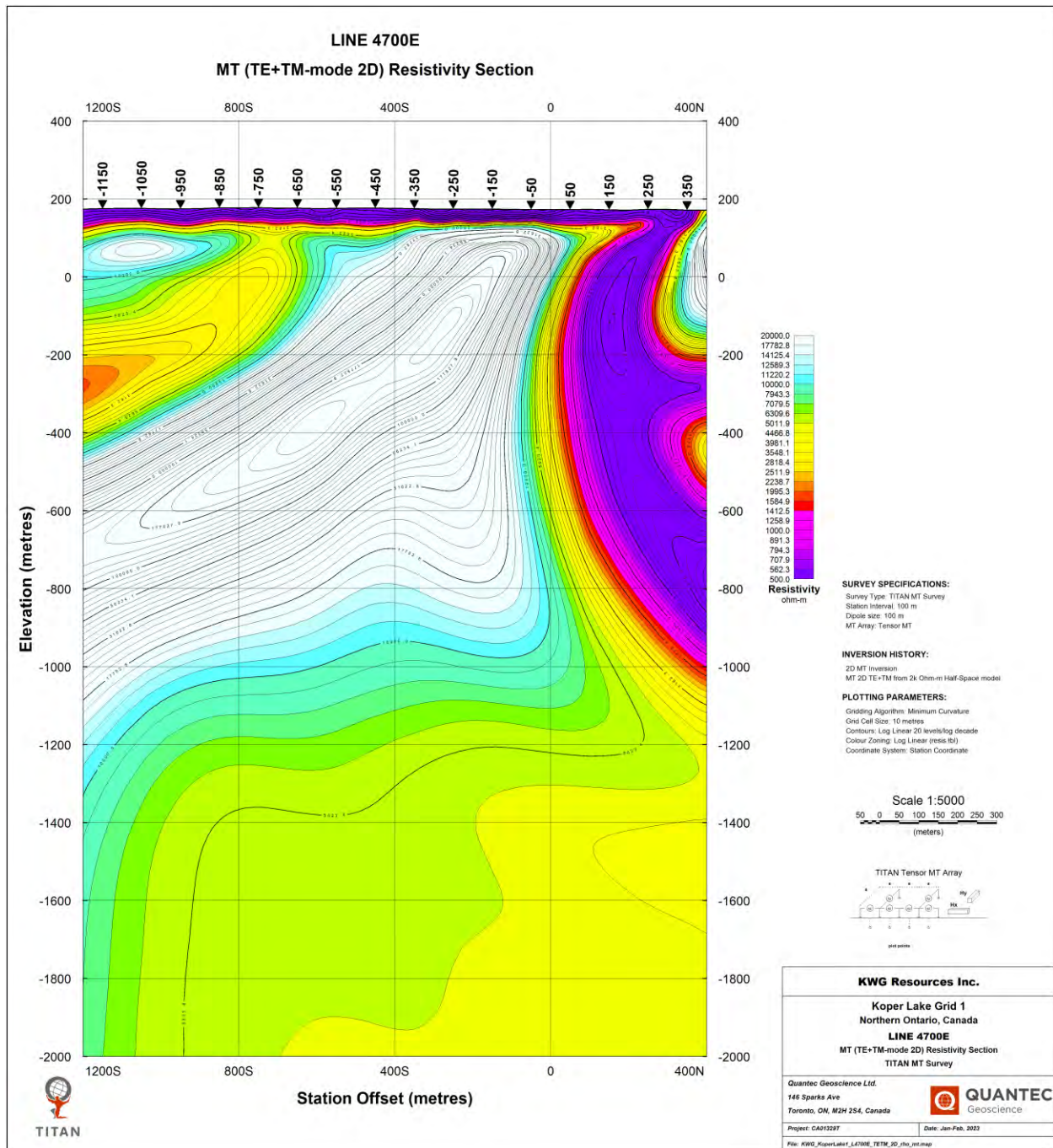
Rodi, W. and Mackie, R.L., 2001. Nonlinear conjugate gradients algorithm for 2-D magnetotelluric inversion, Geophysics, 66, 174--187.

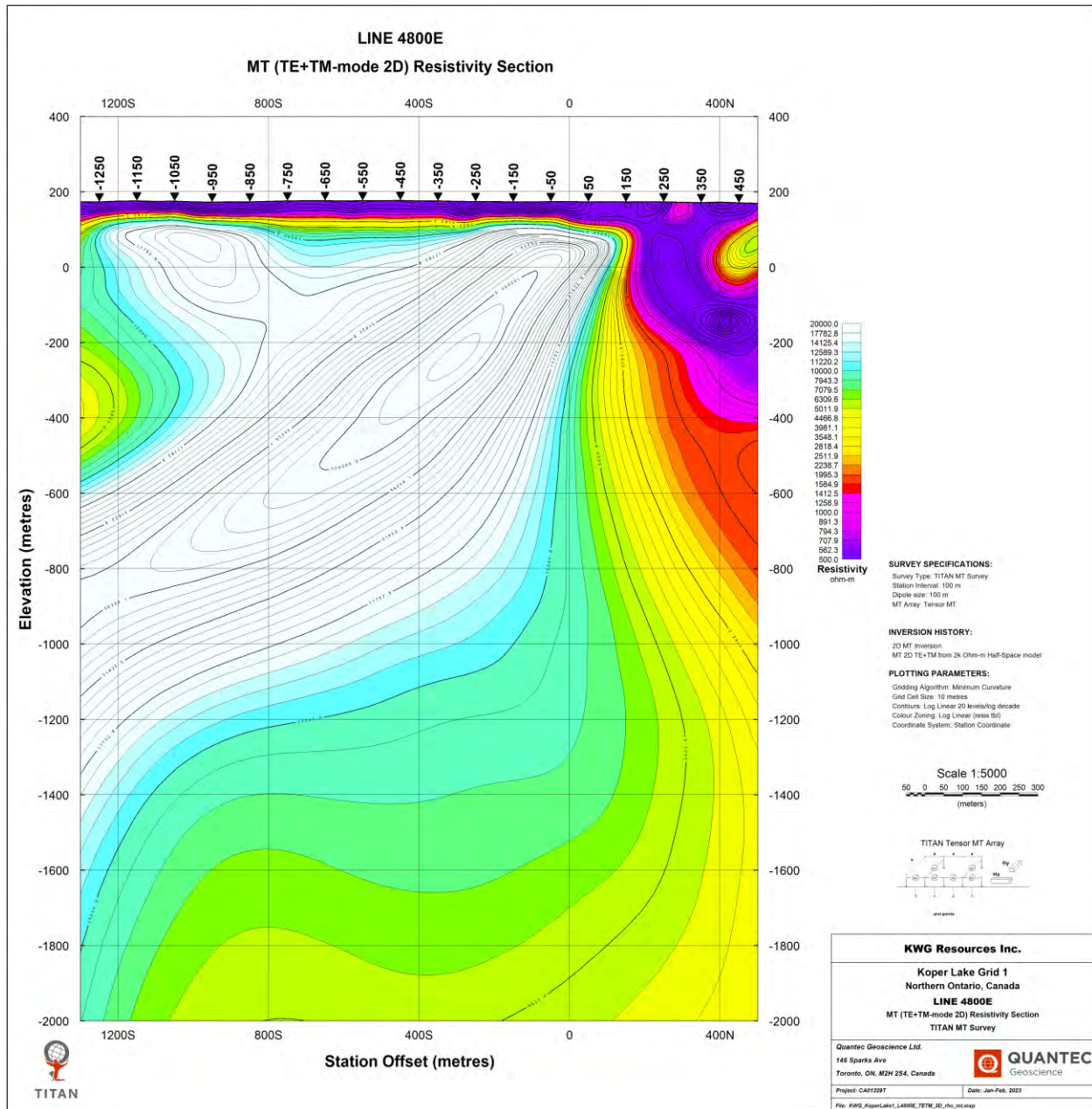
Telford W.M., Geldart, L.P., Sheriff, R.E. and Keys, D.A., 1976. Applied Geophysics. Cambridge University Press, Cambridge.

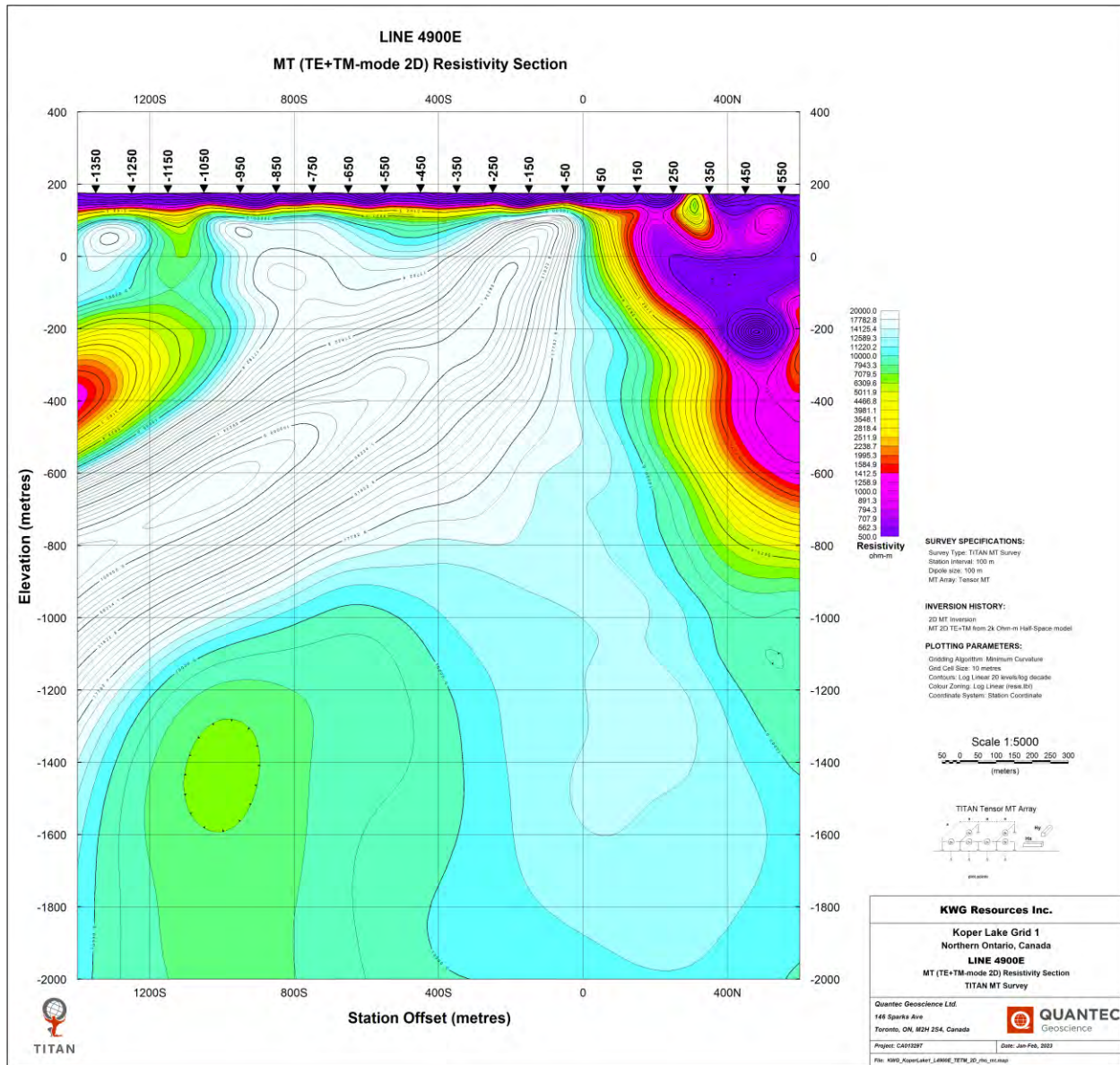
Vozoff, K., 1972. The Magnetotelluric method in the Exploration of Sedimentary basins. Geophysics, 37, 98-141.

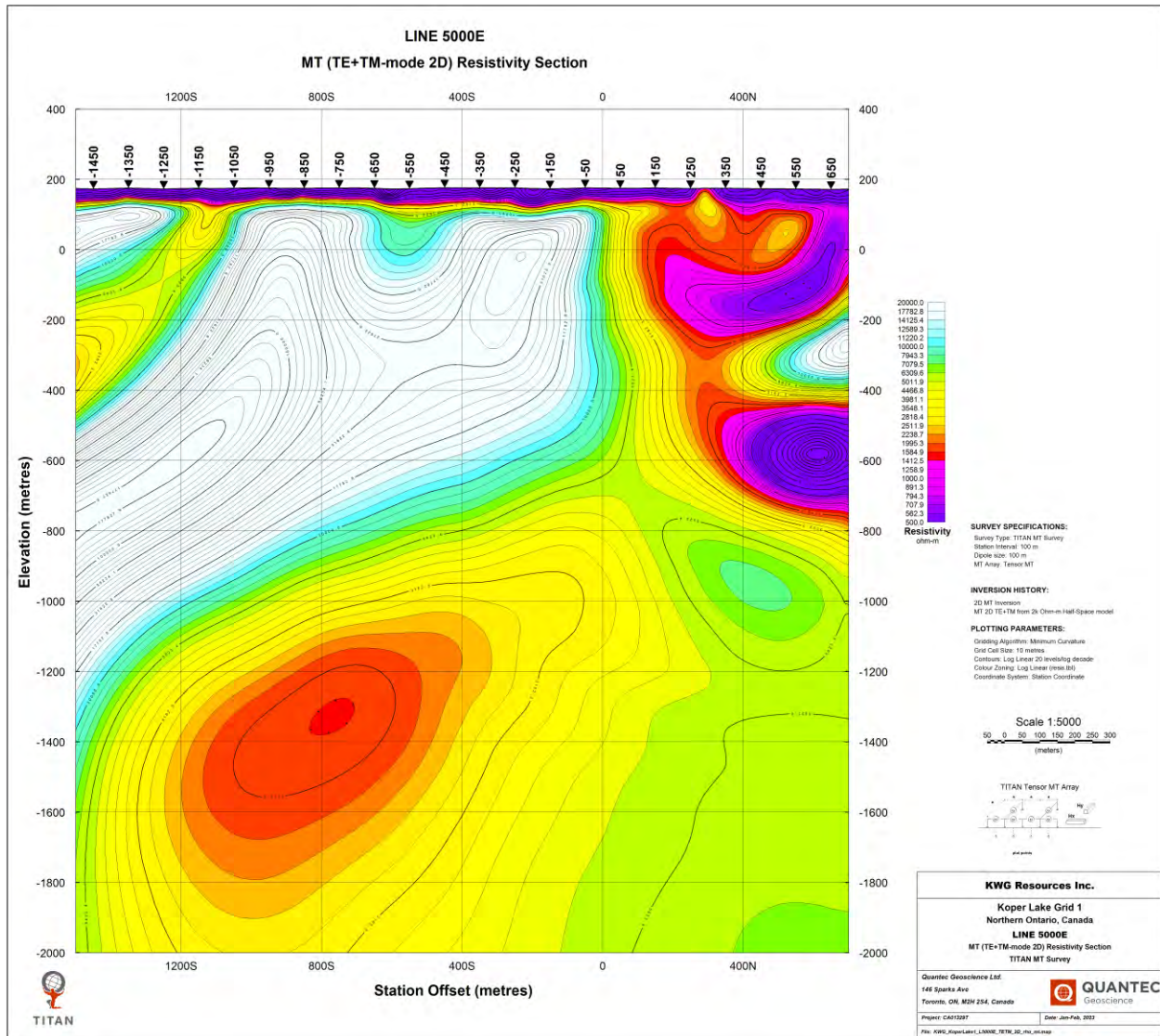
APPENDIX B. RESISTIVITY SECTION MAPS

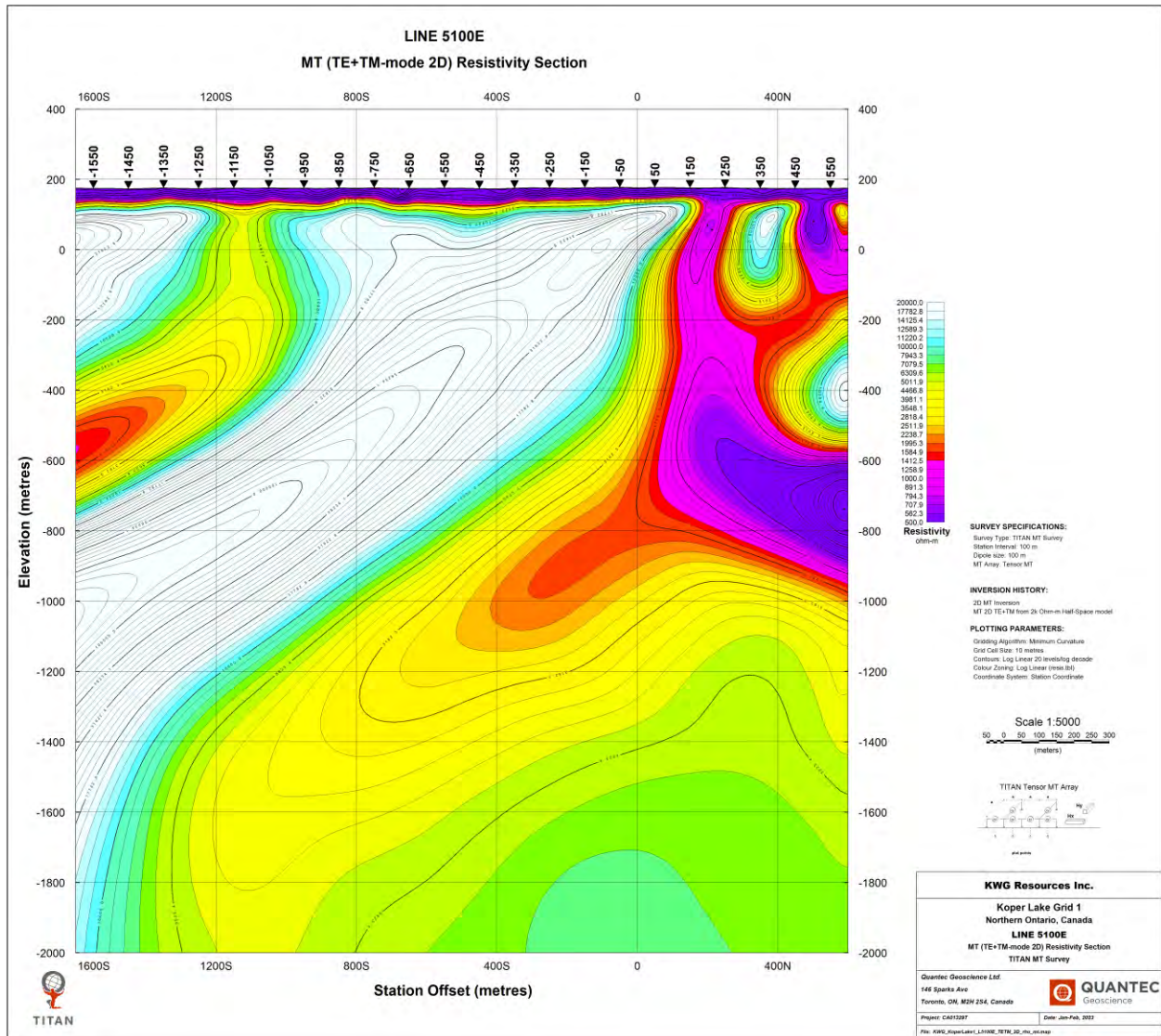
B.1. 2D - MT RESISTIVITY SECTION MAPS – GRID-1

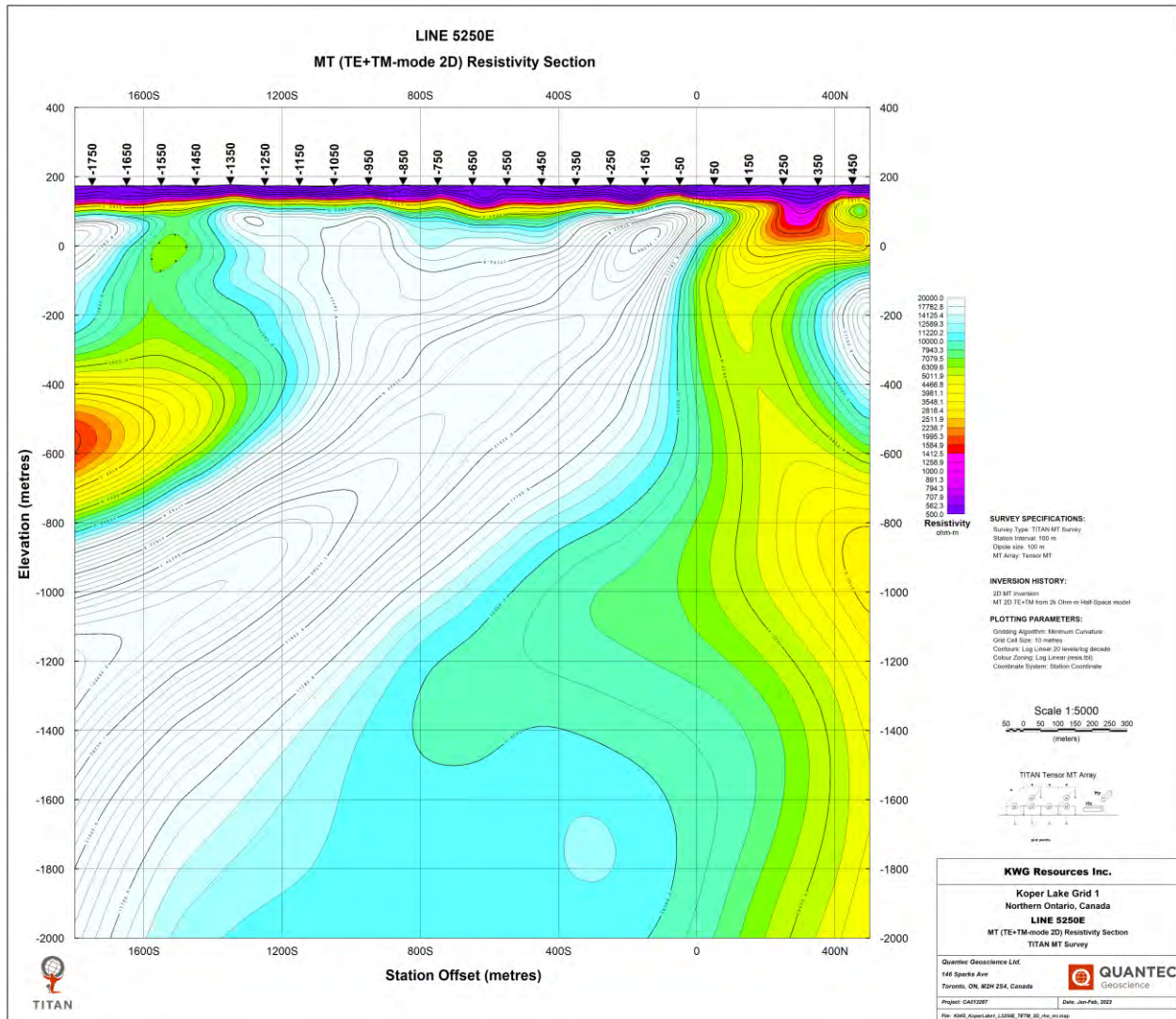


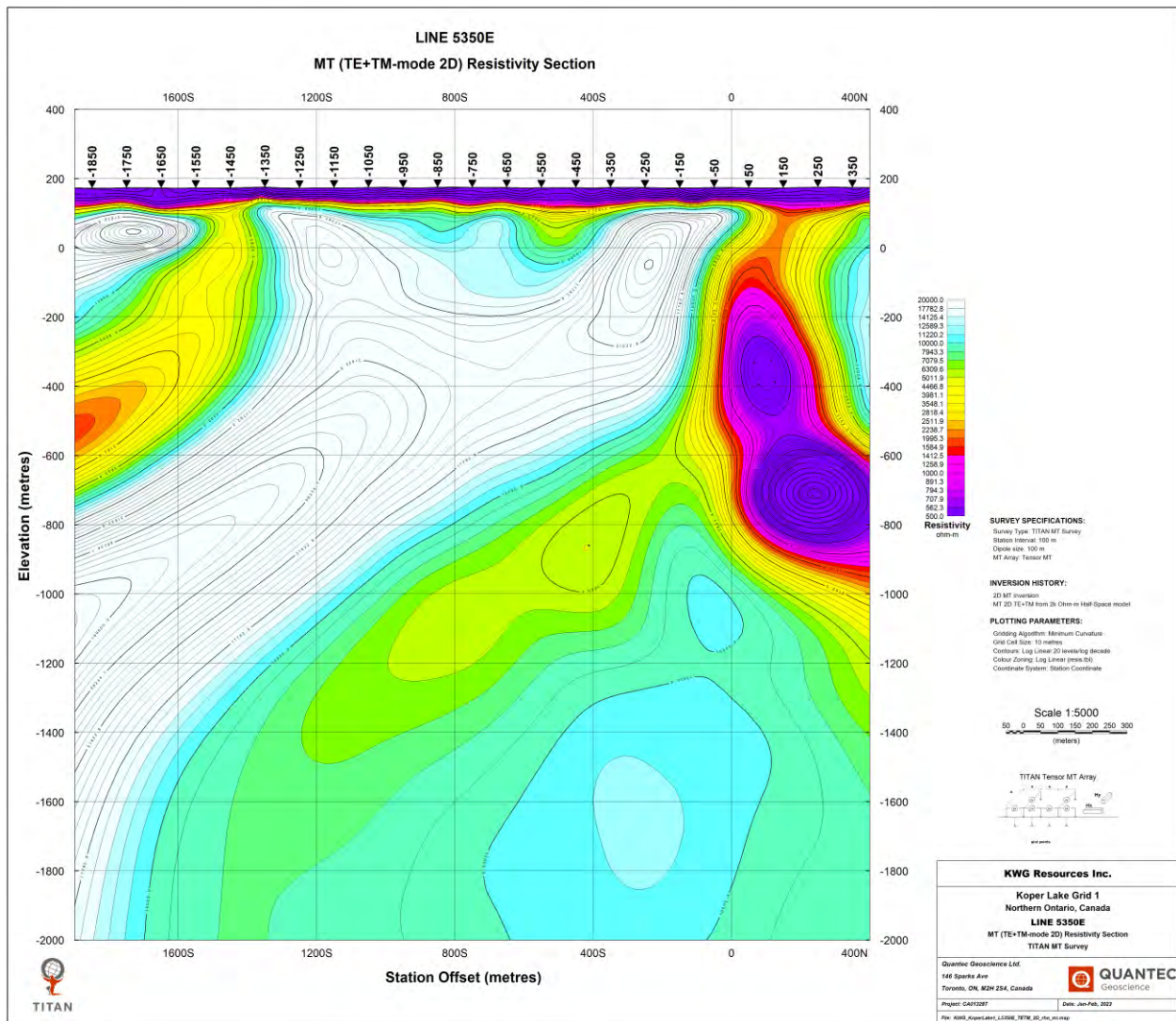


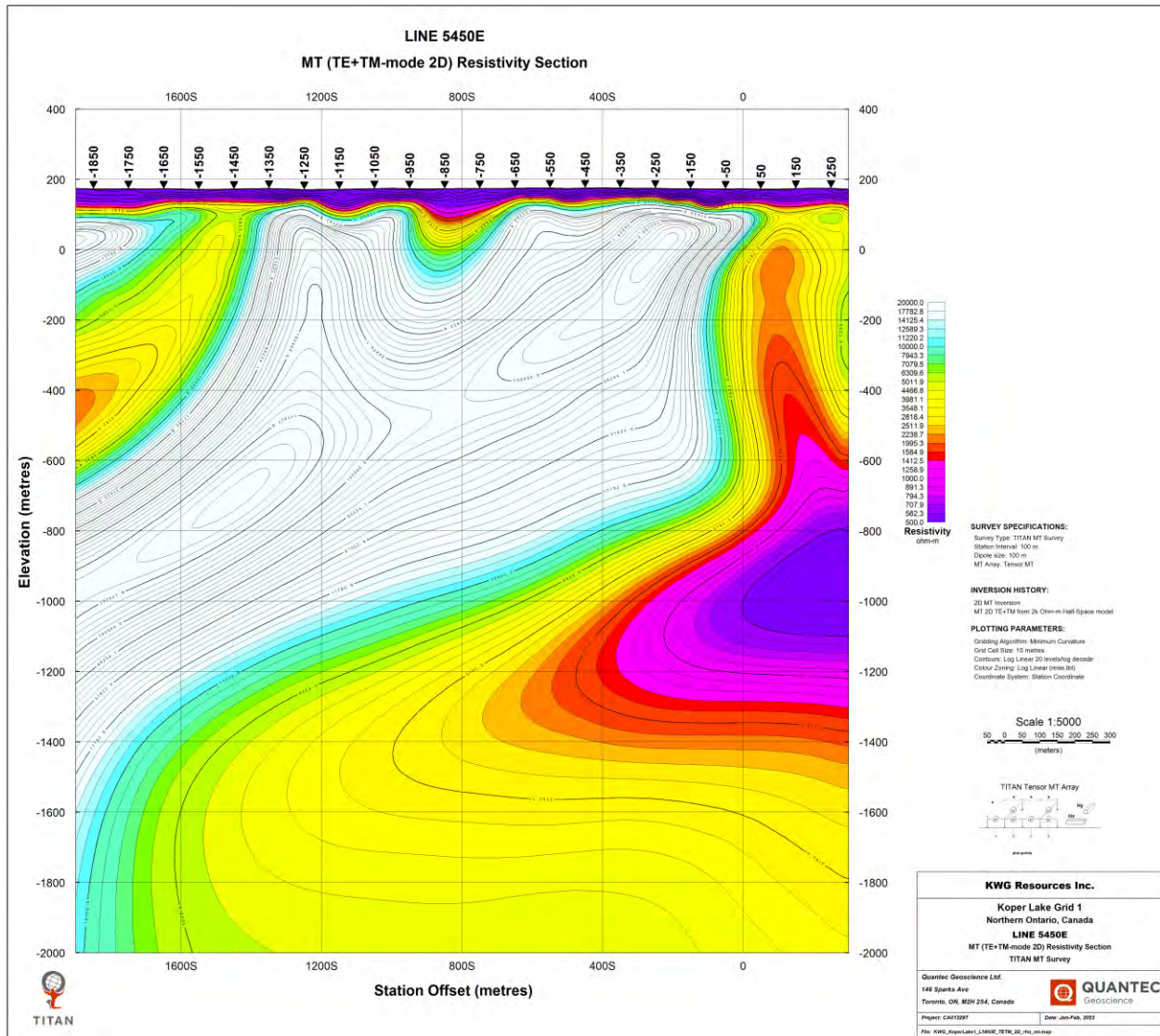




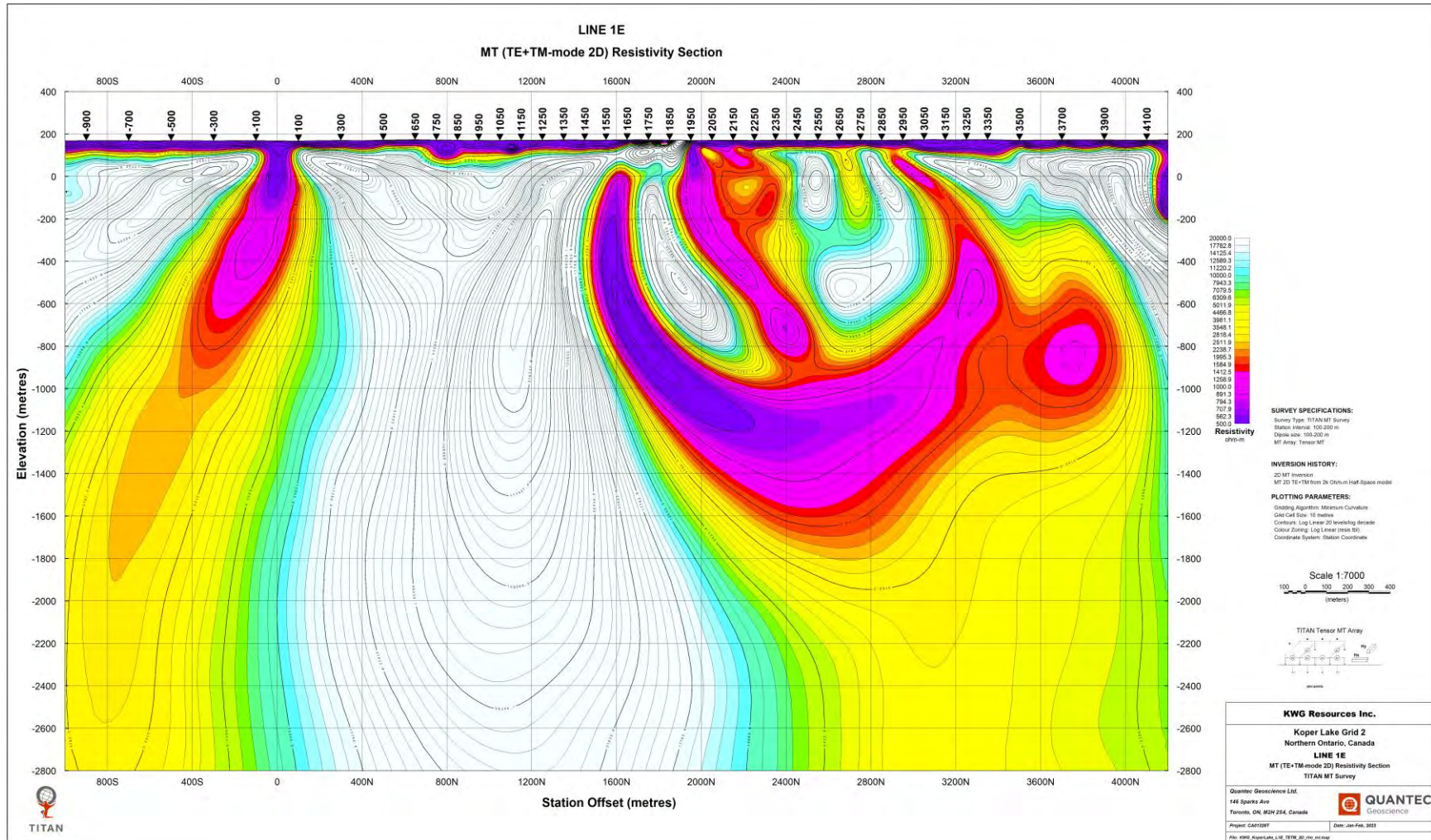


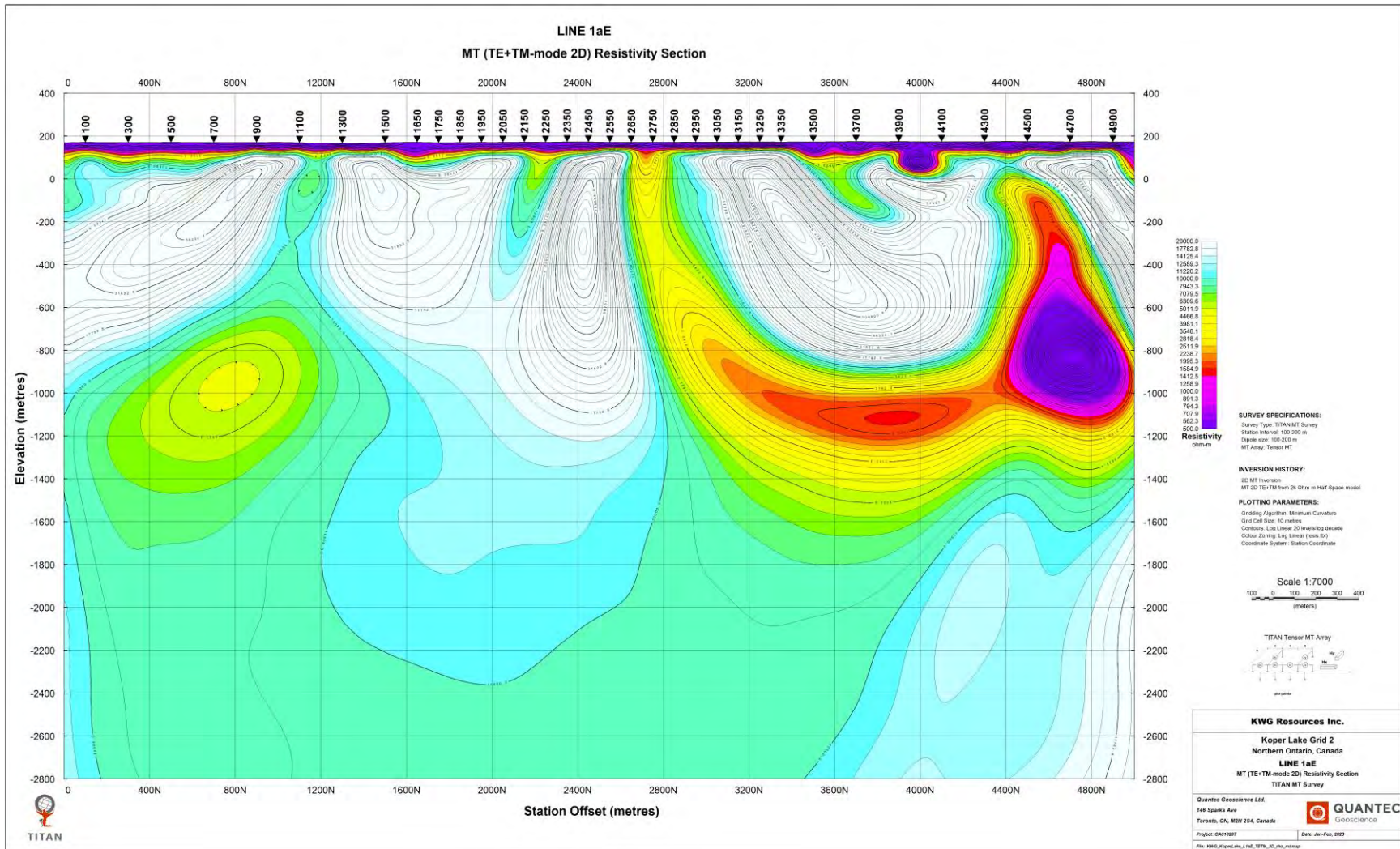


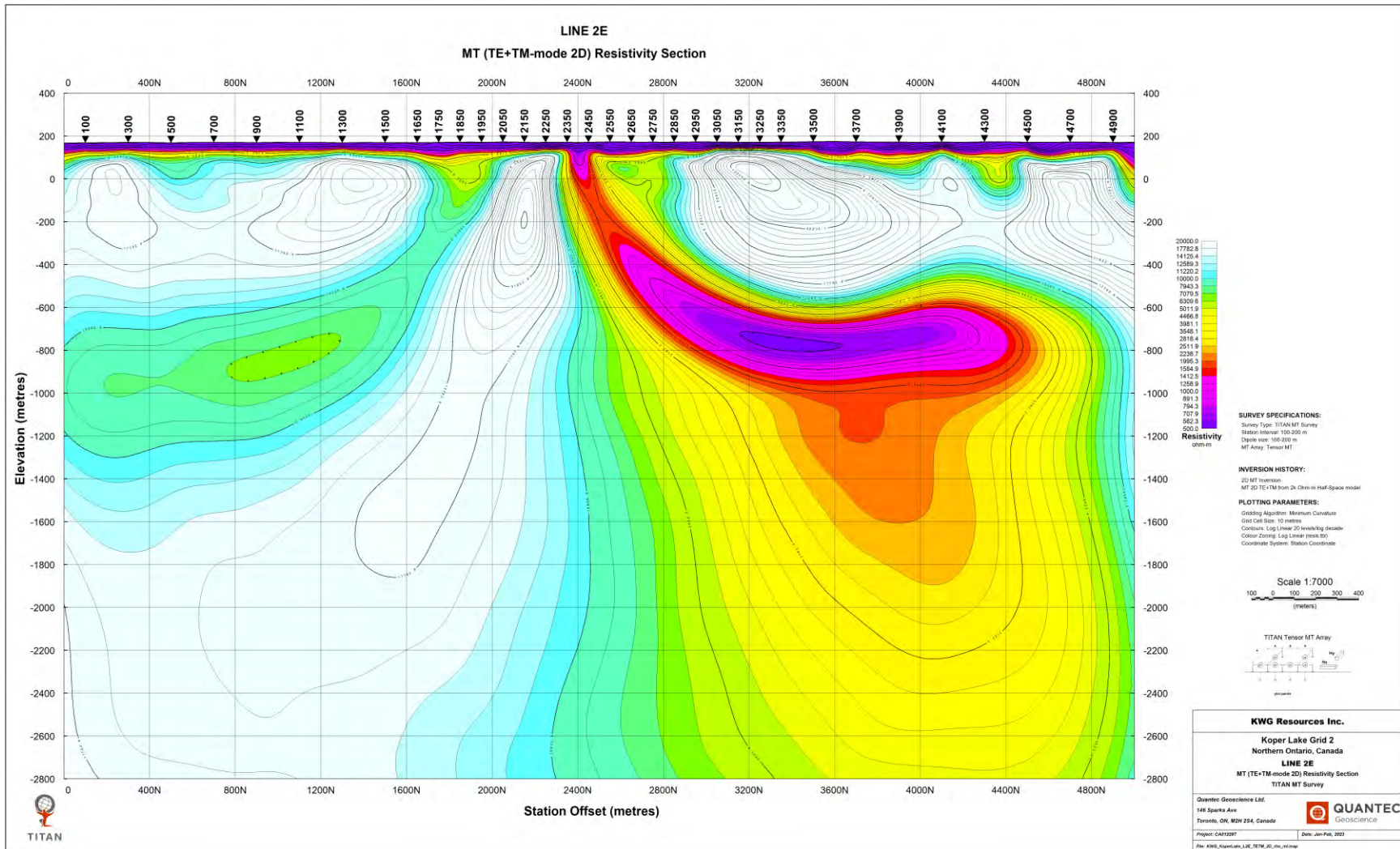


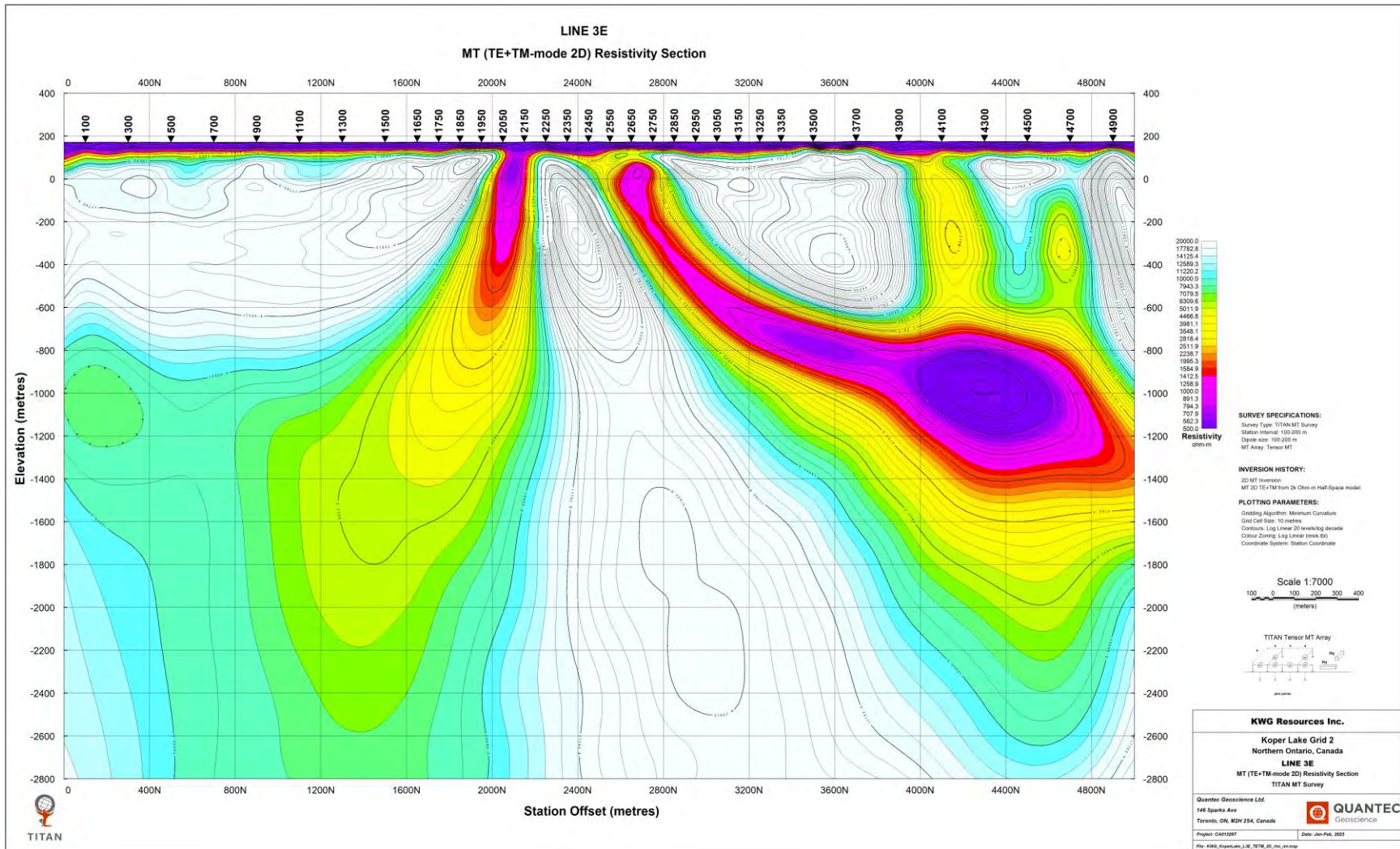


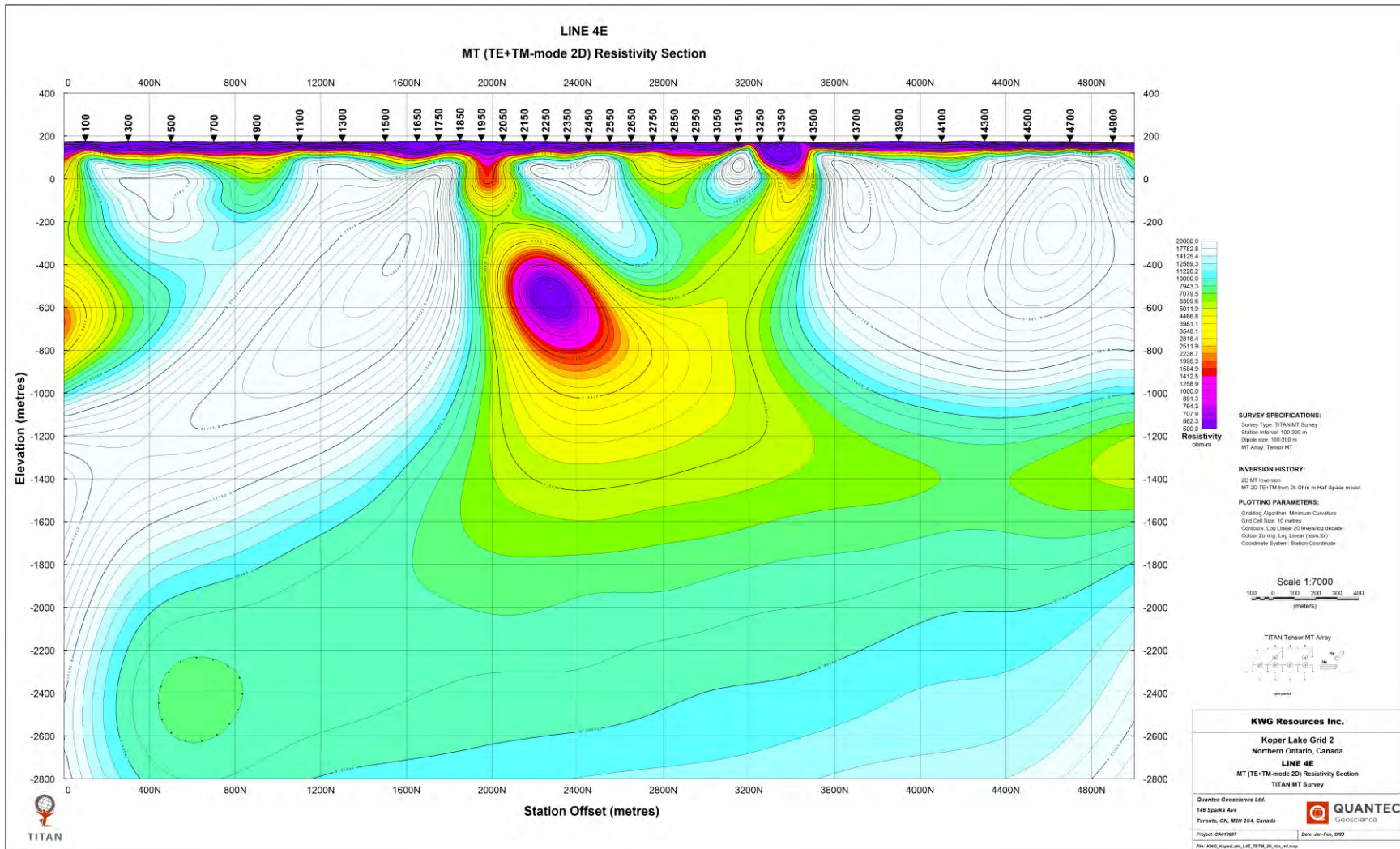
B.2. 2D - MT RESISTIVITY SECTION MAPS – GRID-2





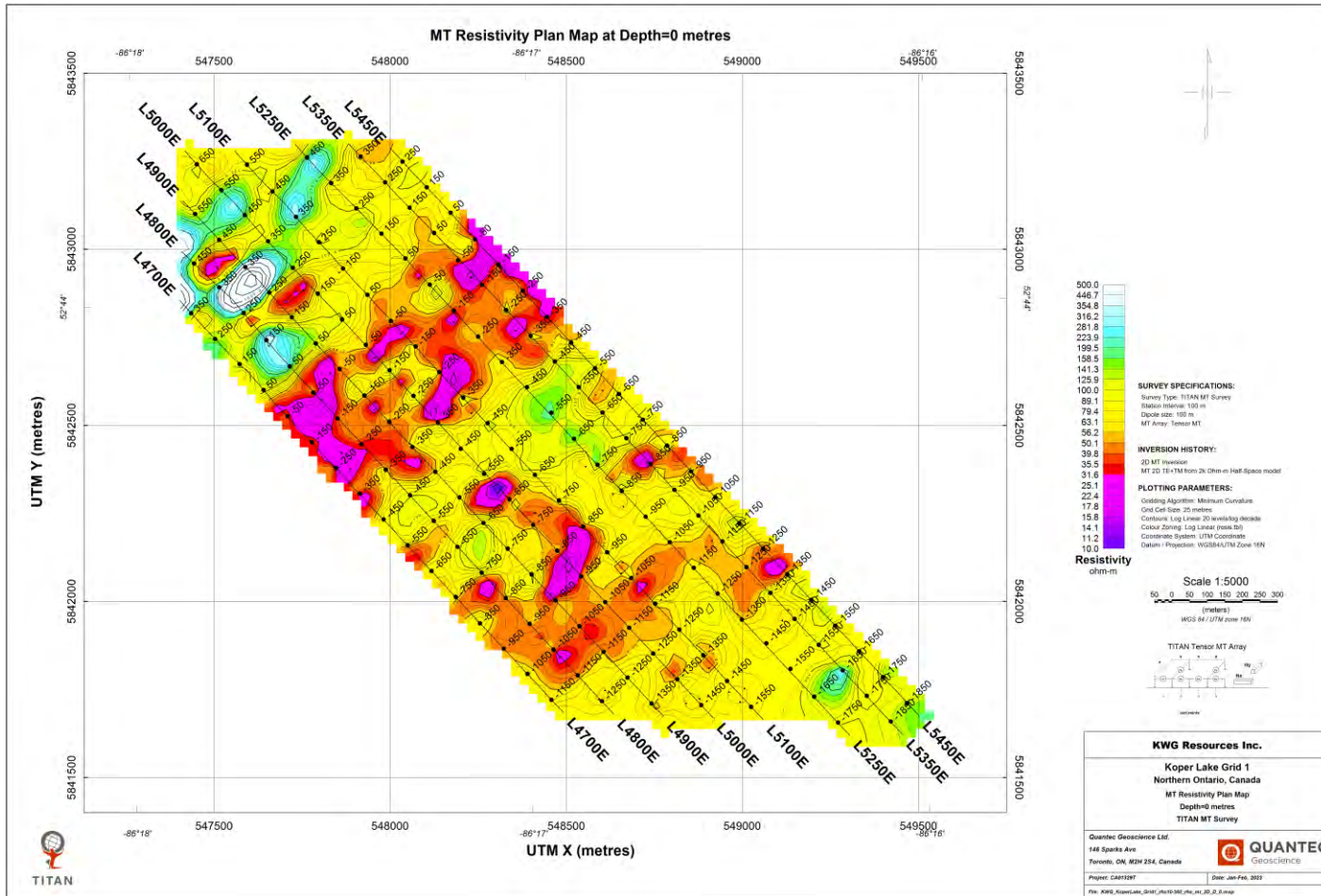


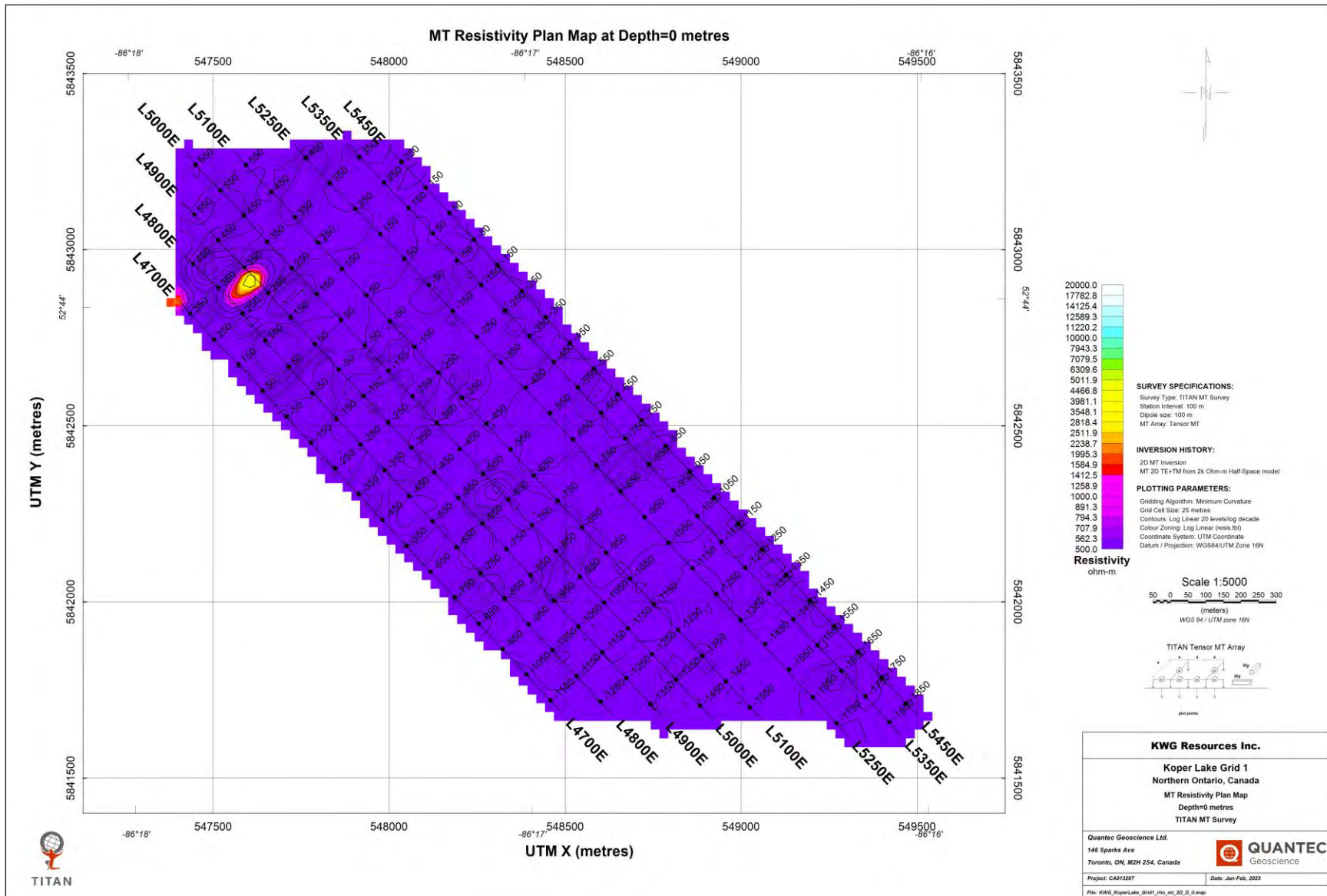


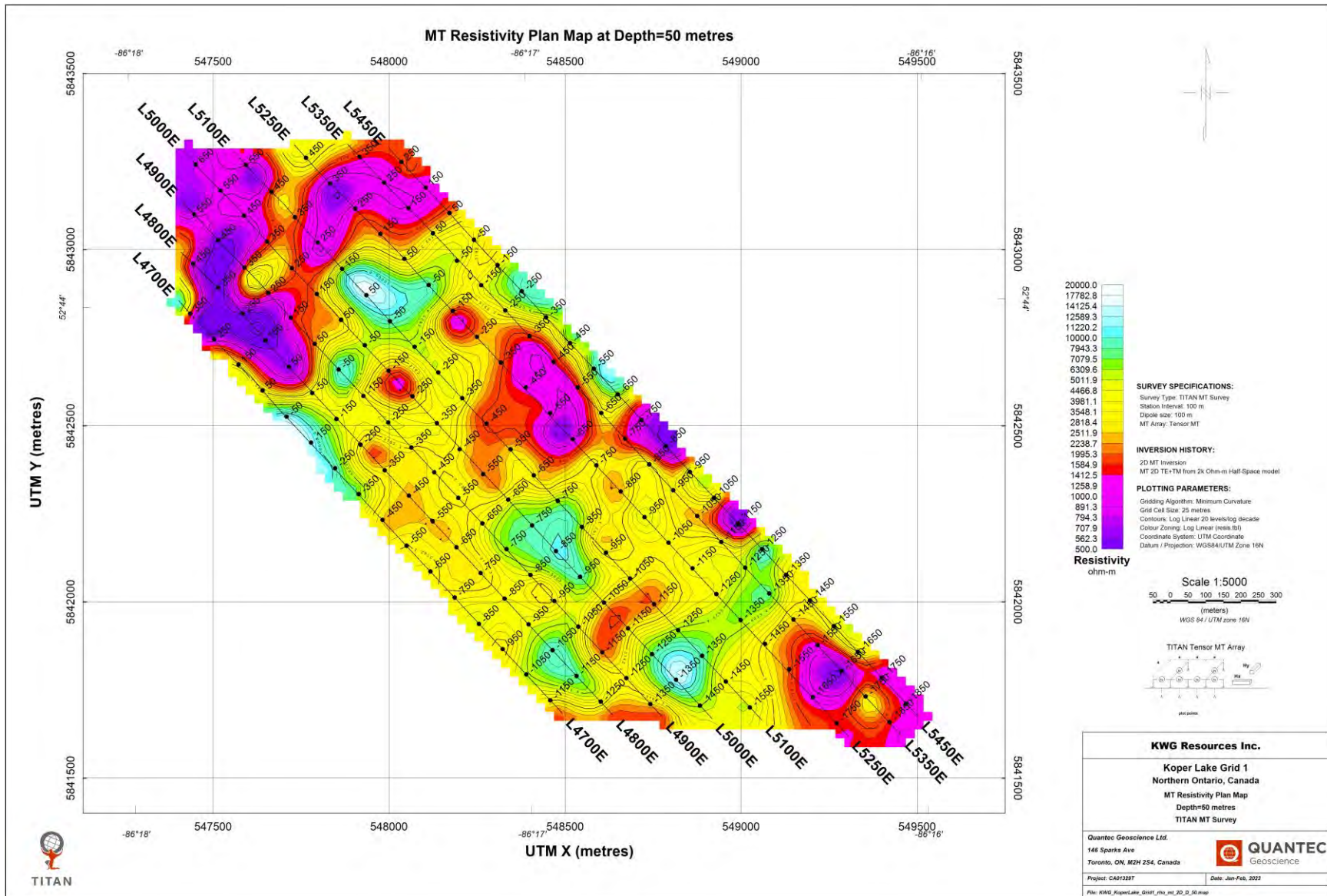


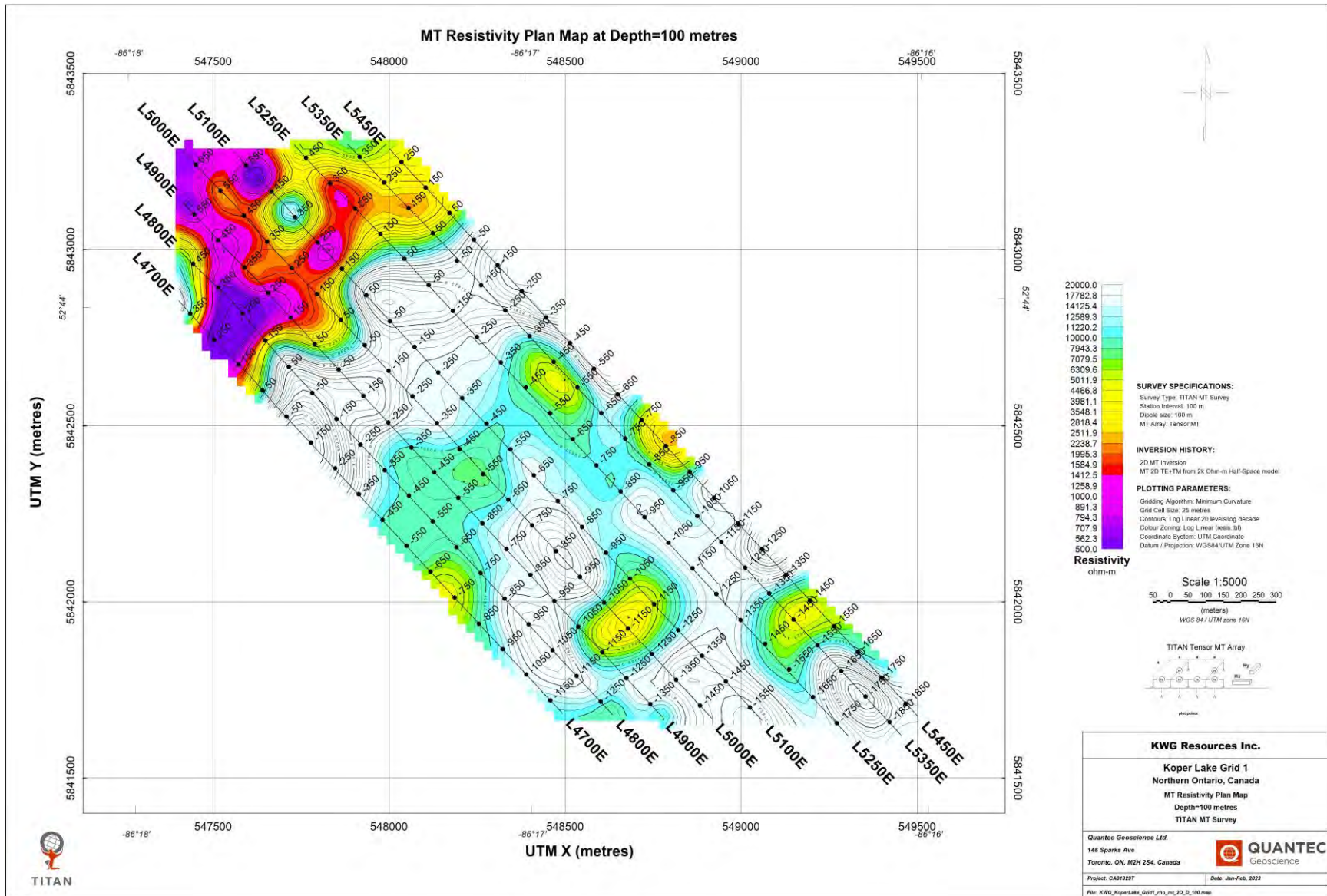
APPENDIX C. RESISTIVITY PLAN MAPS (DEPTH LEVELS)

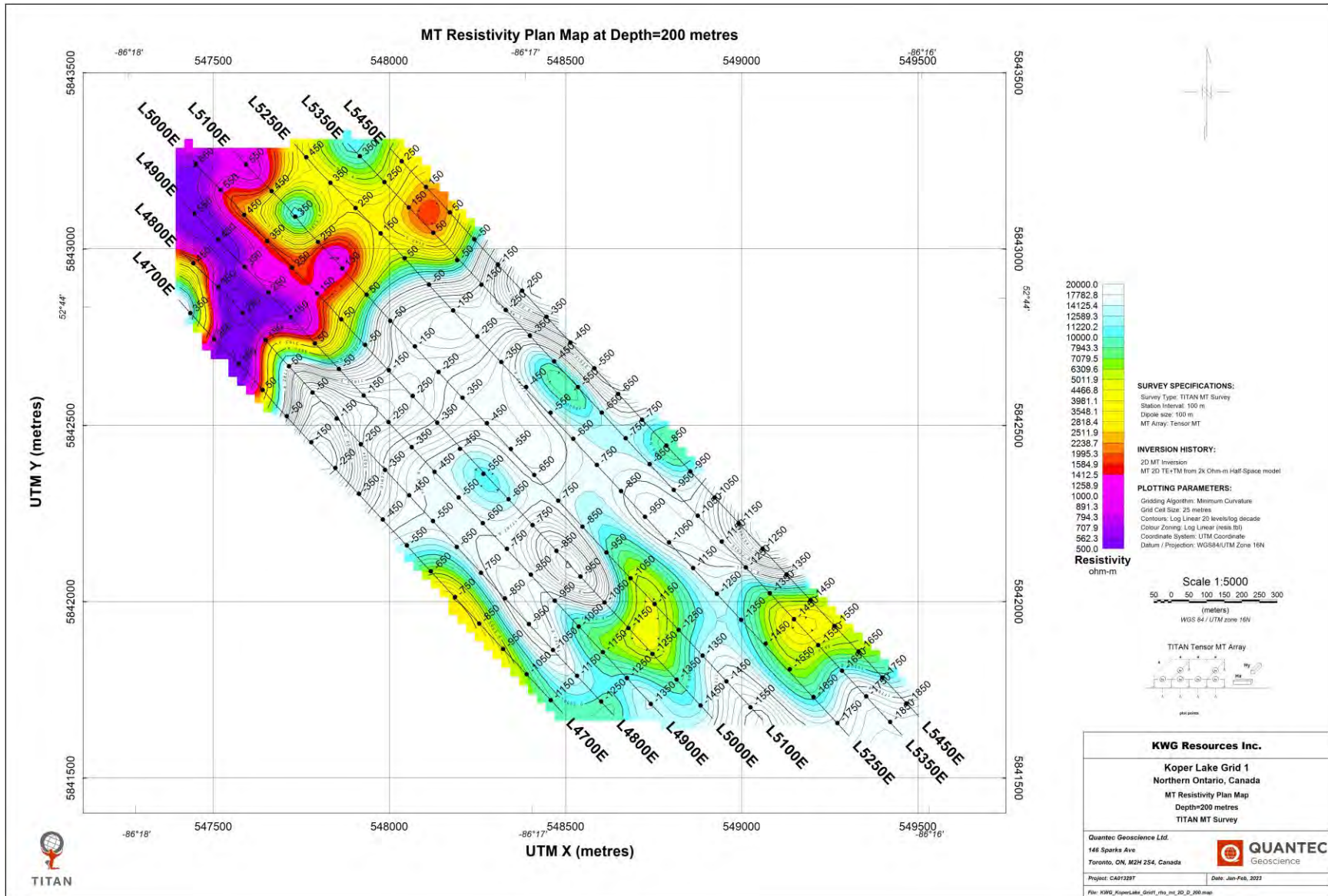
C.1. 2D - MT RESISTIVITY PLAN MAPS – GRID-1

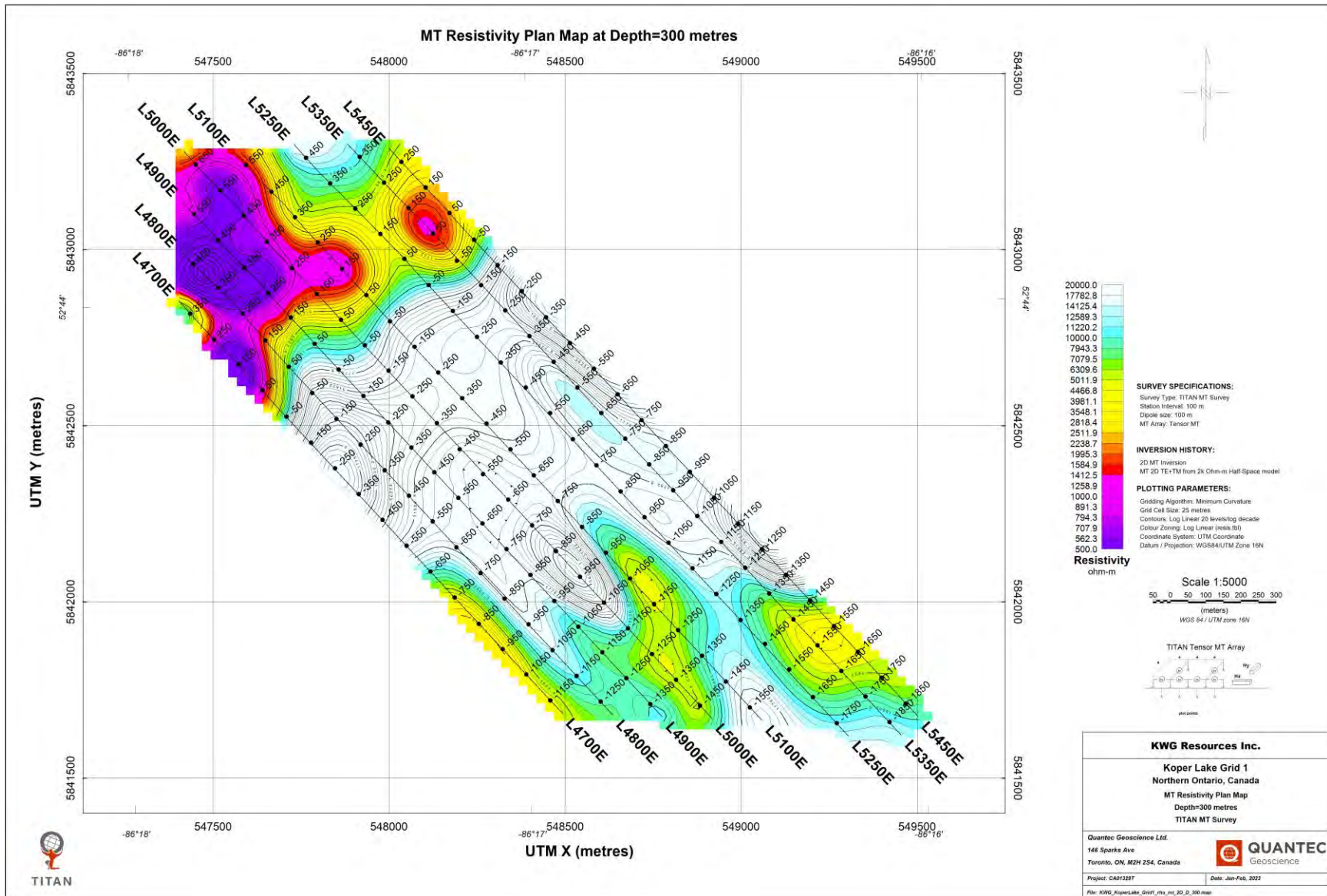


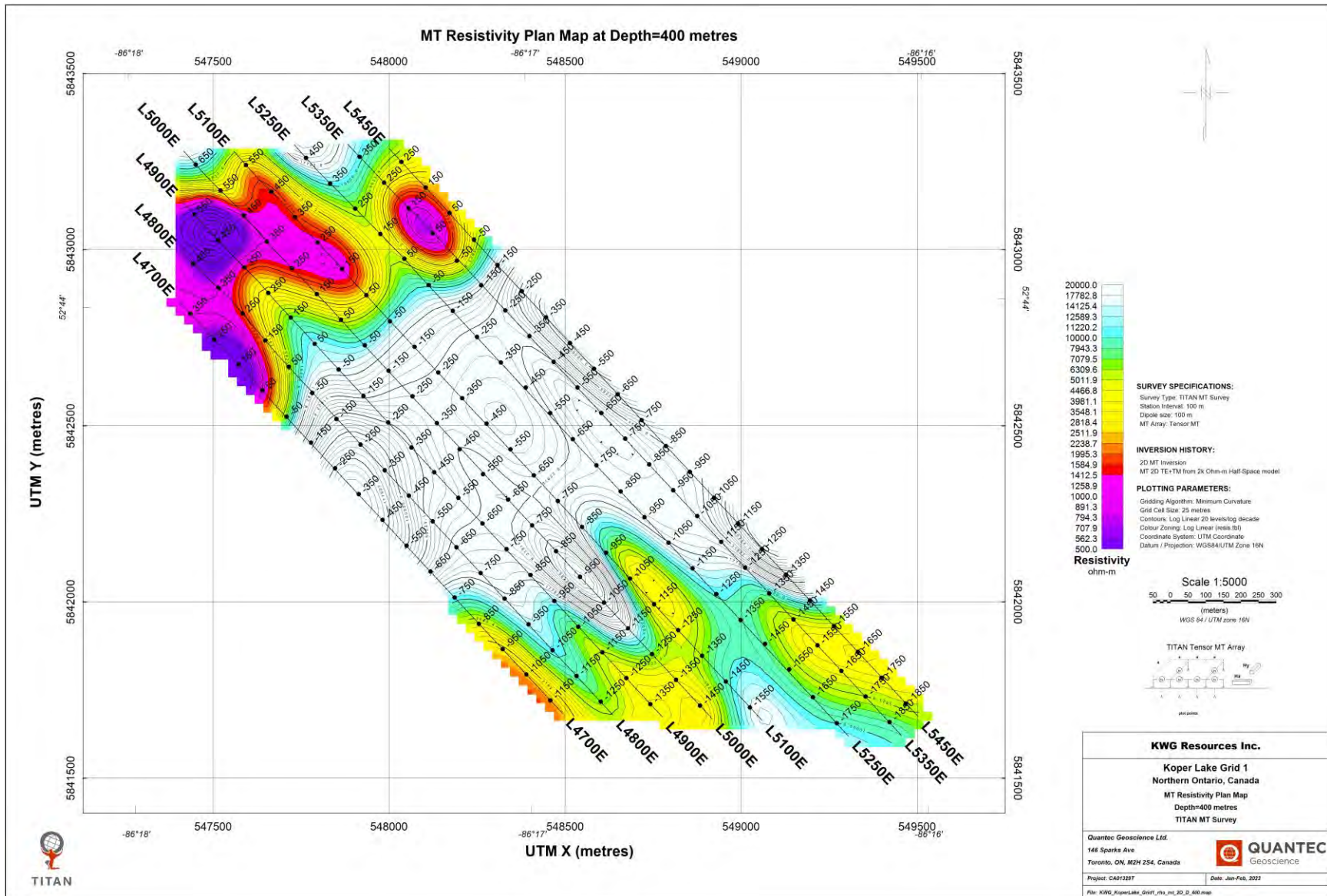


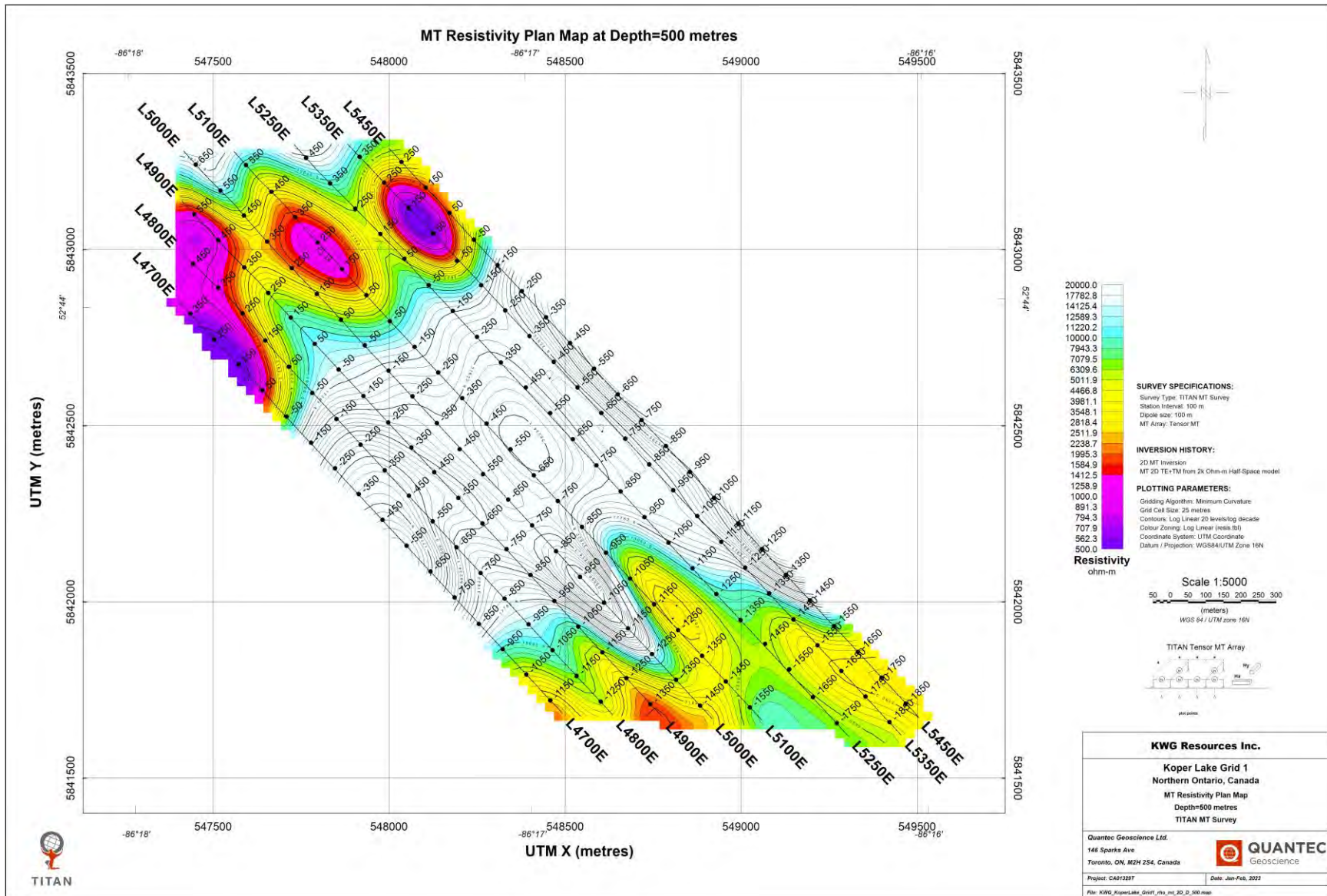


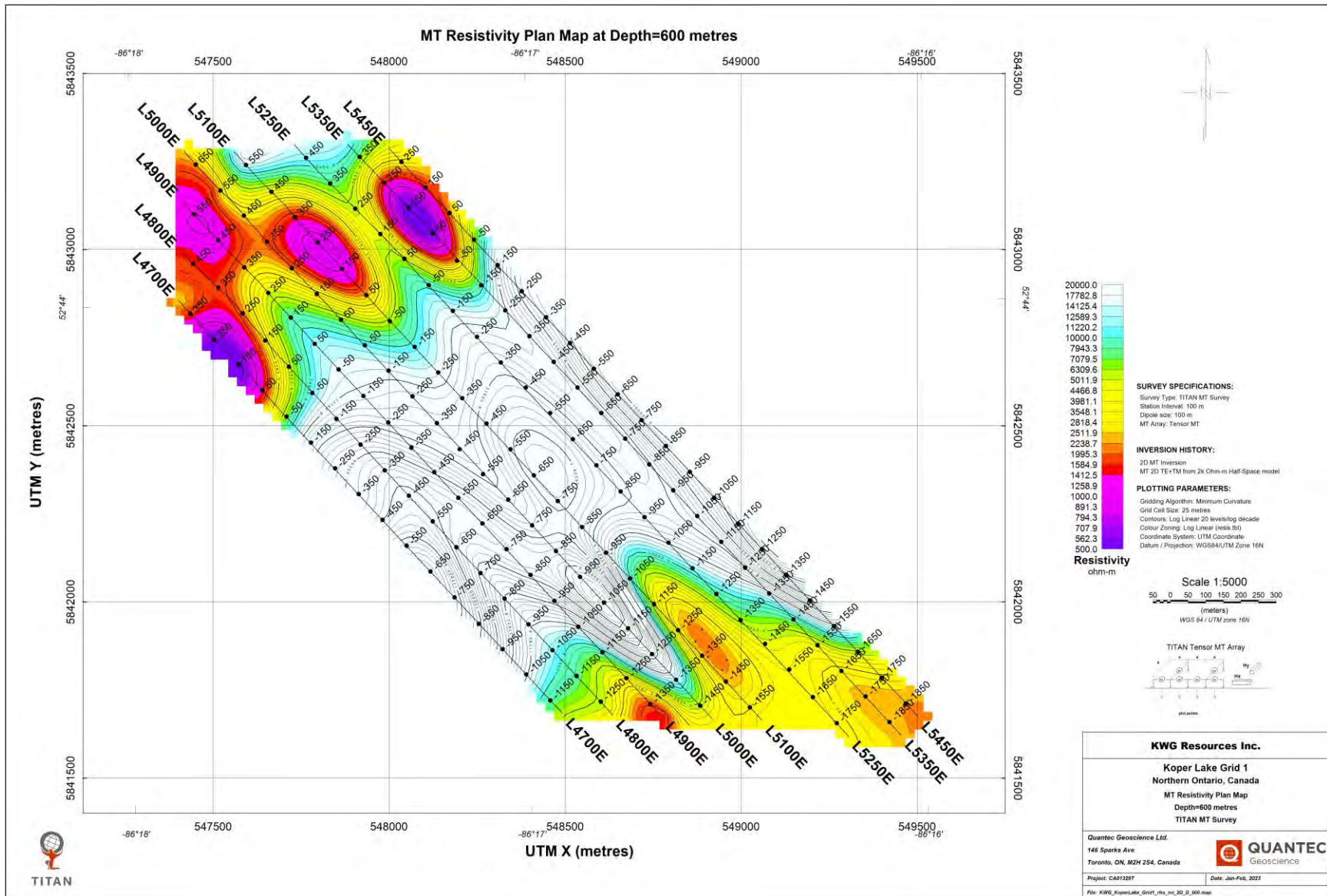


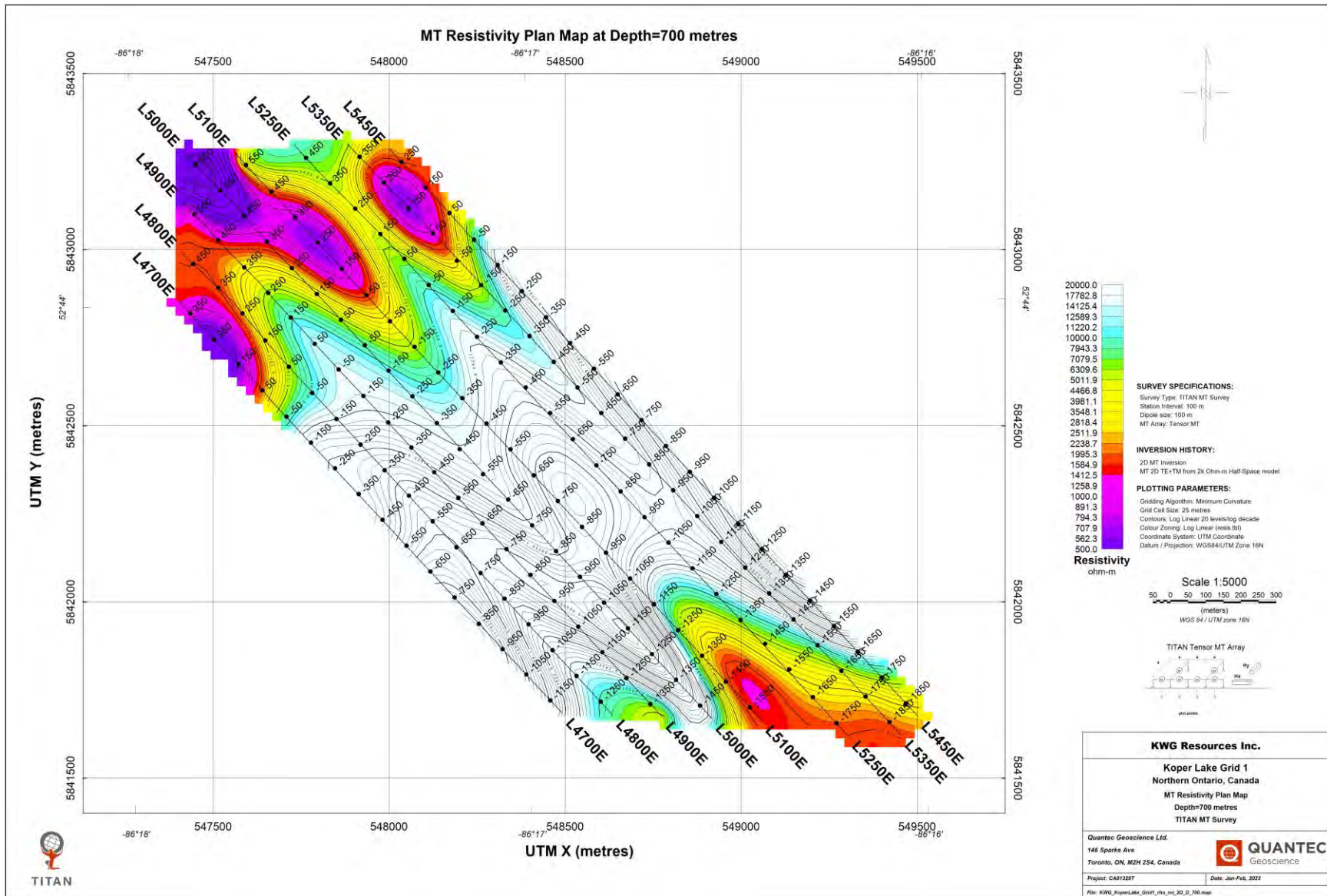


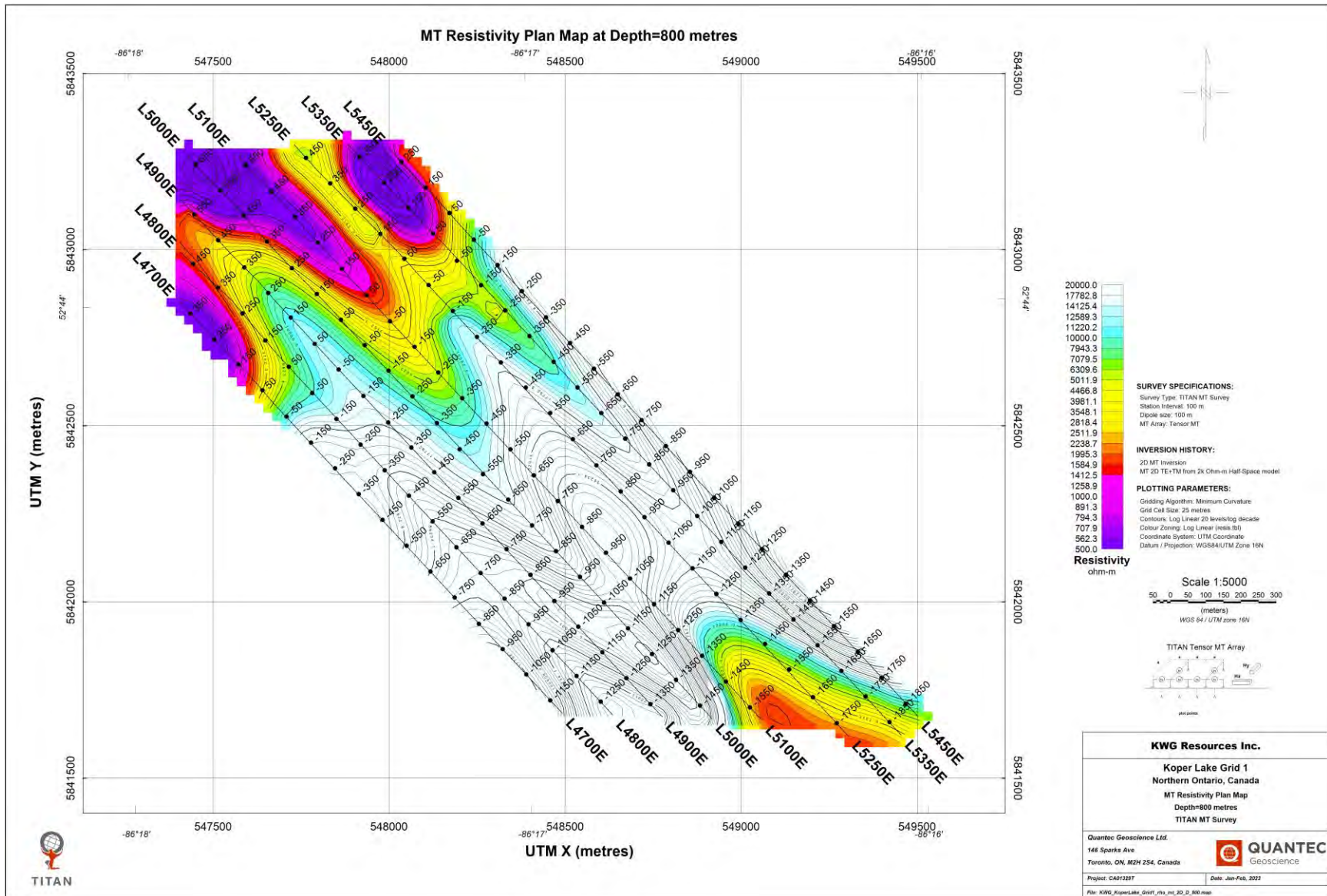


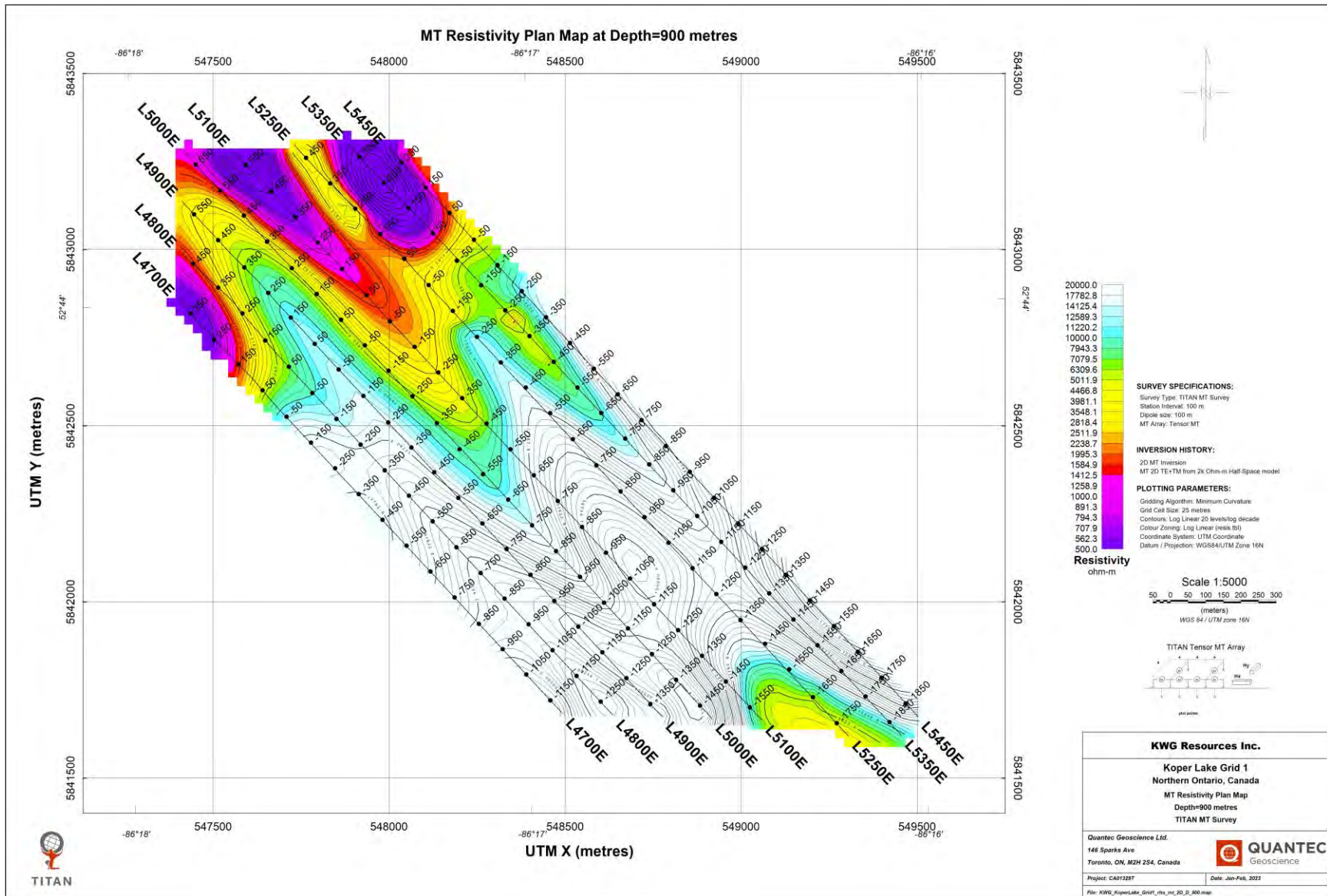


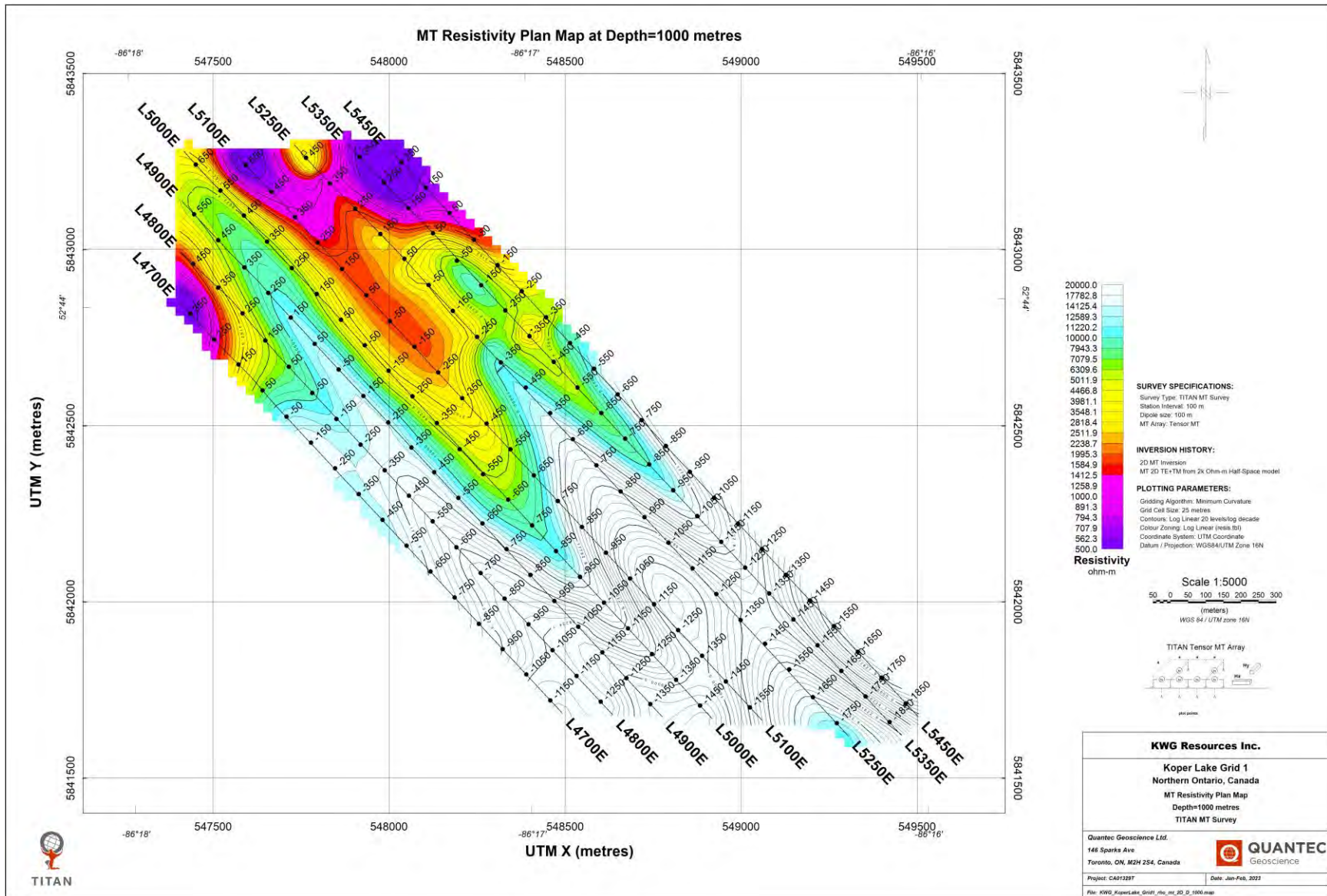


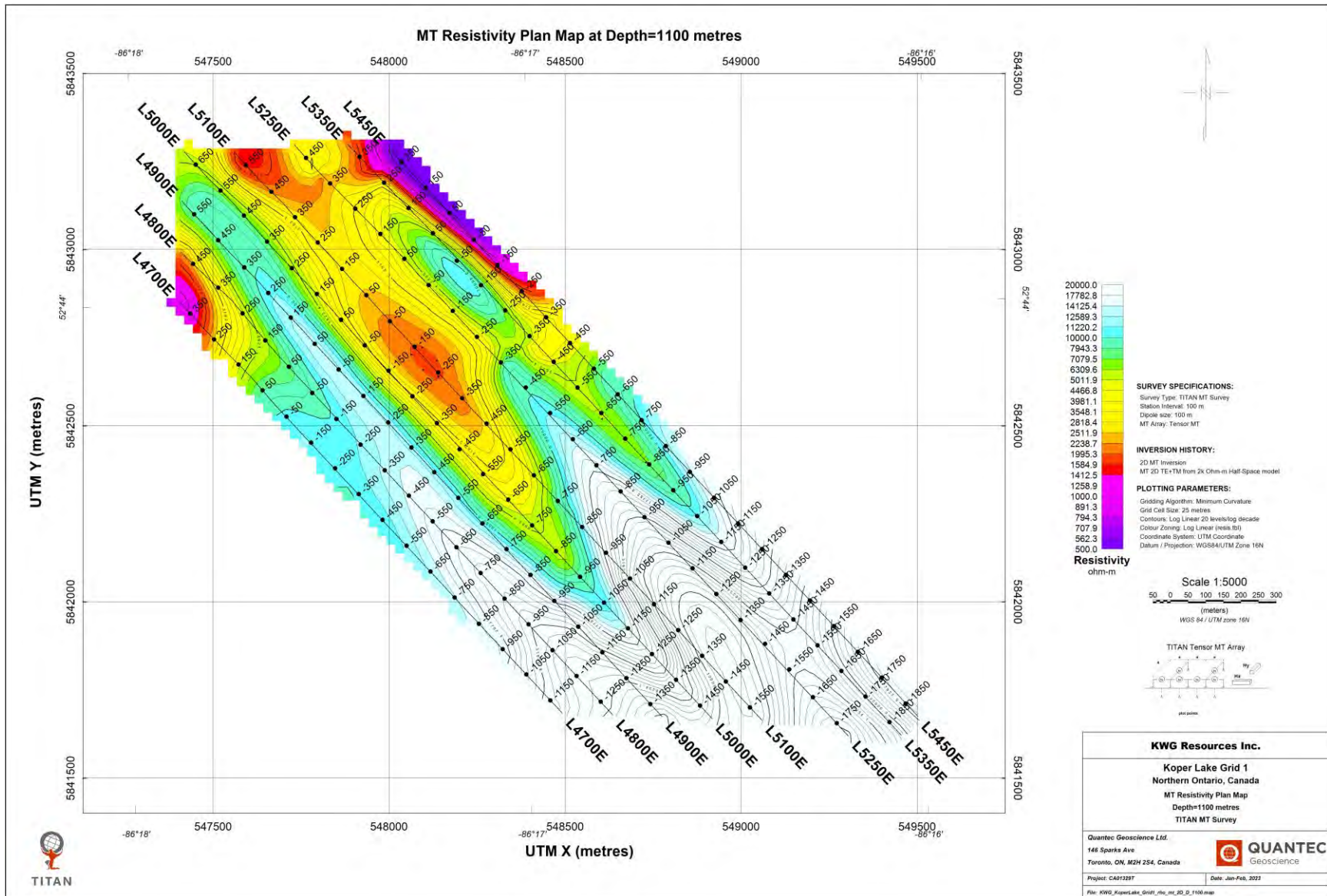


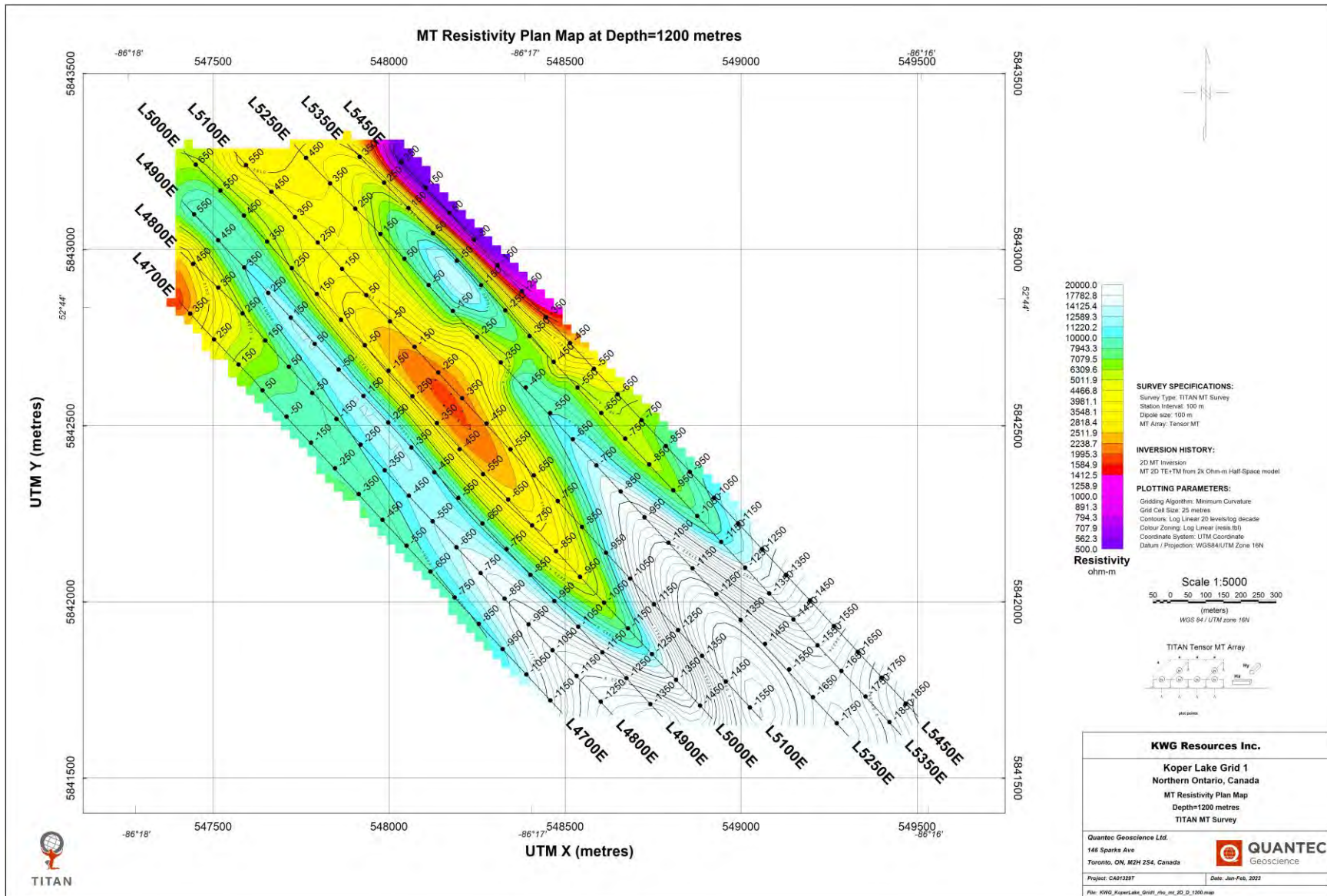


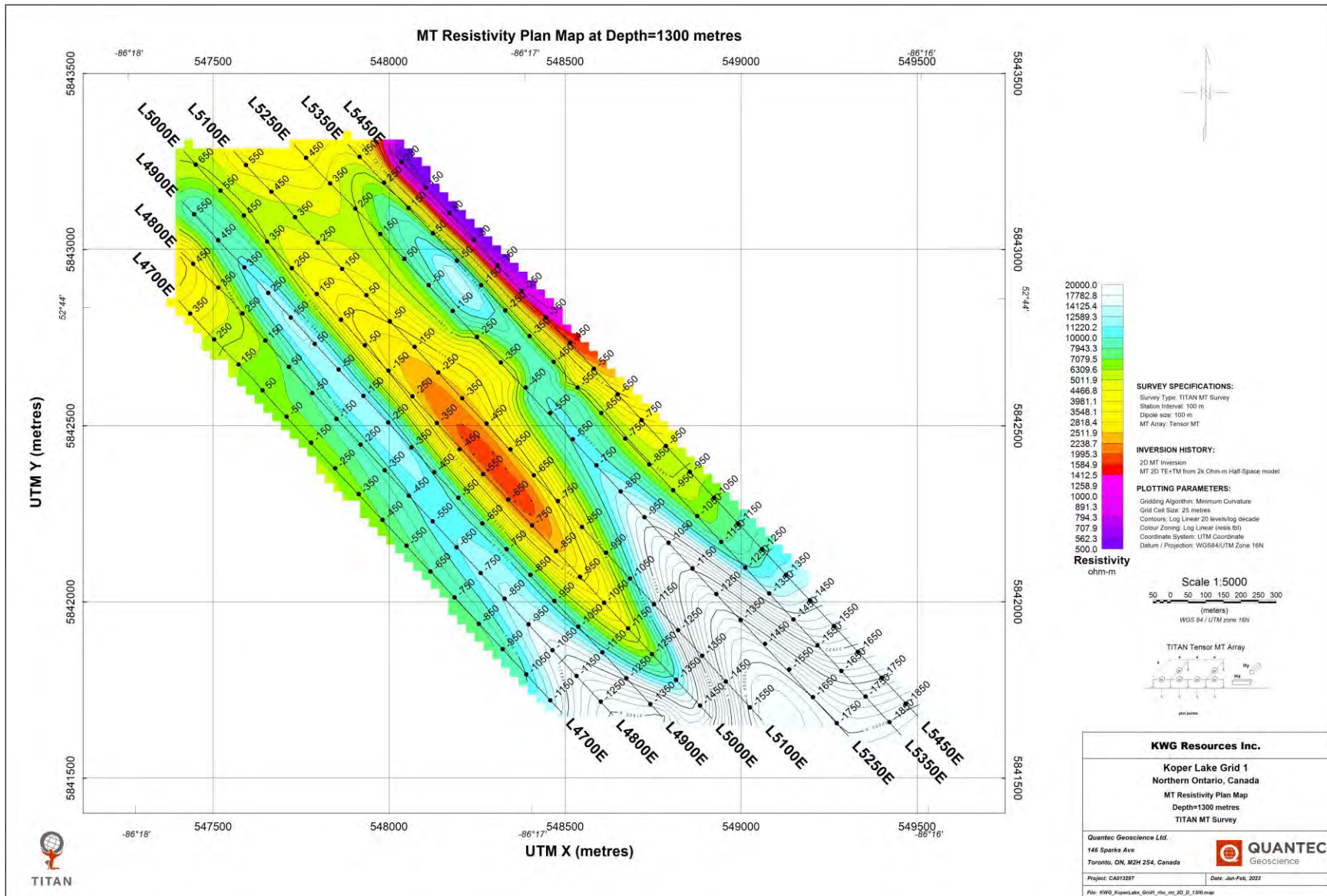


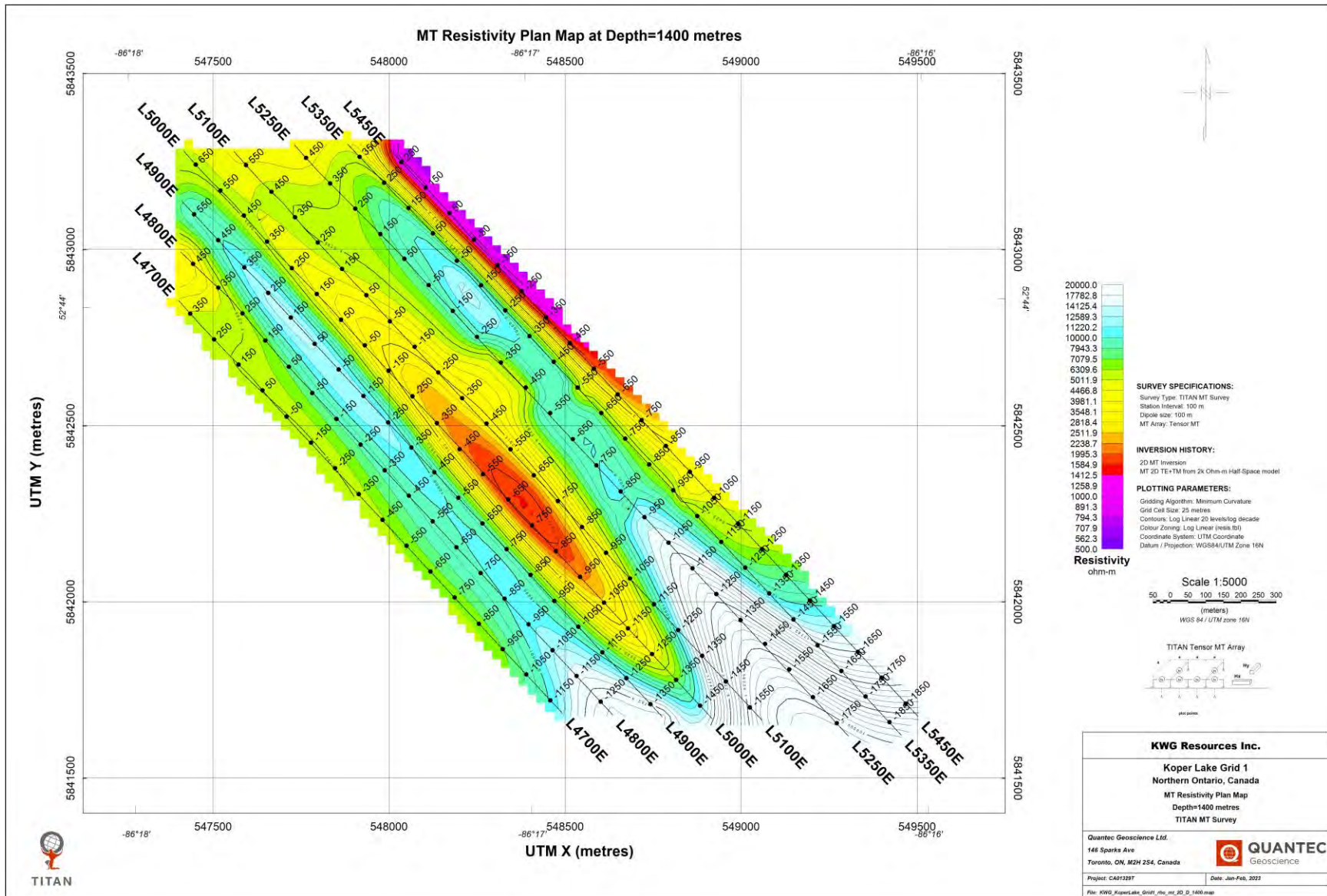


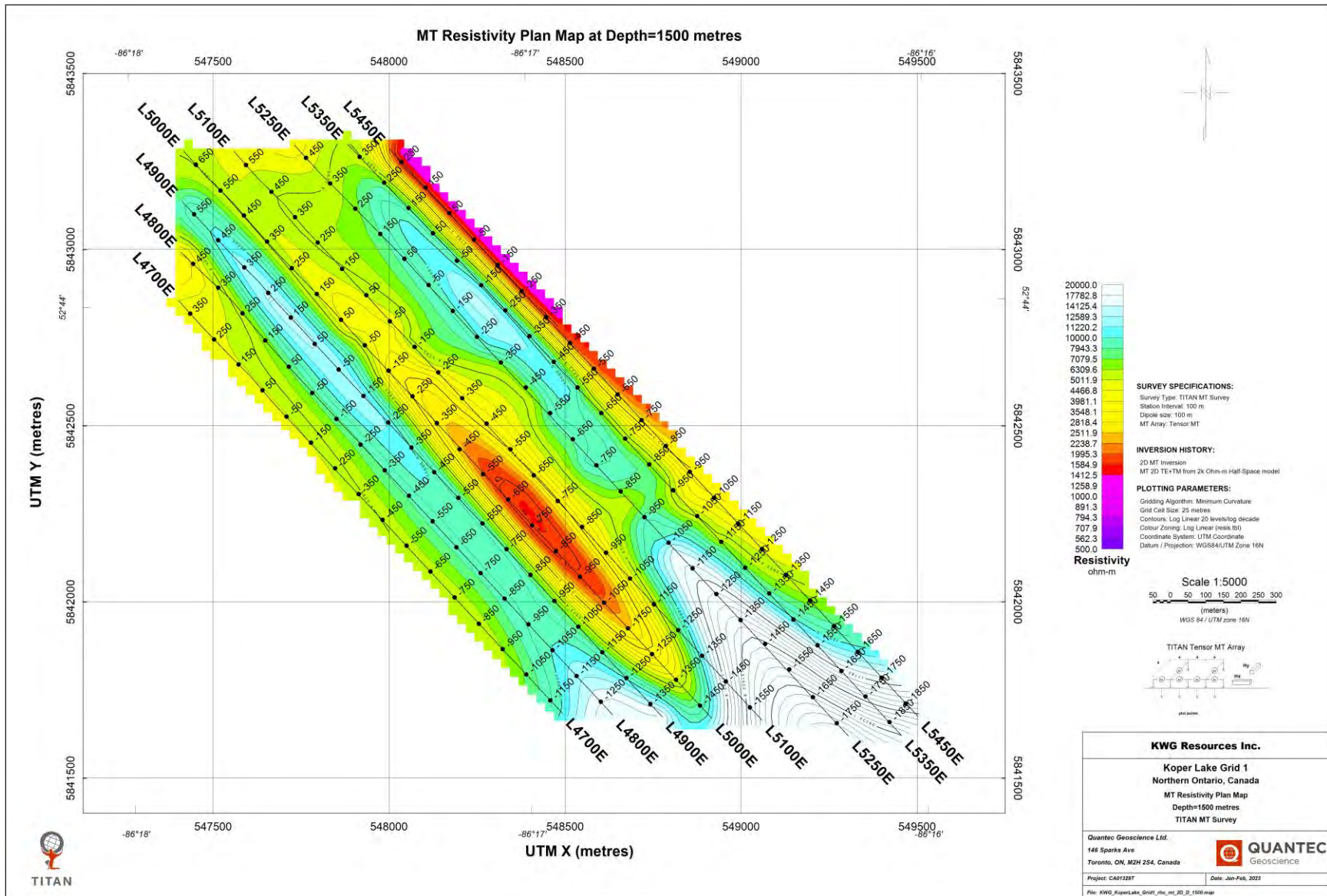


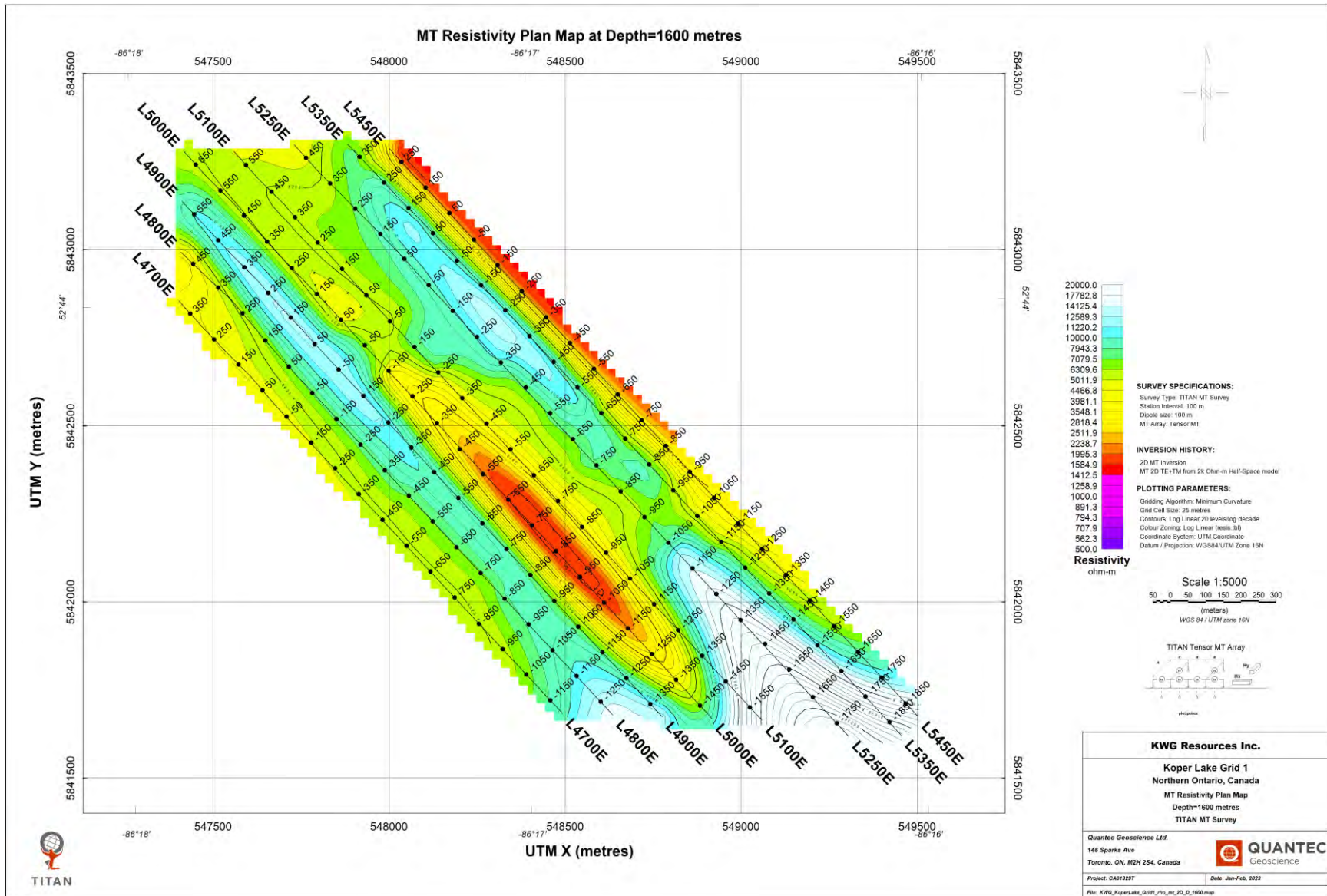


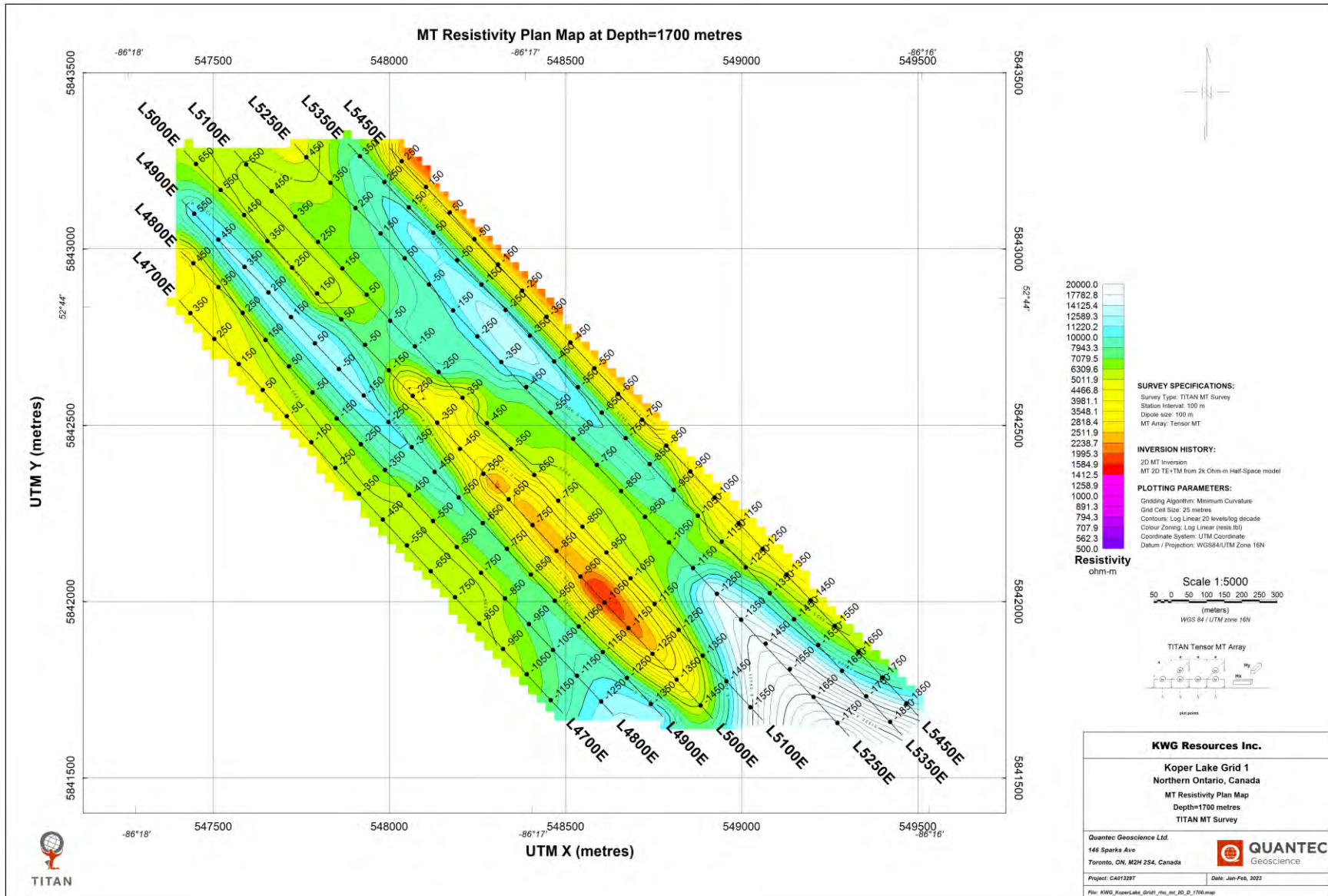


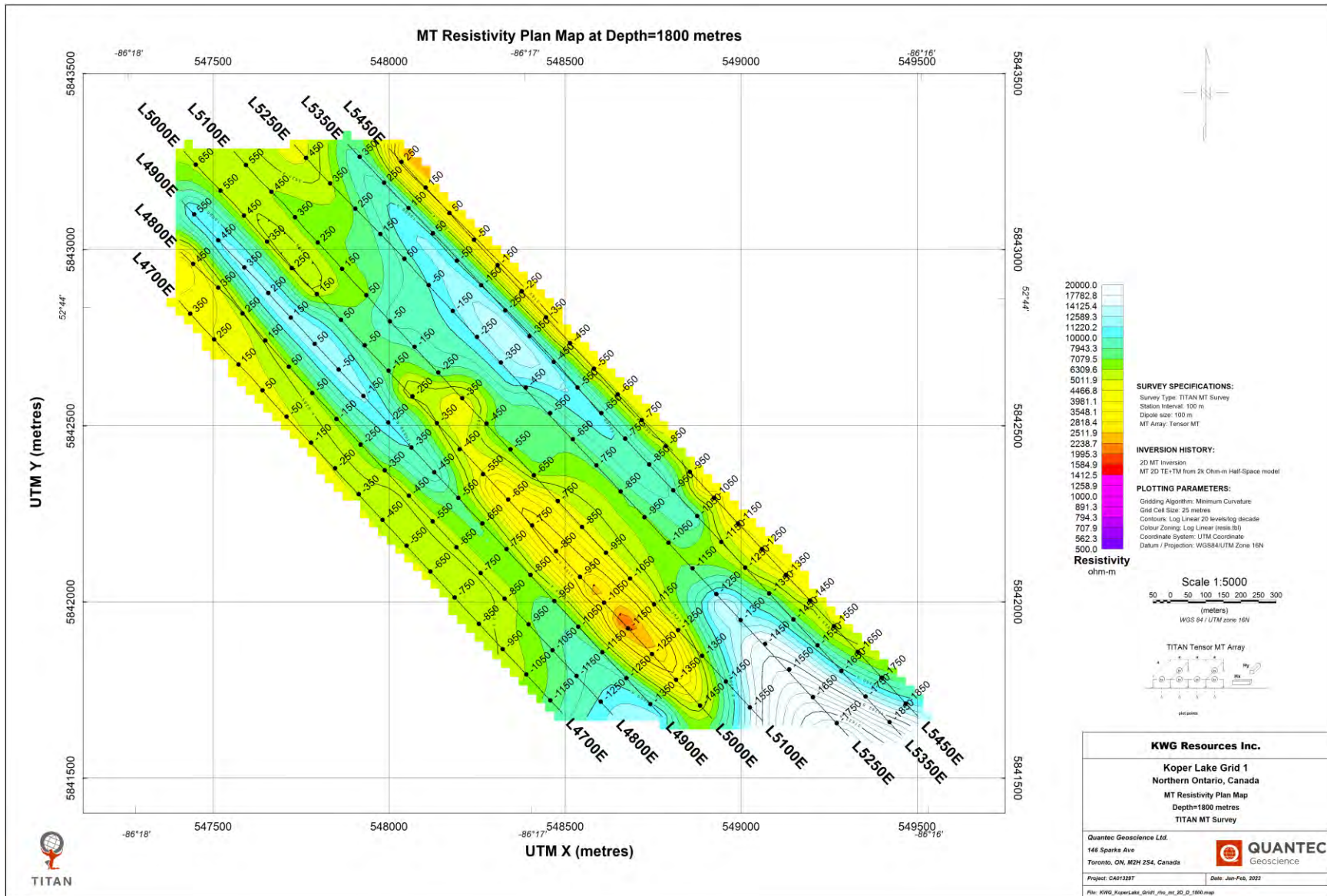


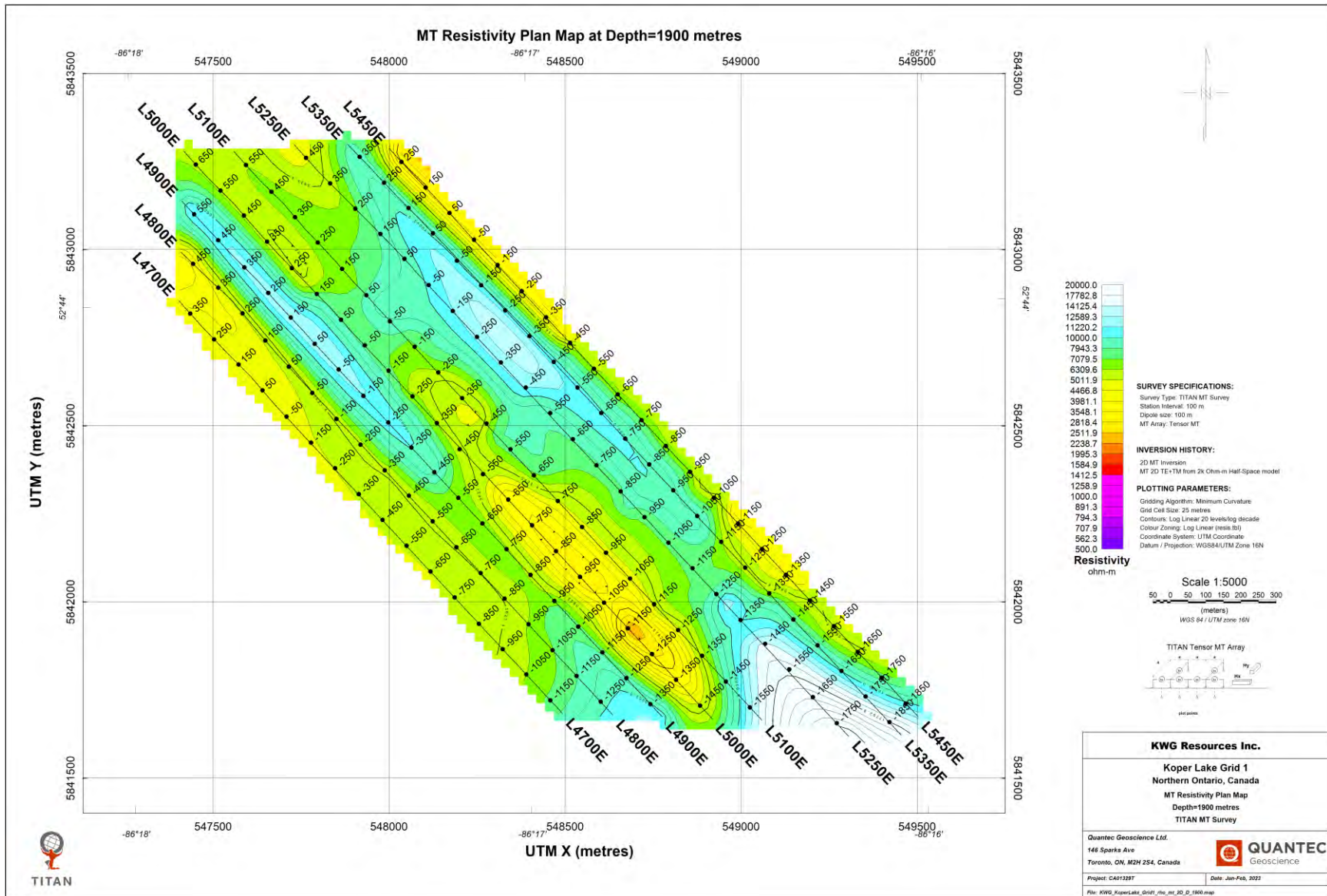


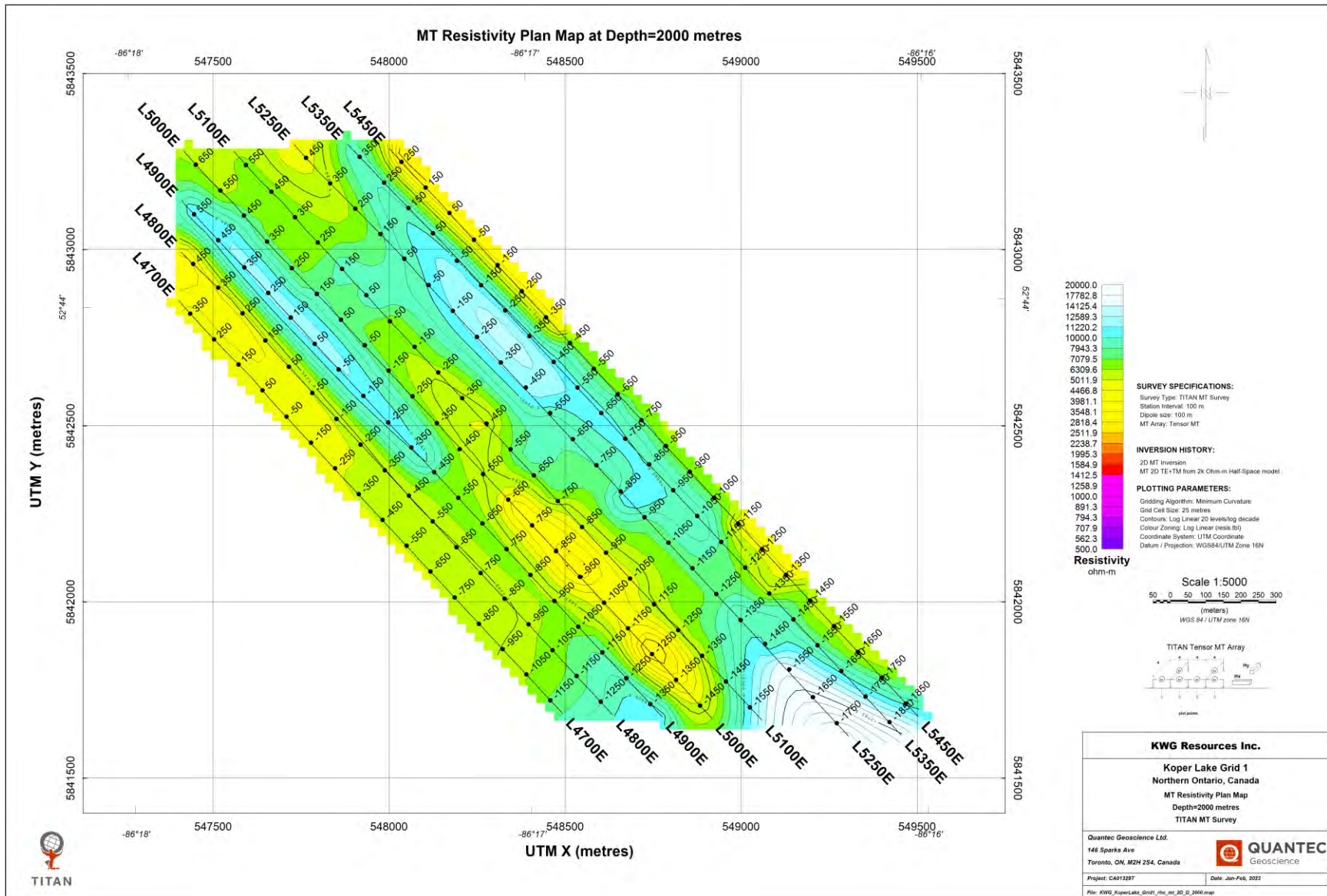




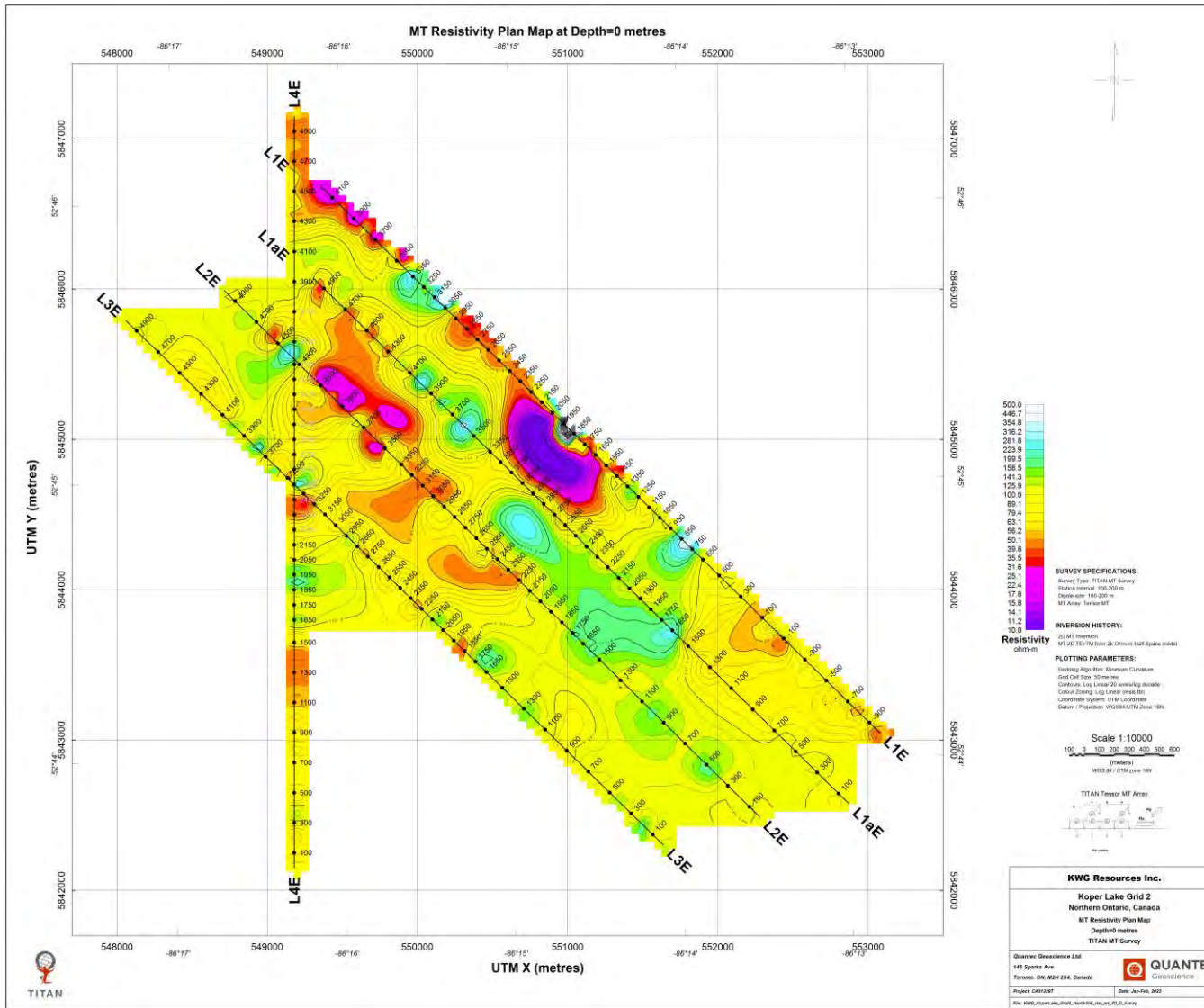


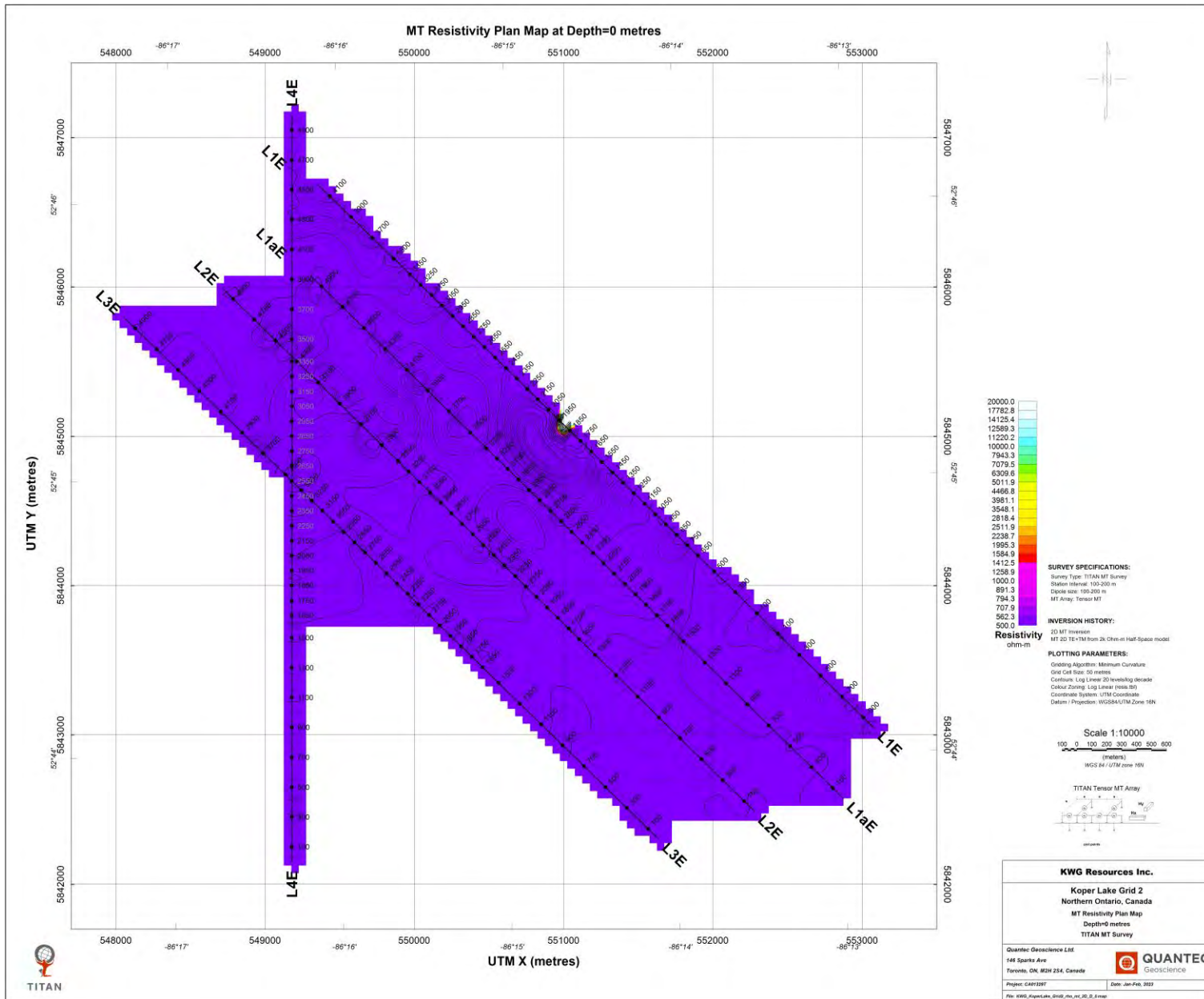


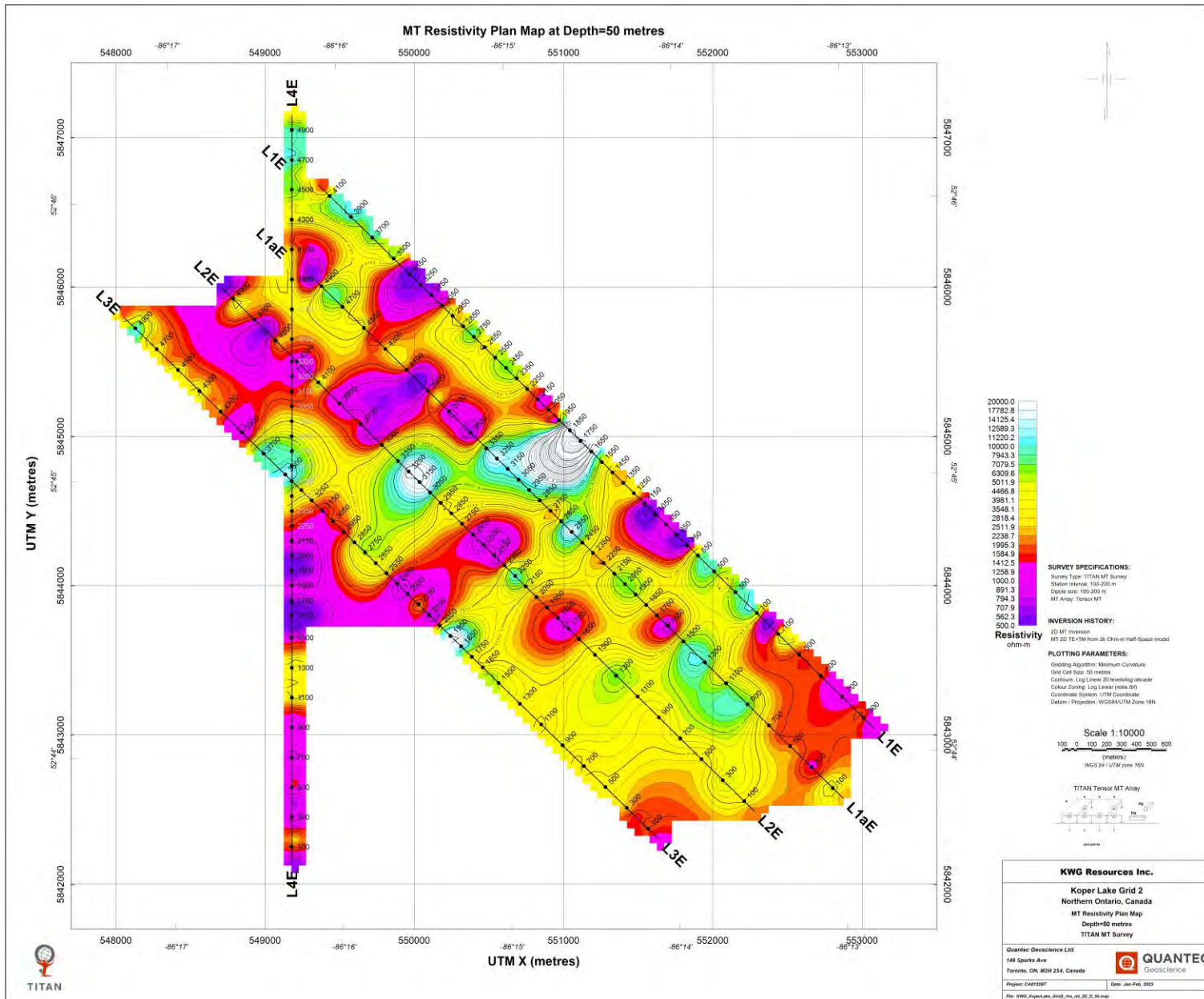


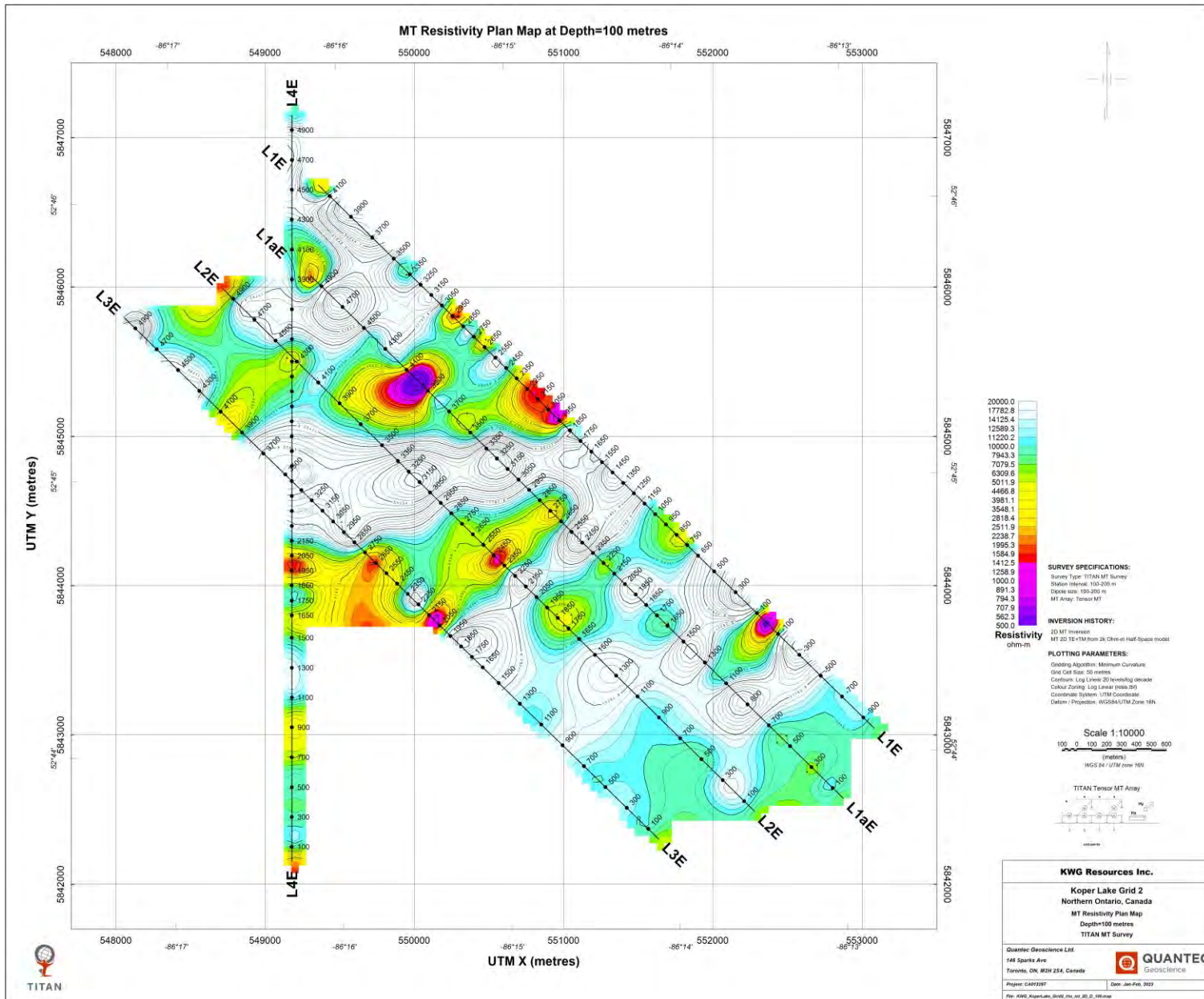


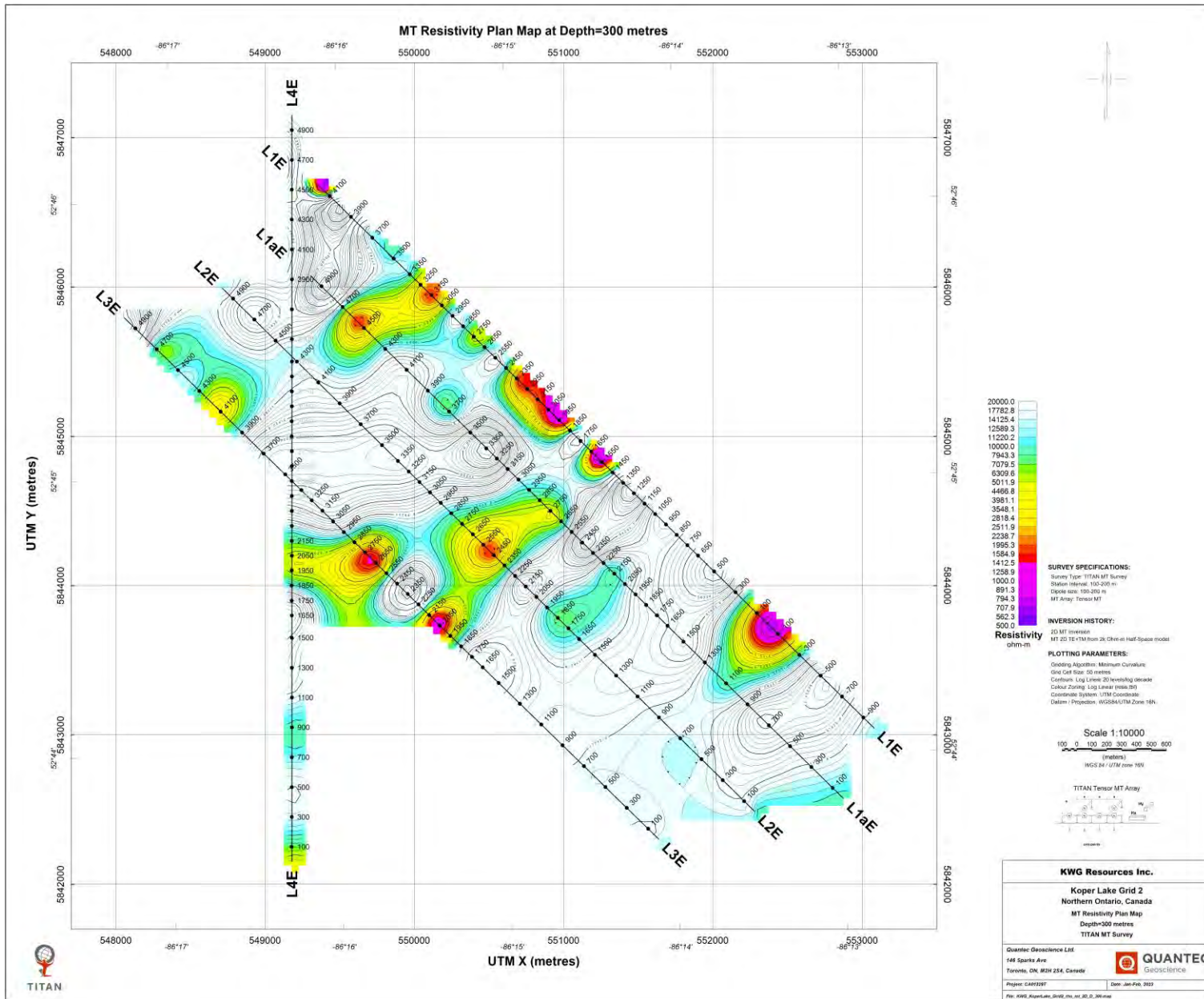
C.2. 2D - MT RESISTIVITY PLAN MAPS – GRID-2

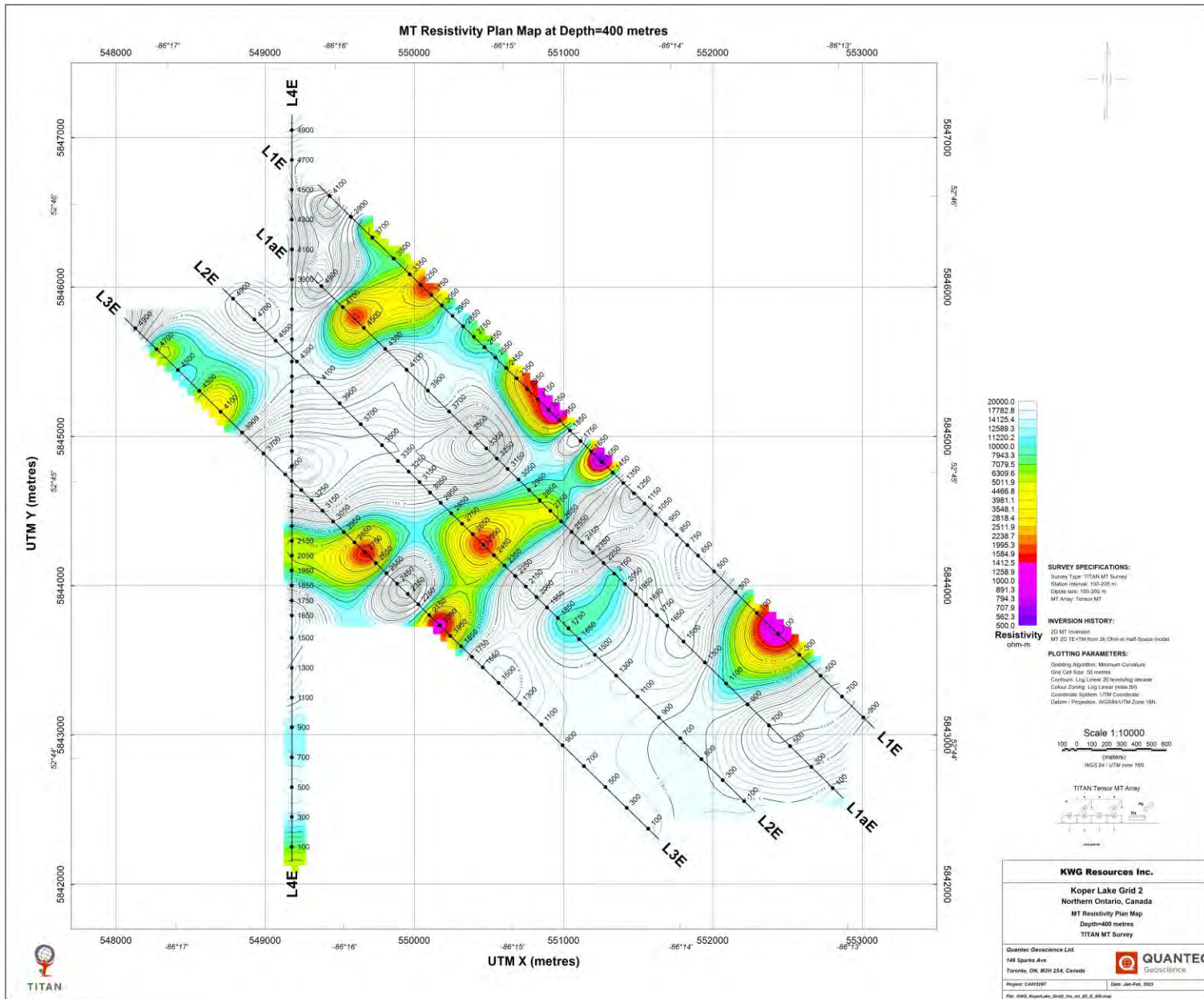


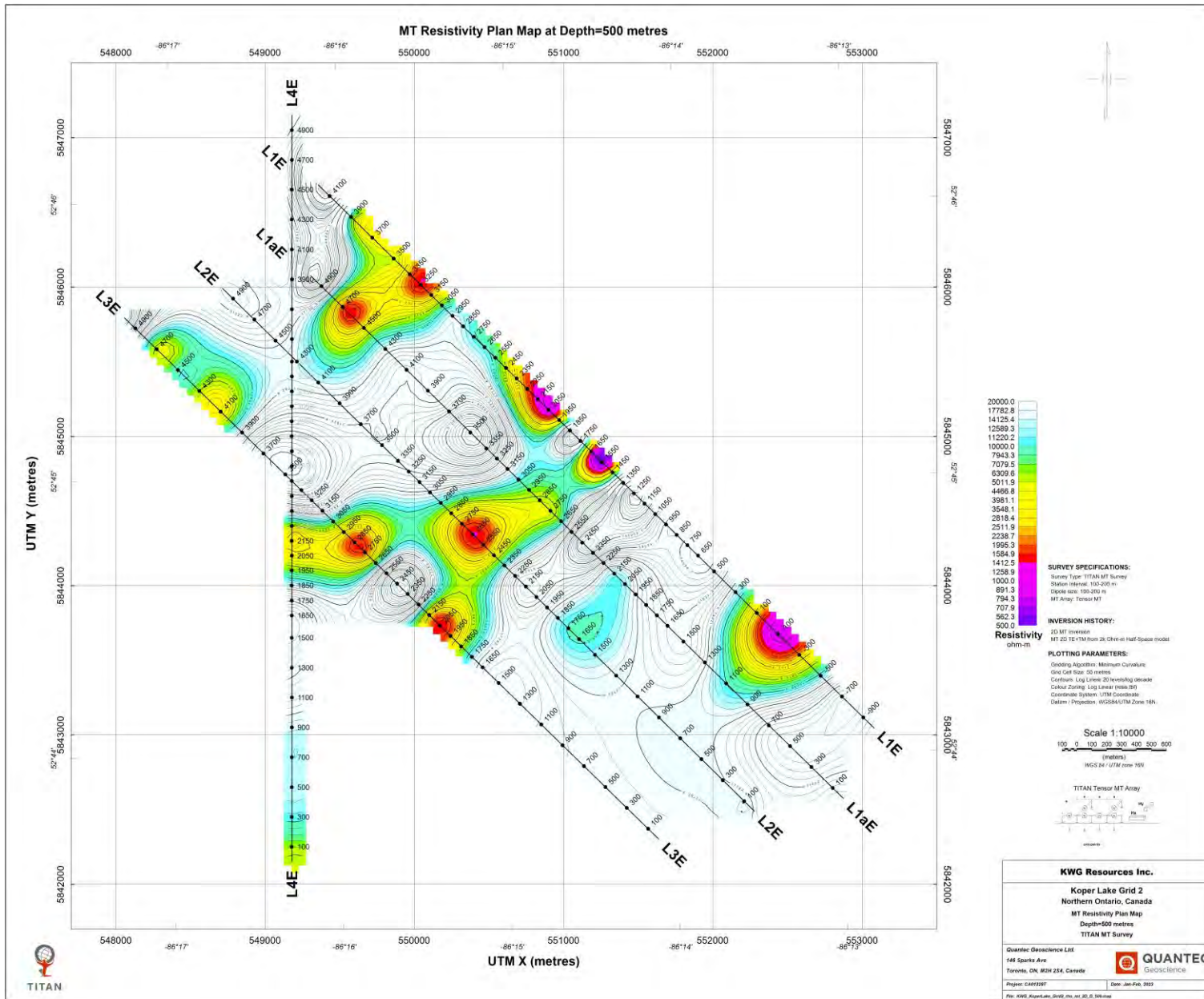


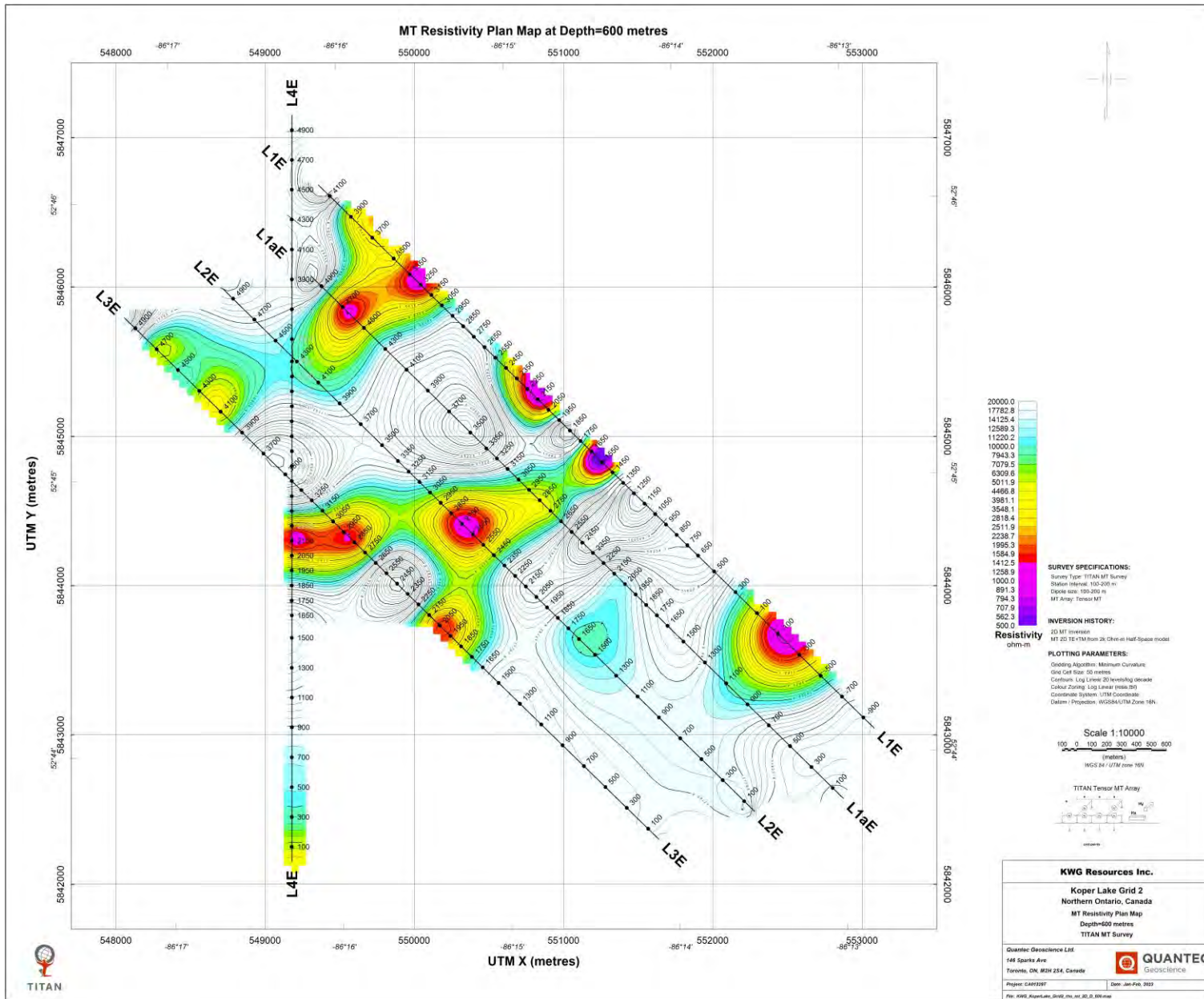


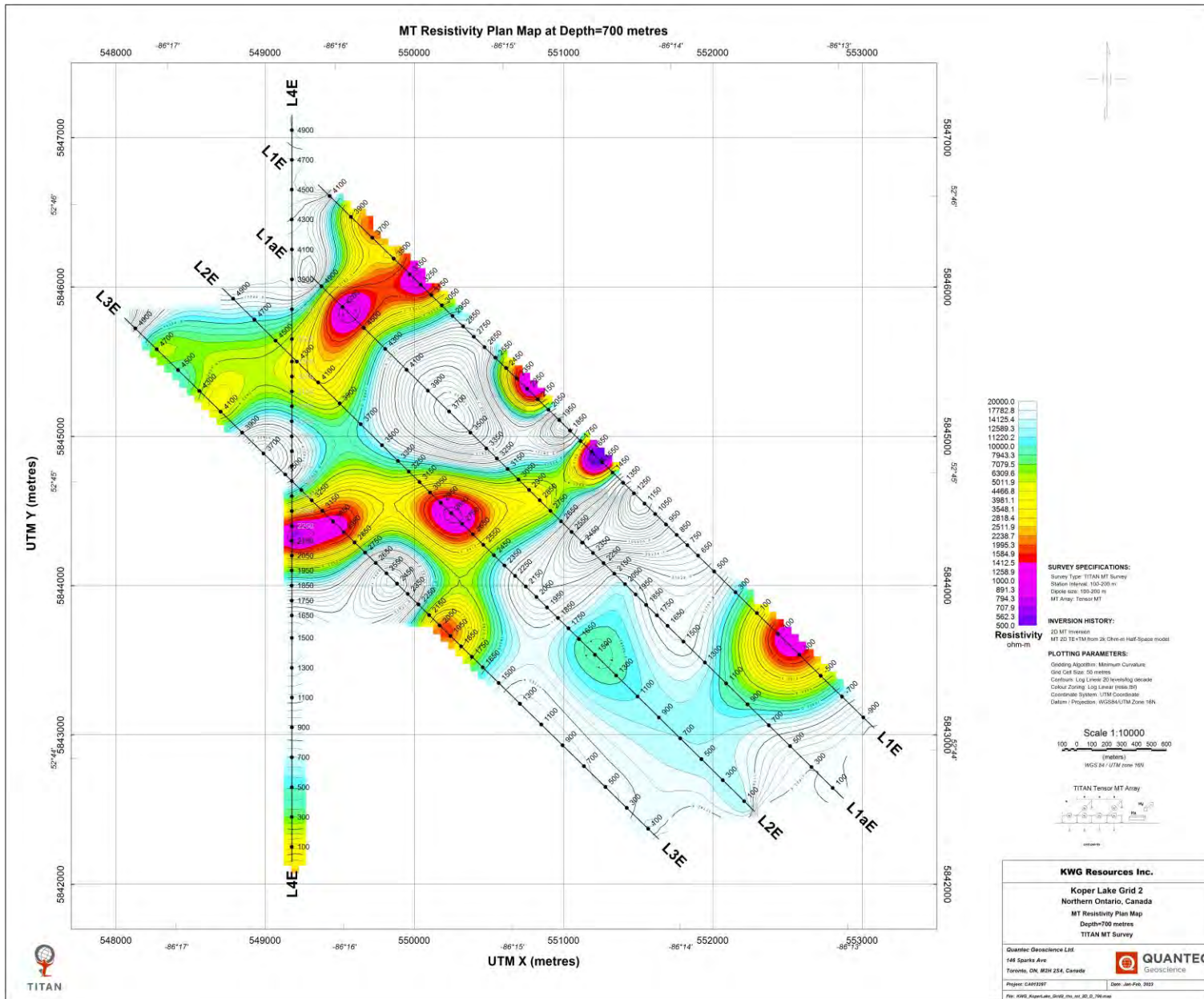


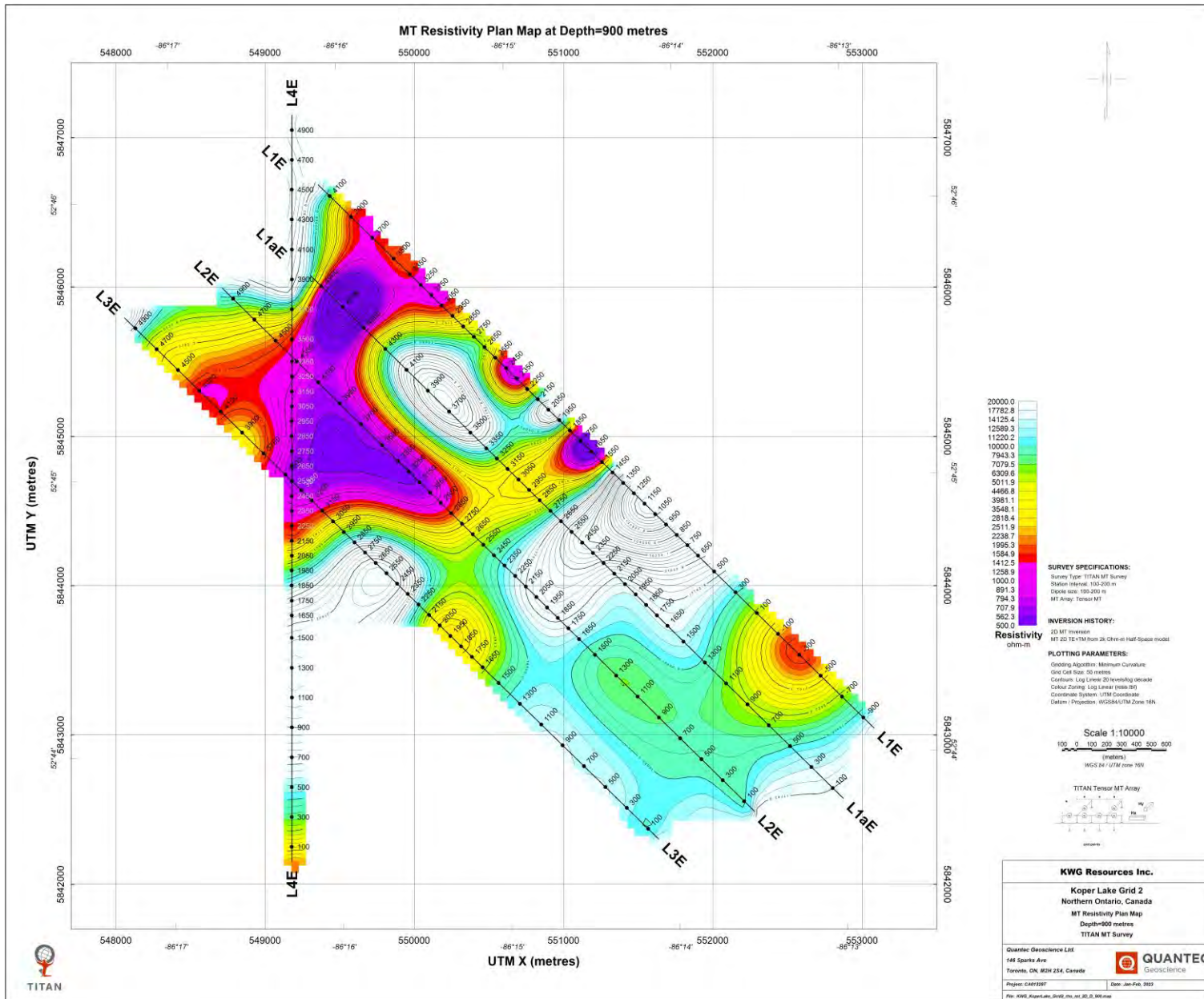


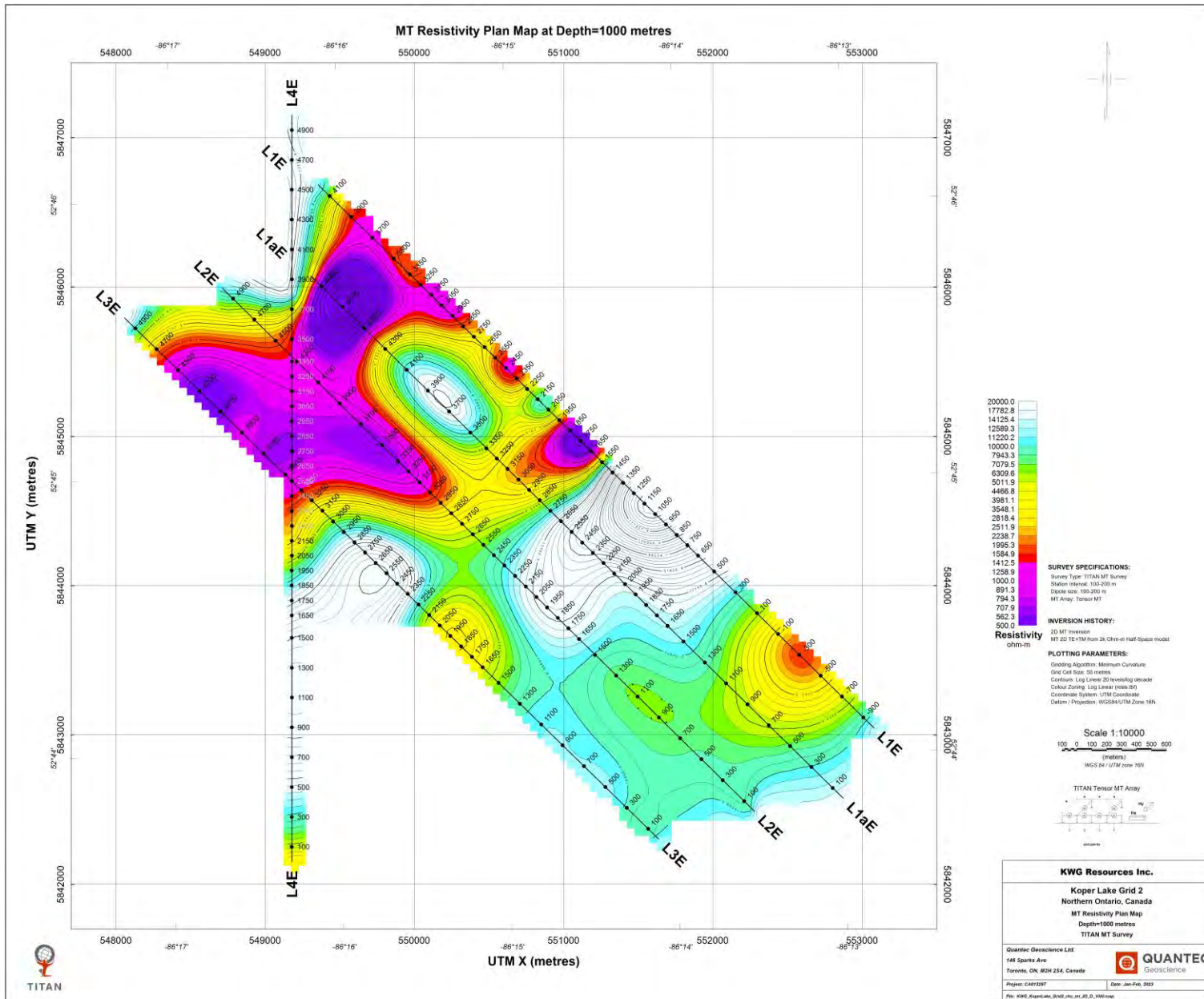


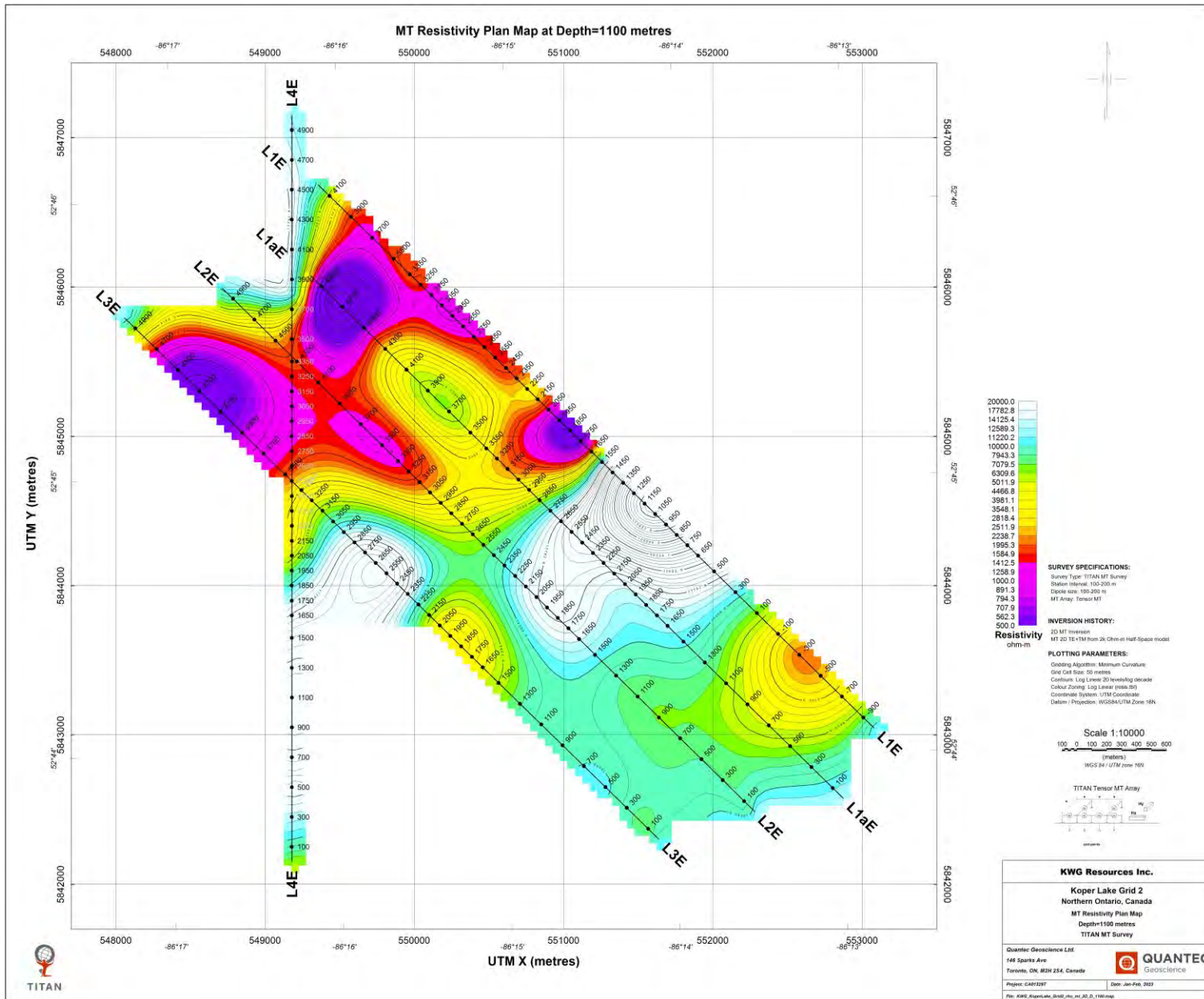


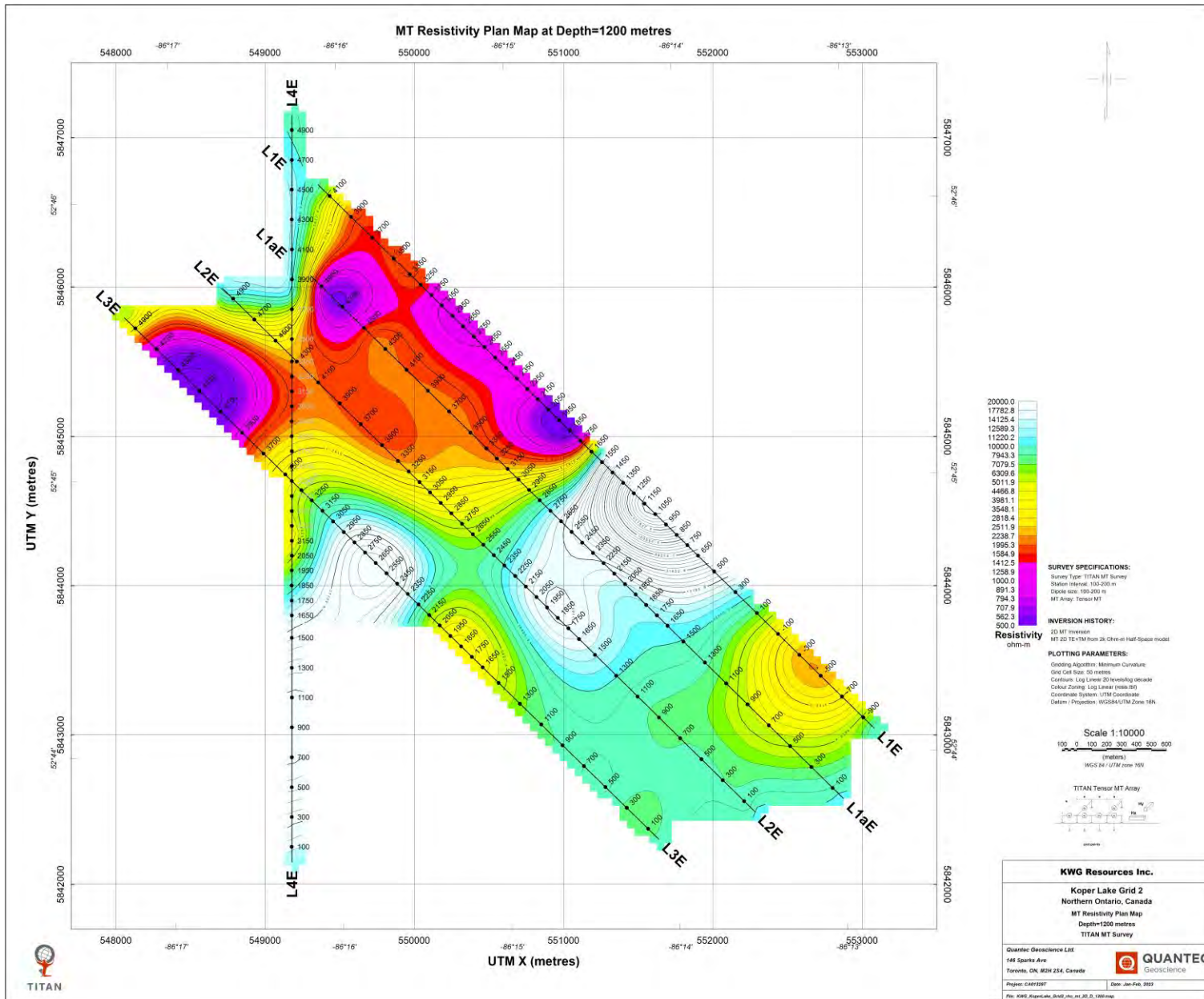


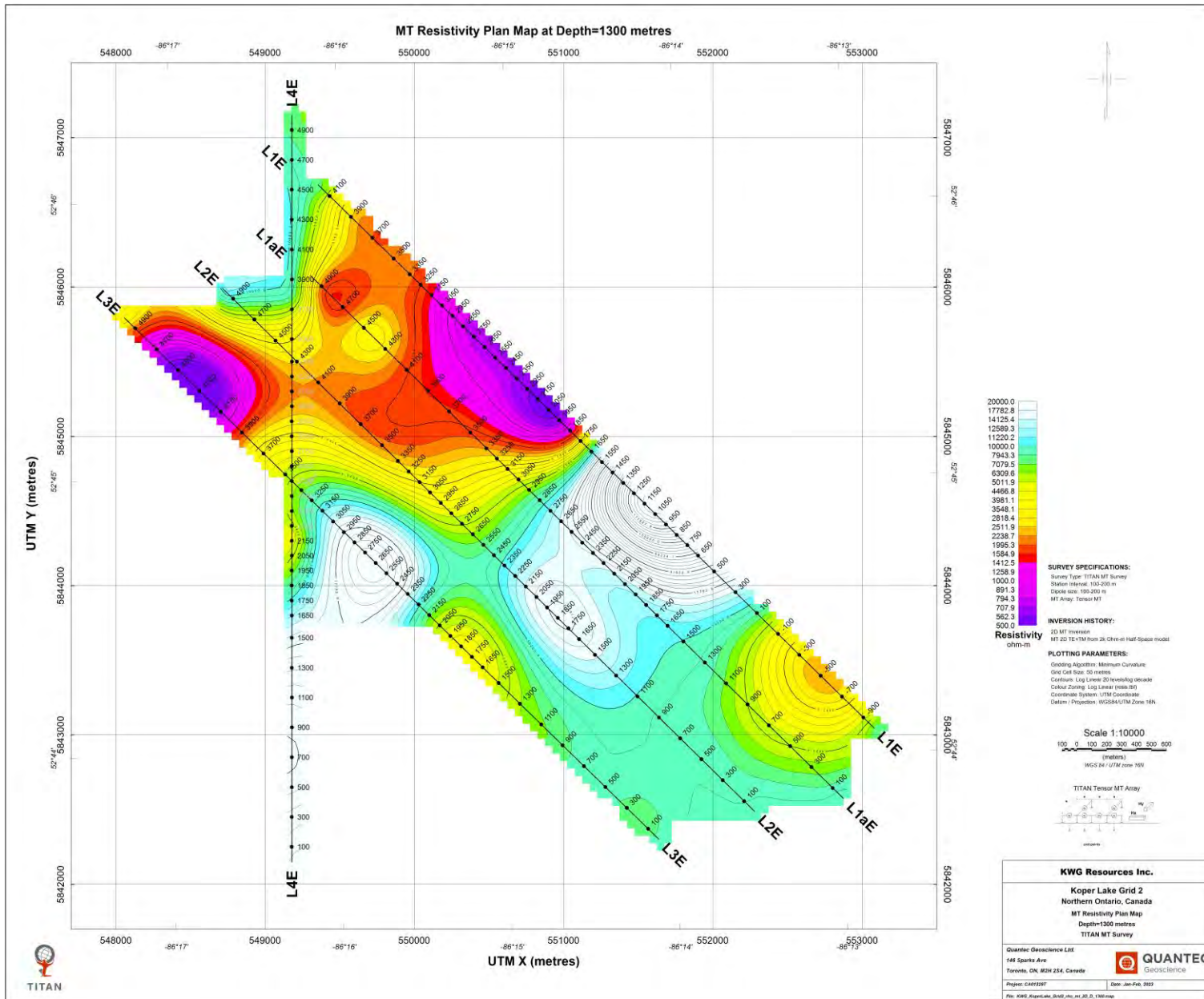


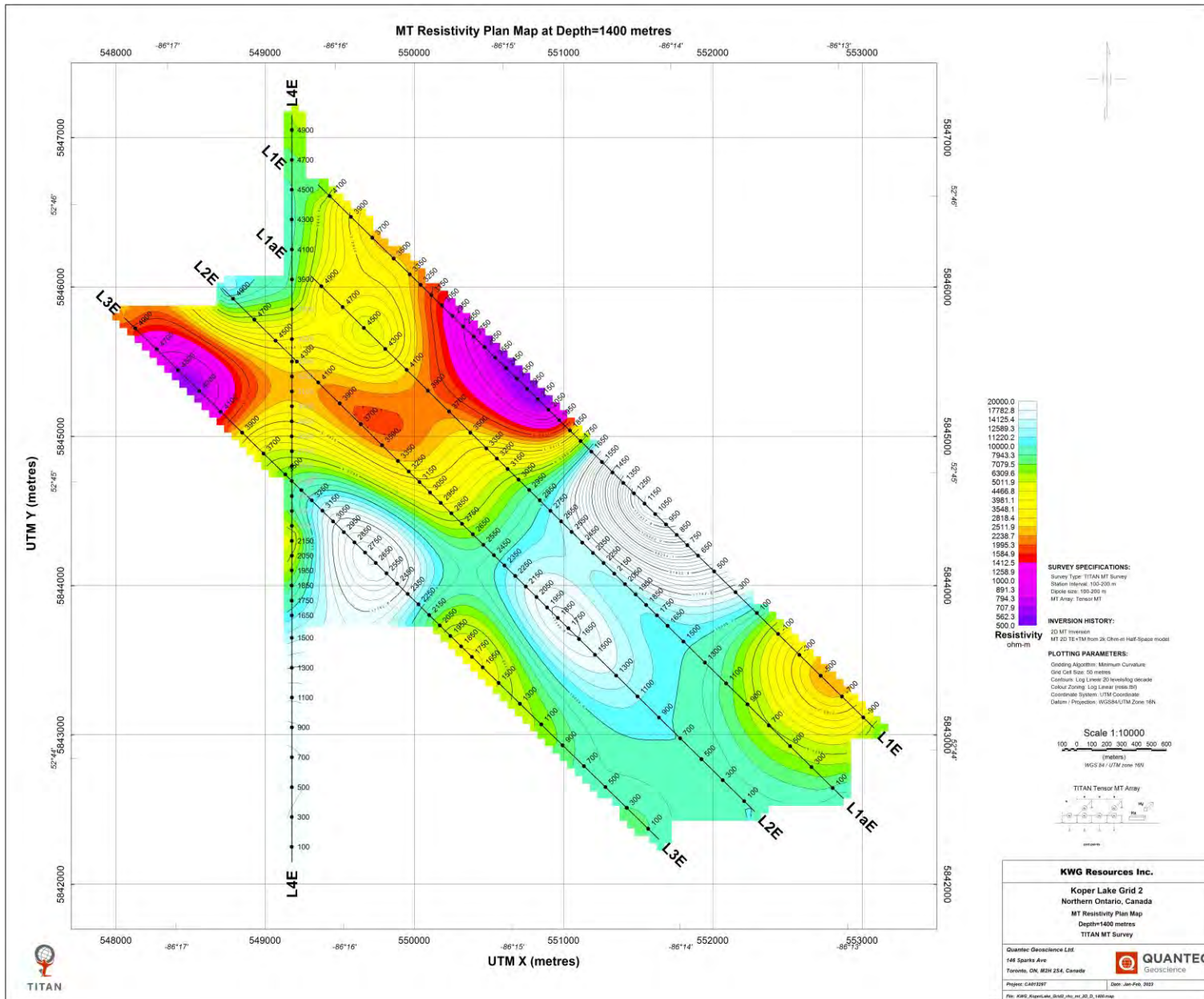


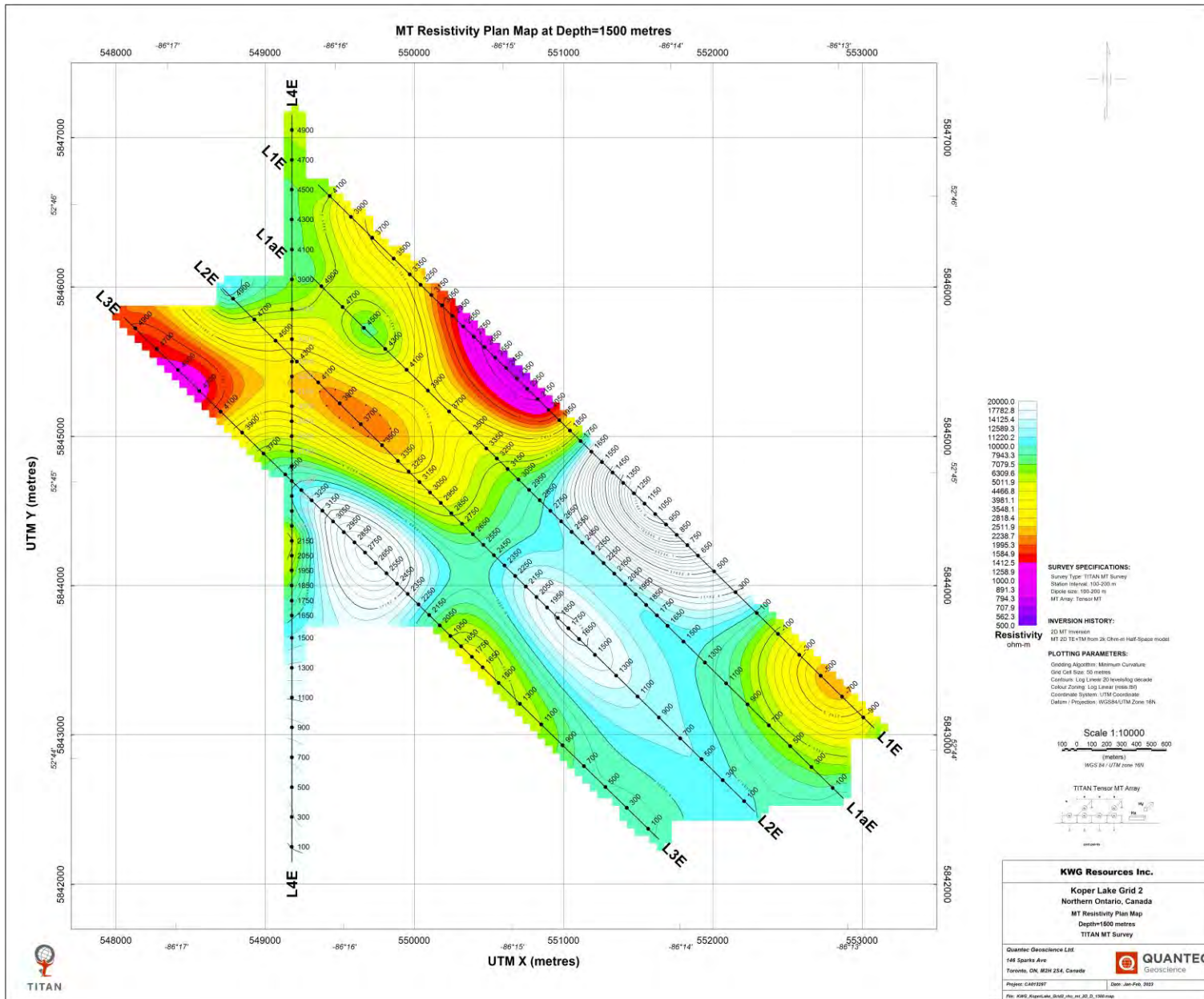


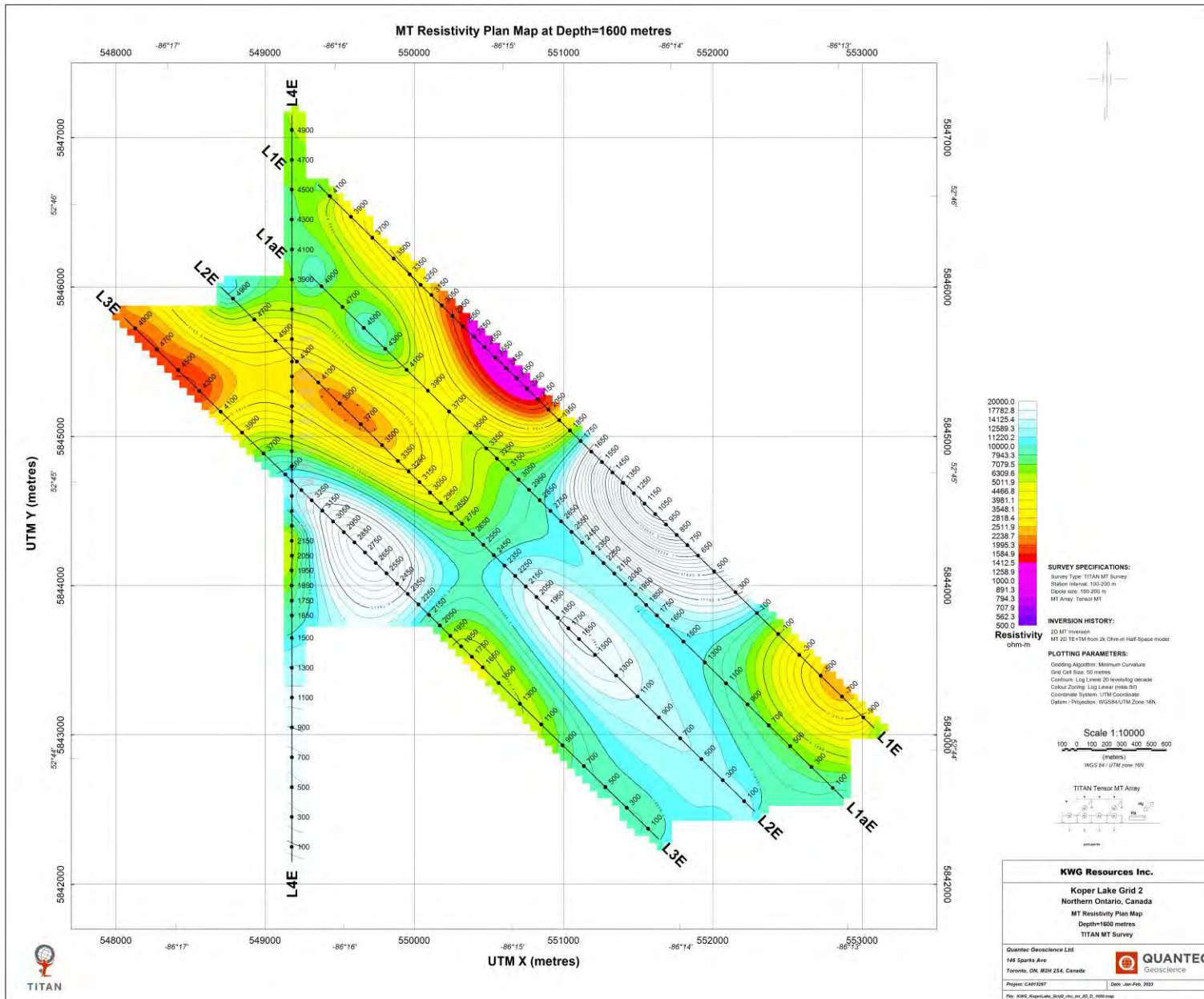


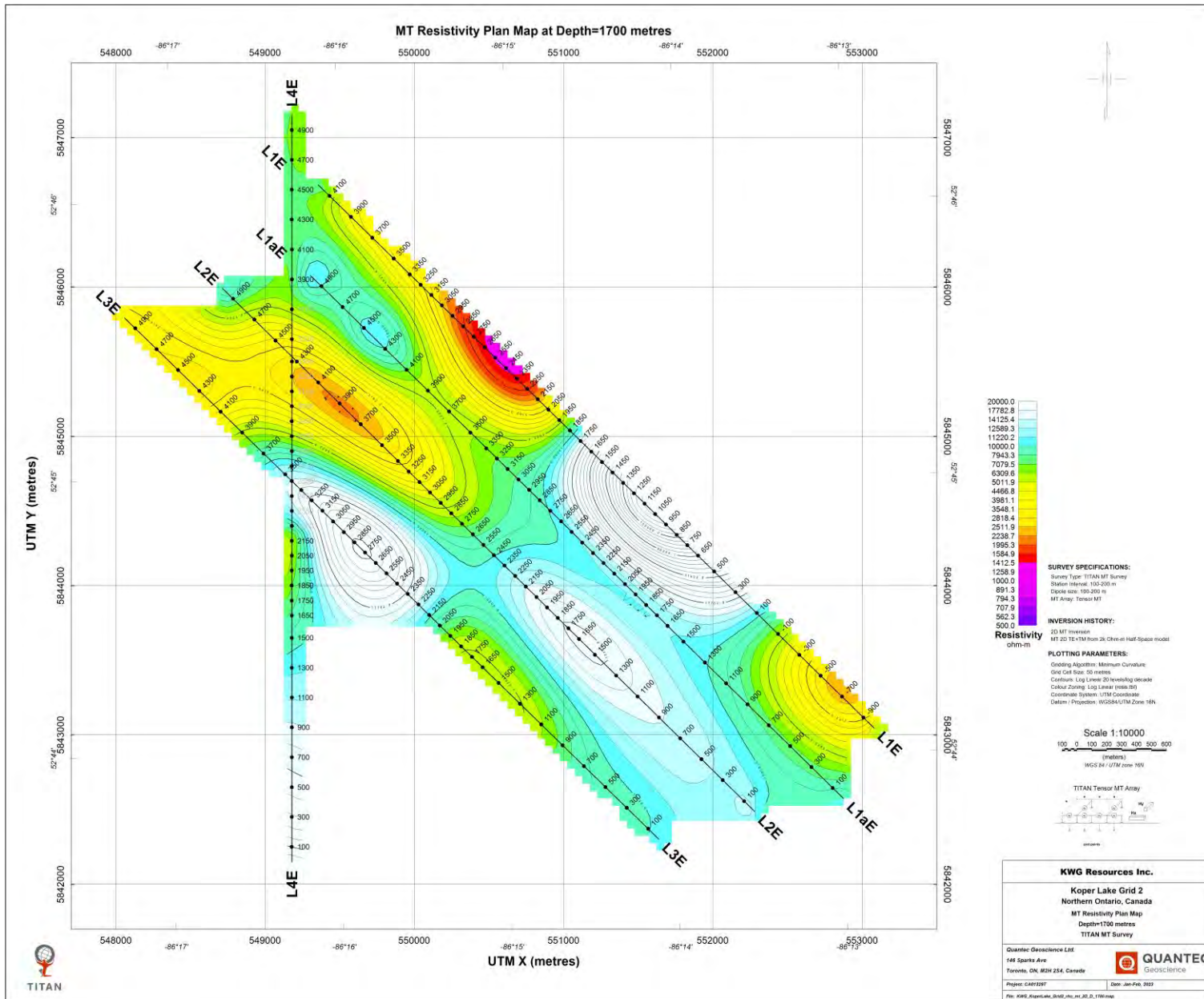


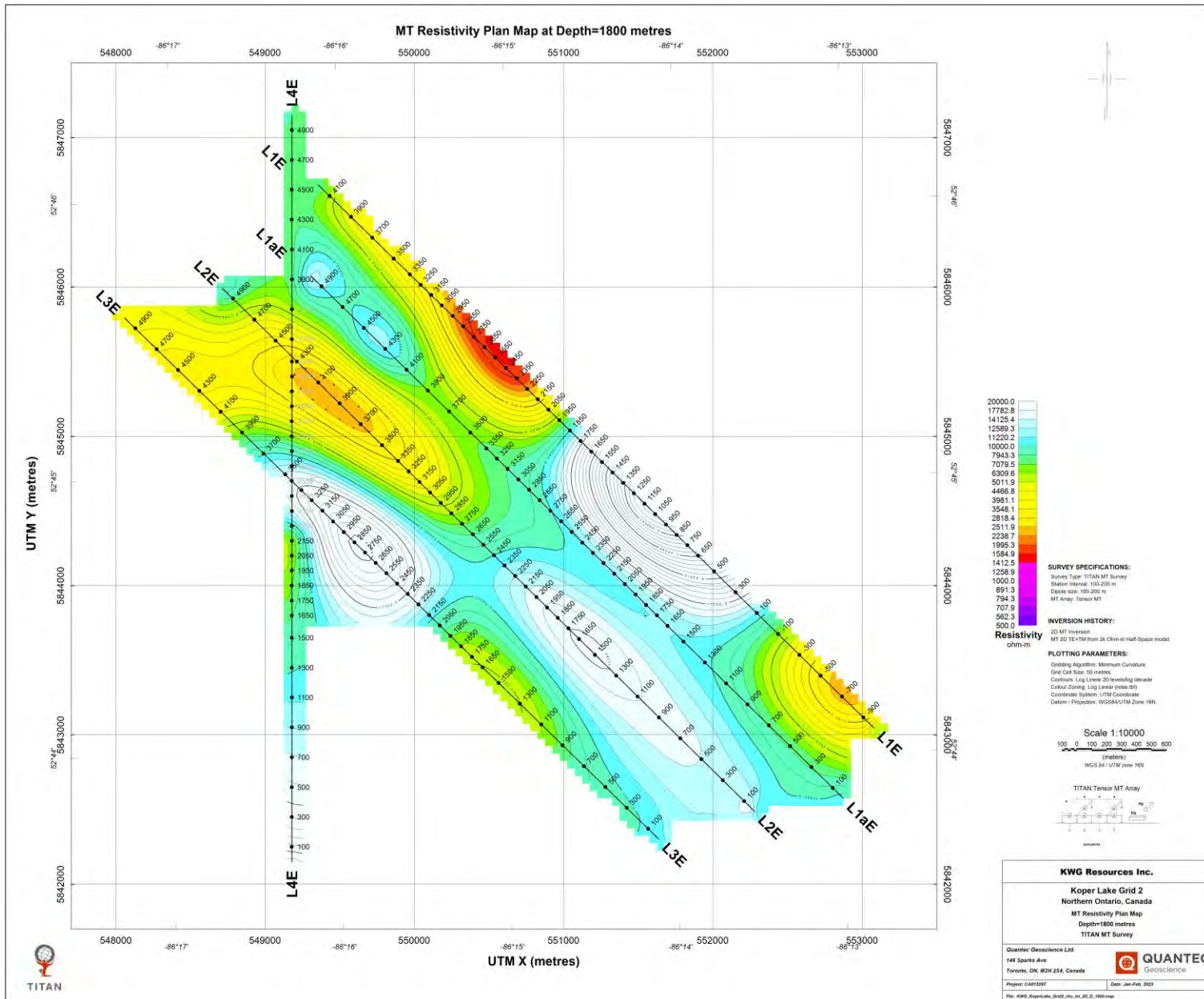


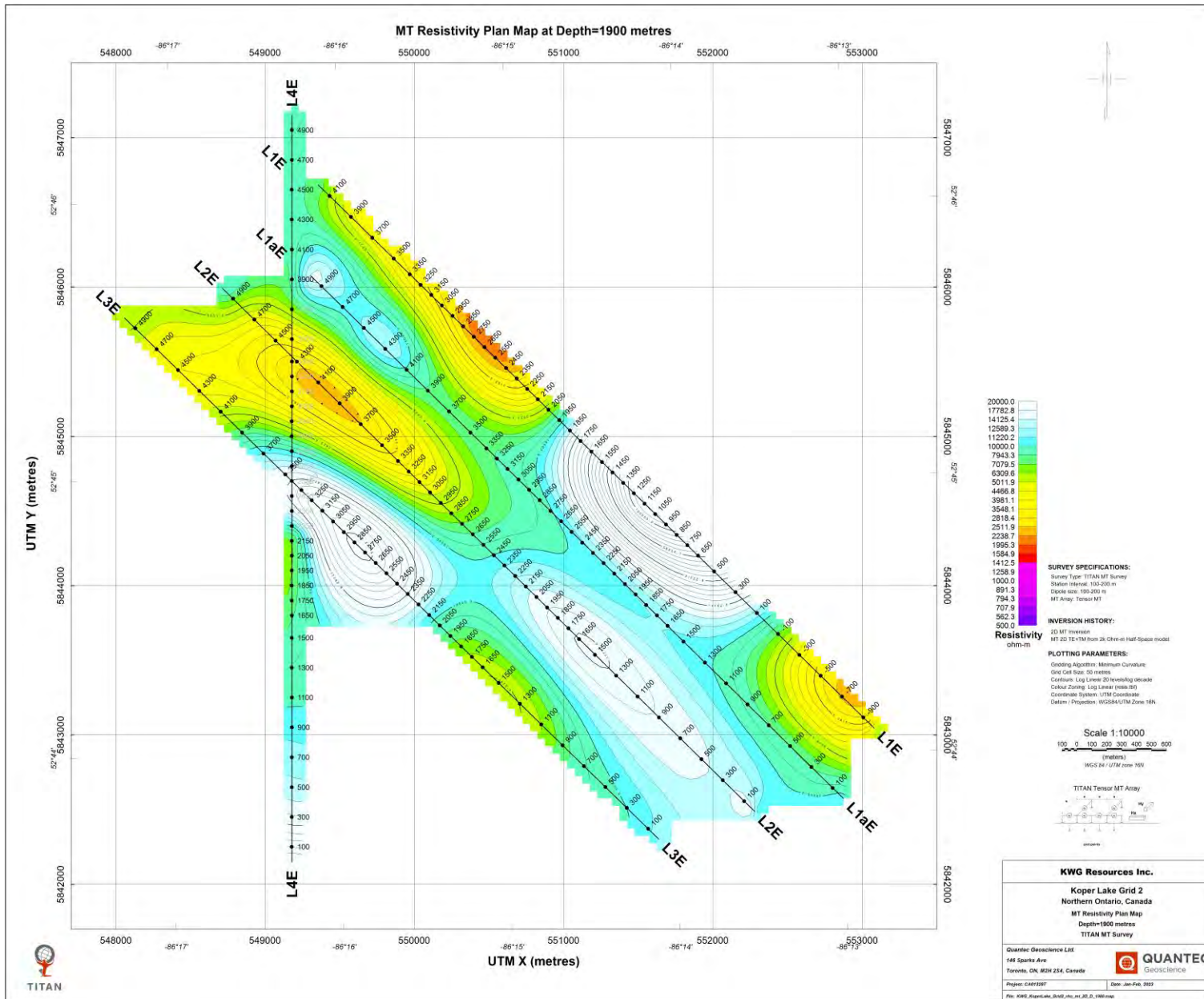


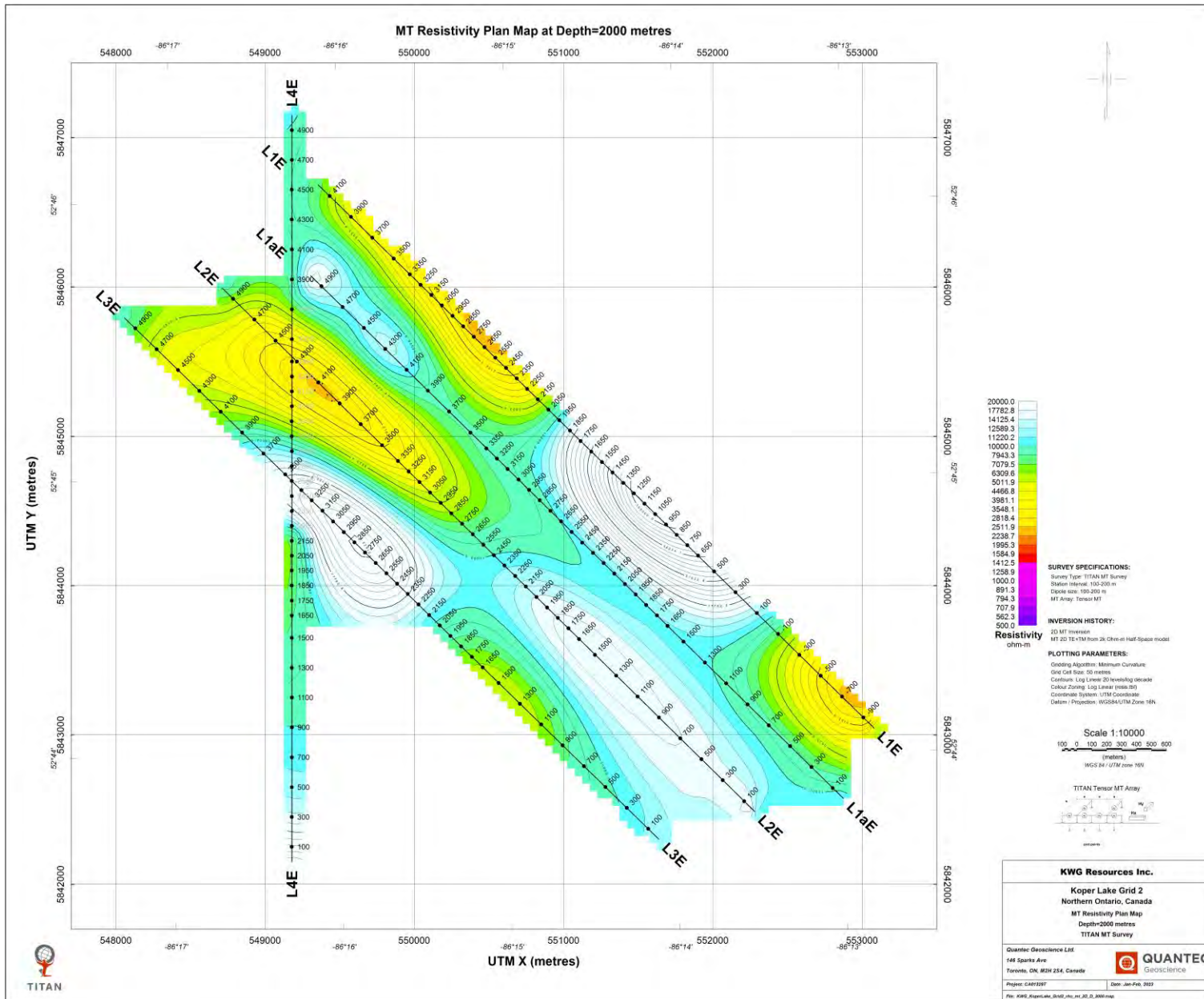


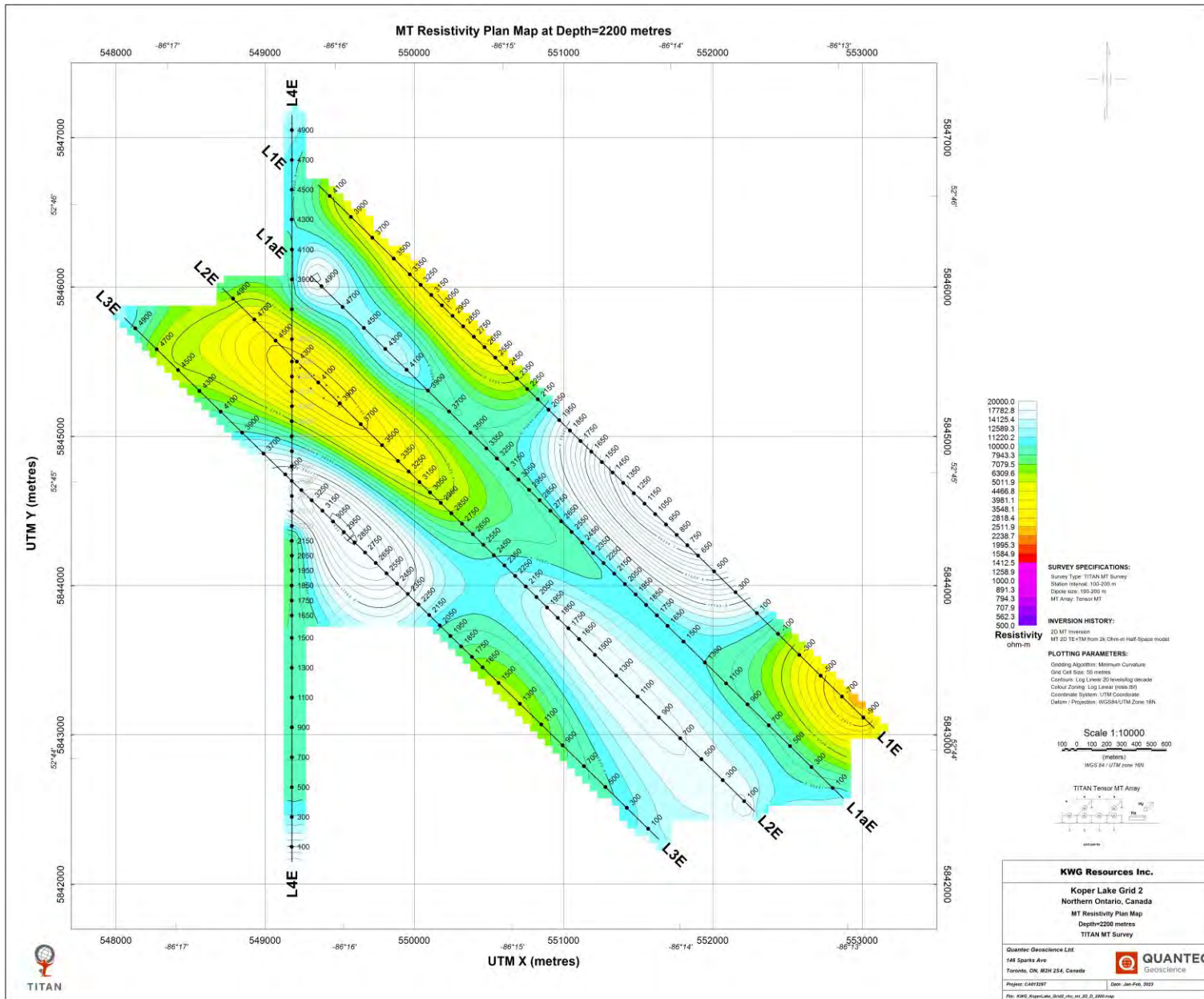


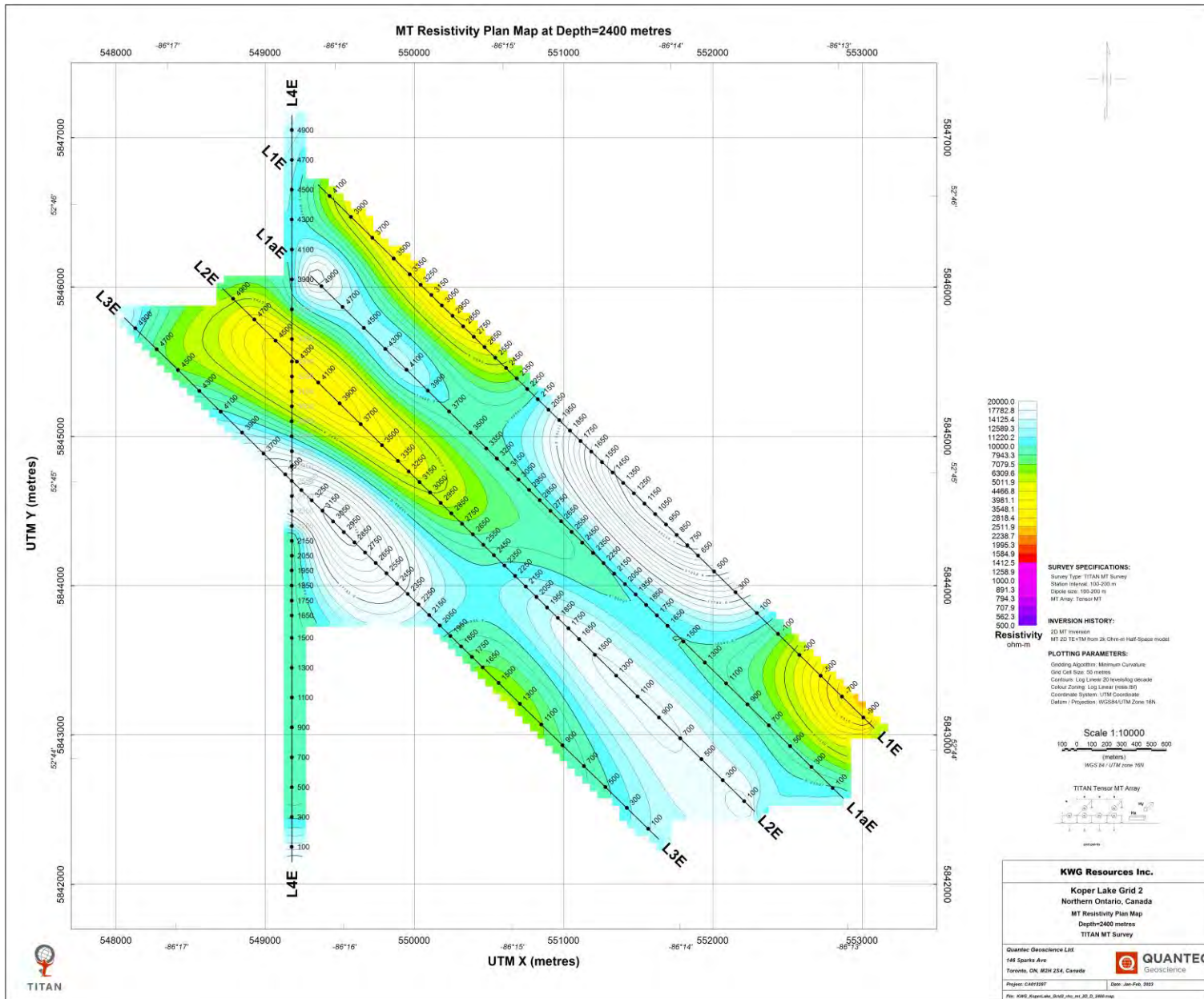


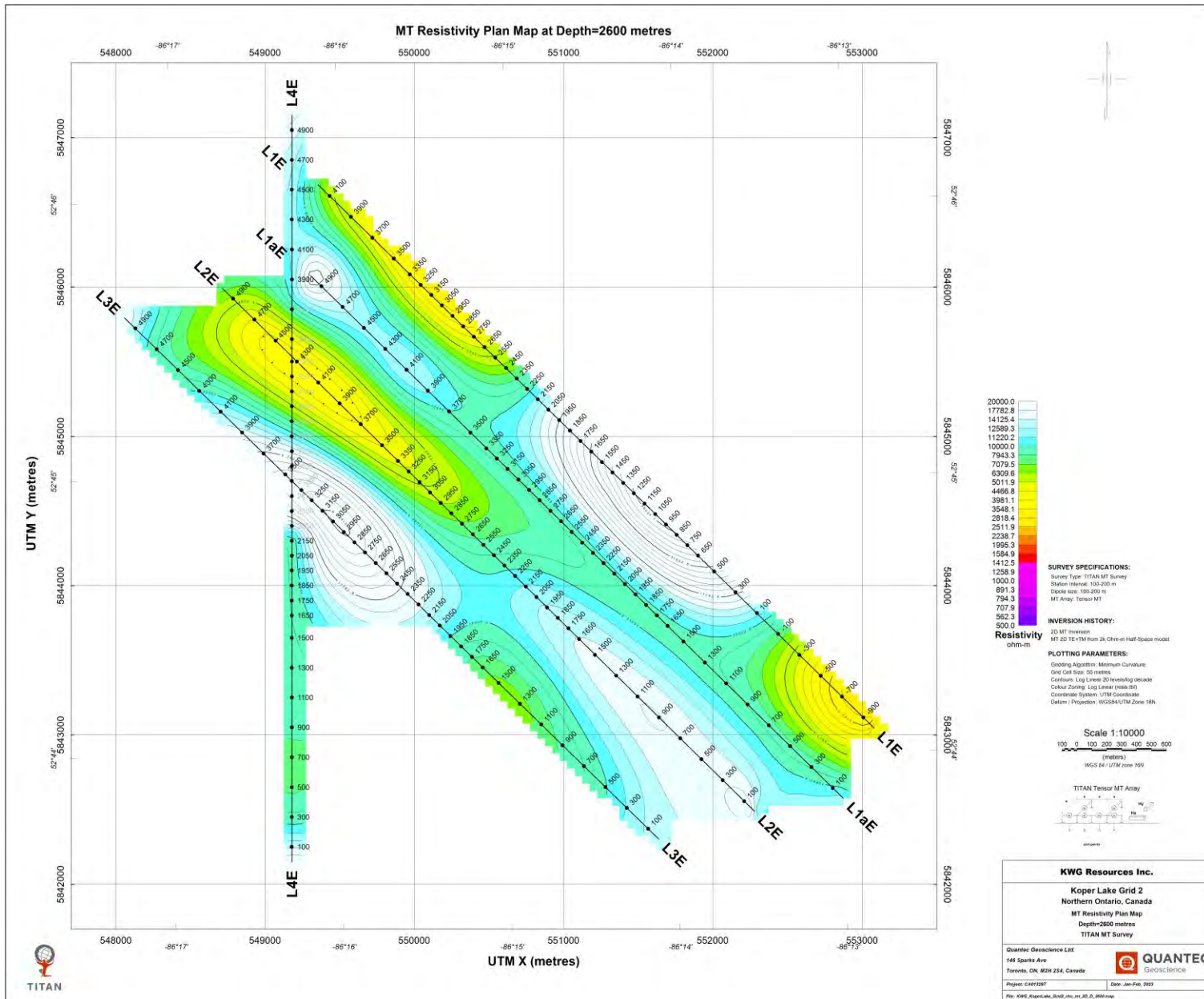


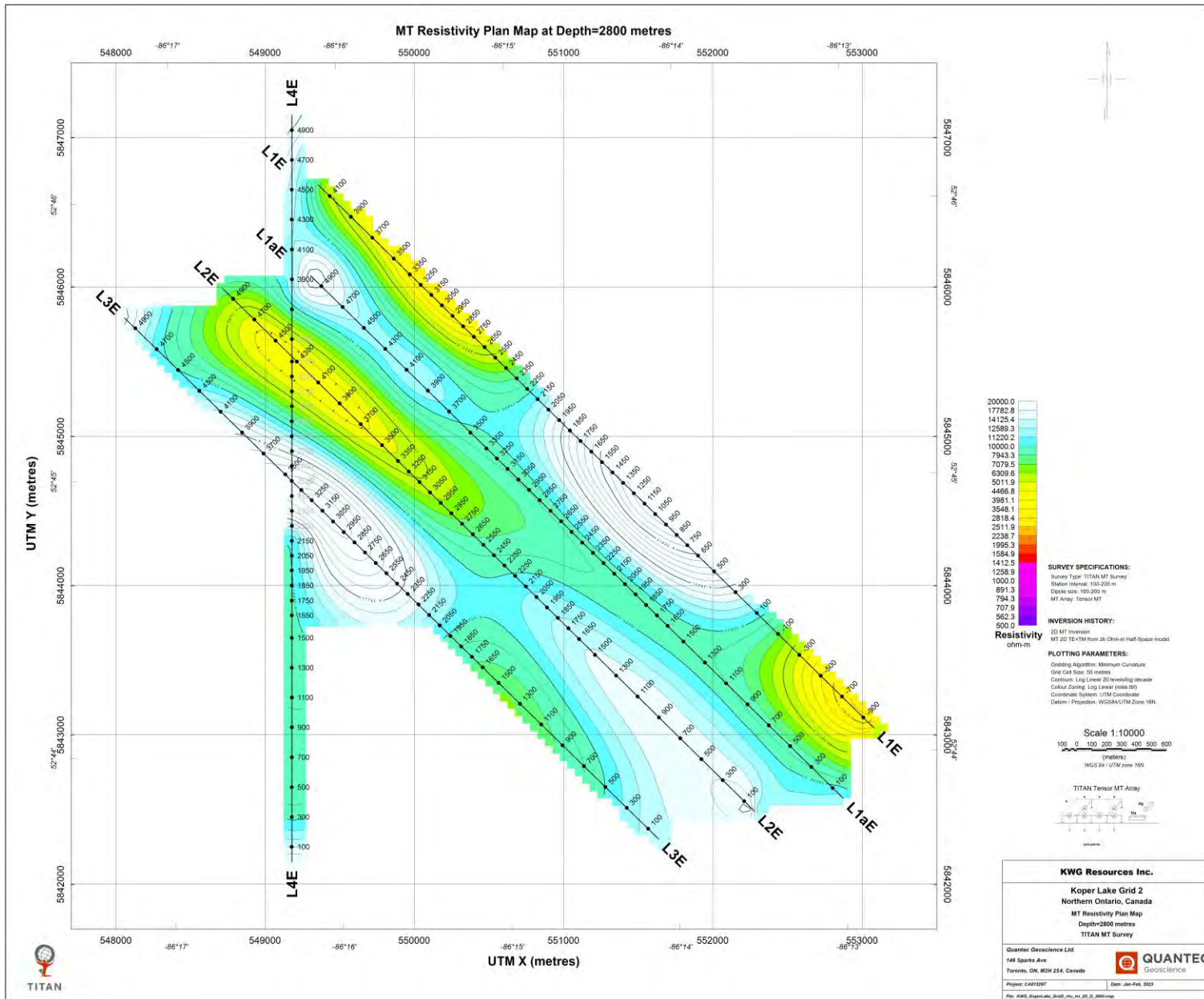


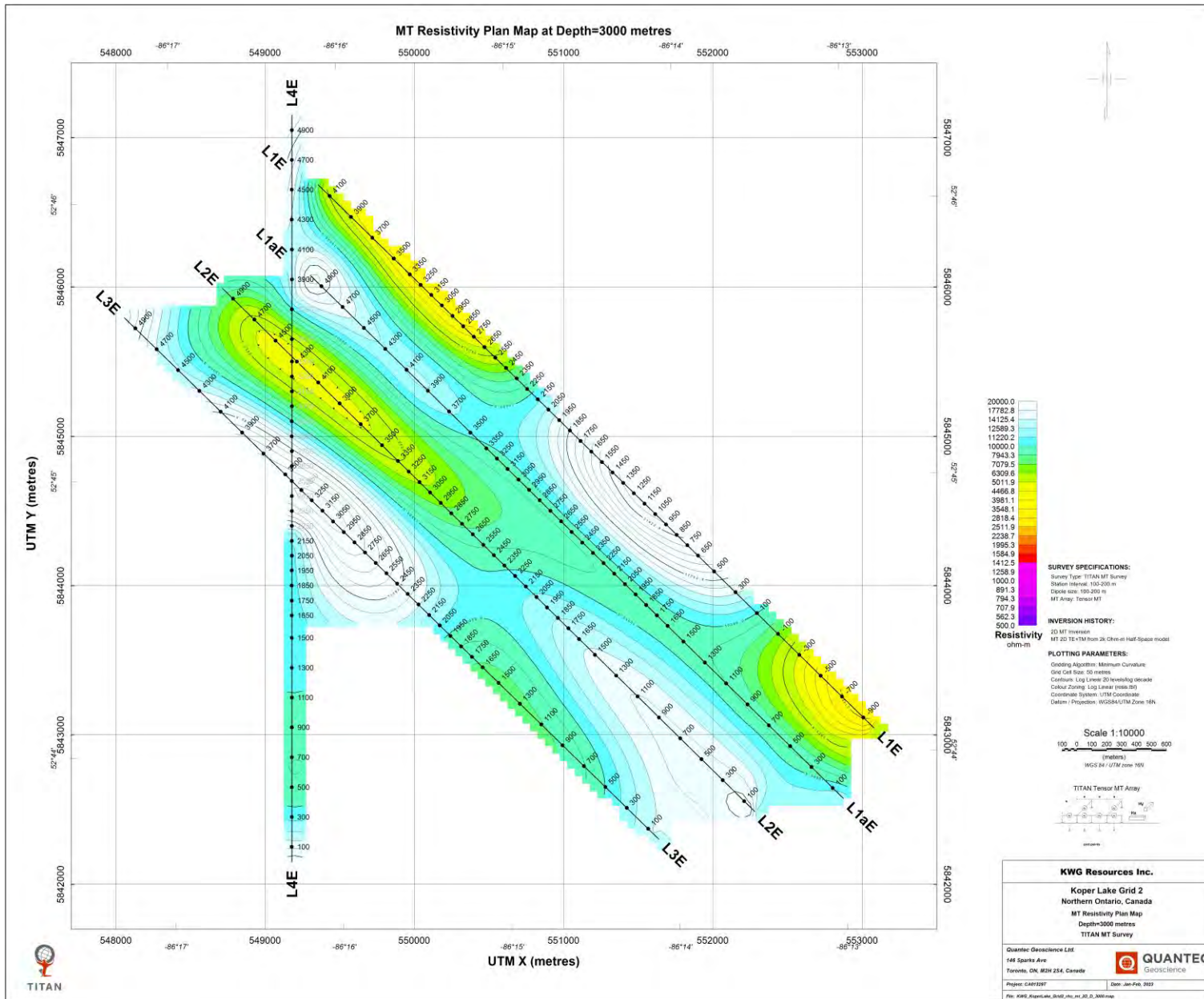












APPENDIX D. GEOTOOLS 2D (CGG) INVERSION CODE

The 2D MT inversion code was developed by Randall Mackie in late 2012 for CGG. The usual approach to MT inversion, and indeed the approach used in this algorithm is that of Tikhonov regularization (Tikhonov and Arsenin, 1977). This algorithm seeks to find regularized inversion models that fit the data to within the prescribed errors. Typically, the regularization is of the form of minimum-structure models. We use the nonlinear conjugate gradients algorithm (Rodi and Mackie, 2001) to minimize the nonlinear objective function:

$$\psi(m) = \frac{1}{2}(d - F(m))^T V^{-1}(d - F(m)) + \tau_1 m^T L^T L m + \tau_2 (m_0 - m)^T D(m_0 - m)$$

where the first term is the squared L-2 norm of the weighted residuals, the second term is the L-2 norm of the model roughness, and the third term is the squared L-2 norm of the variations away from the a-priori model. In this equation, L is the approximation to the depth weighted Laplacian, and D is a diagonal weighting matrix. If minimizing model variations, the second term is modified by changing m to (m₀-m). The inversion is for the complex apparent resistivity and the complex vertical magnetic transfer function (if present).

Doing a 2D MT inversion requires the solution of hundreds of 2D MT forward solutions. The new algorithm for 2D MT forward problems is a finite-difference modeling algorithm based on the network analog to the Maxwell equations (Swift, 1971; Madden, 1972). The model is divided into 2D rectangular blocks of varying dimensions each with a constant conductivity. Additional air layers are added on top of the earth model for the TE mode solution. In the TM mode (E_y, E_z, H_x), the electric fields are eliminated resulting in a second order system of equations for H_x. In the TE mode (E_x, H_y, H_z), the magnetic fields are eliminated resulting in a second order system of equations for E_x. In both cases, the resulting second order system of equations is solved using a parallel sparse matrix solver (PARDISO), which is fast and efficient, after which electric and magnetic fields can be computed at any point in the model.

Some of the related references include:

- Geotools™ 2D inversion (CGG), 2012. Appendix A in: Geotools™, Magnetotelluric and Time Domain EM Data Analysis Software. Reference Document, CGG Multi-Physics Imaging, May 2019.
- Tikhonov, A.N. and Arsenin, V.Y., 1977. Solution of Ill-posed Problems. Washington: Winston & Sons. ISBN 0-470-99124-0.
- Rodi, W. and Mackie, R.L., 2001. Nonlinear conjugate gradients algorithm for 2-D magnetotelluric inversion, *Geophysics*, 66, 174--187.
- Swift, C.M., 1971. Theoretical magnetotelluric and Turam responses from two-dimensional inhomogeneities. *Geophysics*, v. 36, pp. 38-52.
- Madden, T.R., 1972. Transmission systems and network analogies to geophysical forward and inverse problems, ONR Tech. Rep. 72-3.

SUMMARY INFORMATION

QUANTEC OFFICE INFORMATION	
Office:	Quantec Geoscience Ltd.
Address:	146 Sparks Ave., Toronto, ON, M2H 2S4, Canada
Phone:	+1-416-306-1941
Web:	quantecgeo.com
Email:	info@quantecgeoscience.com
PROJECT INFORMATION	
Client Name:	KWG Resources Inc.
Project Name:	Koper Lake Project
Project Location:	Northern Ontario
Project Type:	Titan MT
Project Number:	CA01329T
Project Manager:	Mark Morrison
Project Geophysicist:	Jimmy Stephen
Project Period:	19/01/2023 to 11/02/2023
Report Type:	Summary Report
Report Author(s):	Jimmy Stephen, PhD, PGeo
Report date:	March 8, 2023
Reference	<i>Summary Report for a Titan MT survey over Koper Lake Project (Northern Ontario) by Quantec Geoscience Ltd. on behalf of KWG Resources Inc.</i>
Template version	Version 2021.12.01